

**CIGARETTE SMOKE AND RESPIRATORY
ANTIMICROBIAL HOST DEFENSE**

**DELINEATING THE IMPACT OF TOBACCO SMOKE
ON ANTIMICROBIAL IMMUNITY IN THE
UPPER AND LOWER RESPIRATORY TRACT**

Joshua J.C. McGrath, BSc.

A Thesis

Submitted to the School of Graduate Studies

In Partial Fulfilment of the Requirements For the Degree

Doctor of Philosophy

DOCTOR OF PHILOSOPHY (2021)

McMaster University, Hamilton, Ontario, Canada

**Faculty of Health Sciences, Medical Sciences Graduate Program
(Infection & Immunity)**

TITLE: Delineating the impact of tobacco smoke on antimicrobial immunity in the upper and lower respiratory tract

AUTHOR: Joshua J.C. McGrath, BSc (Hons) McMaster University

SUPERVISOR: Dr. Martin R. Stämpfli, PhD McMaster University

COMMITTEE: Dr. Dawn M.E. Bowdish, PhD McMaster University

Dr. Judah A. Denburg, MD McMaster University

Dr. Mark D. Inman, MD PhD McMaster University

NUMBER OF PAGES: *xxiii*, 220

LAY ABSTRACT

Cigarette smoke exposure is well known to have many harmful effects on human health, including through its ability to promote various infectious diseases such as influenza. However, the mechanisms by which it promotes infection are not fully known. This is an important knowledge gap given that over 1.1 billion individuals continue to smoke worldwide, and a large number of people are exposed to the harmful effects of second-hand smoke, both with fatal consequence. The central goal of this thesis was to gain a better understanding of this relationship between cigarette smoke and infectious disease, specifically by assessing how smoke exposure impacts immune responses in the upper and lower airways.

In the first study, we found that smoke exposure interferes with the ability to activate immunoglobulin (Ig)A antibody responses in the nasal passages of mice, which may have important implications for human nasal vaccination strategies. The second study investigated different methods with which to best measure antibodies in human respiratory samples. Finally, in the third study we defined a role for a specific molecule, CSF3, in worsening health in a mouse model of concurrent cigarette smoke and influenza infection. Overall, this work provides new insights into the ways in which smoking can increase the risk of respiratory infection, thereby informing the future design and testing of vaccines and treatments for use in our highly smoke-exposed global population.

ABSTRACT

Cigarette smoke is the leading cause of preventable mortality worldwide. This excess death is attributable to an increased risk of acquiring a variety of conditions, including chronic respiratory/cardiovascular diseases and various types of cancer. Smokers are additionally predisposed to develop infectious diseases, notably including pneumonia caused by the influenza virus, one of the most prevalent and burdensome pathogens in existence today. Although cigarette smoke is well known to modulate many aspects of the immune system, the specific mechanisms by which this predisposition is mediated are incompletely understood. Also unclear is the effect of cigarette smoke on responses to intranasal immunization strategies aimed at eliciting immunity against pathogens such as influenza in the upper airways, where protection may substantially contribute to sterilizing immunity.

This PhD thesis focused primarily on addressing these knowledge gaps. In the first study, we assessed the effect of cigarette smoke on antibody induction following intranasal immunization in the upper airways of mice, finding that smoke exposure attenuated antigen-specific IgA induction in the upper respiratory tract, reproductive tract, and systemic circulation. In addition, we found that these nasal IgA demonstrated a reduced antigen-binding avidity in the acute post-immunization period. Mechanistically, deficits in nasal IgA were associated with a reduced accumulation of antigen-specific IgA antibody-secreting cells (ASCs) in the nasal mucosa, induction of these cells in nasal-draining lymphoid tissues, and upregulation of molecules critical to ASC homing (vascular cell adhesion molecule-

1; VCAM-1) and IgA transepithelial transport (polymeric immunoglobulin receptor; pIgR) in the nasal mucosa. Ultimately, in tandem with recent clinical work published by others, our study strongly suggests that cigarette smoke can attenuate IgA induction in the upper airways, which may have implications for aspects of intranasal vaccine efficacy. Thus, smoking status should be more consistently considered in the design of clinical trials for IgA-oriented intranasal vaccines.

The second study did not assess smoking and host defense directly, but rather served to optimize protocols for assessing immunoglobulins in human mucoid respiratory samples as a precursor to future studies in smoking-related disease. In this regard we found that, relative to phosphate-buffered saline (PBS), dithiothreitol (DTT)-based processing of human sputum samples increased total IgA yields, decreased IgE yield, and improved the detection of a specific IgG autoantibody. These findings suggest that processing choices for human mucoid respiratory samples should be made with specific goals in mind as they pertain to antibody isotype(s) of interest.

Finally, in the third study we investigated potential mechanisms by which cigarette smoke exposure promotes influenza, given that smokers are at increased risk of acquiring the pathogen, progressing to severe disease, and being admitted to hospital/ICU following infection. In doing so, we found that concurrent smoke exposure increased morbidity, hypoxemia, pulmonary edema, neutrophilia, and ultimately mortality in a mouse model of H1N1 infection. These changes were associated with an increased accumulation of viral (v)RNA in cells independent of

any change in the shedding of replication-competent viral particles. Using a novel dysregulation score approach, we found that interleukin (IL)-6 and colony-stimulating factor (CSF)3 expression was highly exacerbated in the lungs and circulation of smoke-exposed, infected mice relative to controls. Supplementation of recombinant (r)CSF3 increased morbidity, hypothermia and edema, while blockade of the cognate receptor (CSF3R) improved alveolar-capillary barrier function. On the cellular level, single cell RNA-sequencing revealed a shift in the distribution of *Csf3*⁺ cells towards neutrophils. Finally, deep transcriptional analysis of neutrophils revealed a gene signature that was largely indicative of an exacerbated form of typical disease with select unique regulatory elements. Ultimately, this work identifies potential therapeutic targets (CSF3R signaling, excess vRNA accumulation) for the treatment of cigarette smoke-augmented influenza, and warns against clinical rCSF3 therapy to treat neutropenia during viral infectious disease.

In conclusion, the work presented in this PhD dissertation expands our understanding of the relationship between cigarette smoke and antimicrobial host defense as it pertains to both IgA immunity in the upper airways, and the pathogenesis of cigarette smoke-augmented influenza.

“Then she began to read.

Her father had taught her about hands. About a dog's paws. Whenever her father was alone with a dog in a house he would lean over and smell the skin at the base of its paw. This, he would say, as if coming away from a brandy snifter, is the greatest smell in the world! A bouquet! Great rumours of travel! She would pretend disgust, but the dog's paw was a wonder: the smell of it never suggested dirt. It's a cathedral! her father had said, so-and-so's garden, that field of grasses, a walk through cyclamen — a concentration of hints of all the paths the animal had taken during the day.

A scurry in the ceiling like a mouse, and she looked up from the book again.”

- **Michael Ondaatje, *The English Patient***

ACKNOWLEDGEMENTS

This PhD began partially as a means with which to further delay choosing a career, and partially as a last-ditch smoking cessation strategy (I hypothesized that it would be pretty ridiculous to continue smoking while studying smoking). In the end, it turned out to be one of the best decisions I ever made. Over the past six years I lost an addictive, destructive habit and gained so much more – a wealth of experiences both personal and scientific, a stronger sense of confidence, some highly impactful mentors, and a number of invaluable friendships. I have many people to thank for helping me along the way, without whom I would not be where I am today.

First I have to thank my supervisor, Dr. Martin Stämpfli. One day in early 2015, after listening to one of his lectures I approached his office as he was on his way out to London. I asked if I could join his lab for a Master's degree, out of the blue. He was kind enough to take a chance on me, and promptly threw me into the deep end of science. Martin, you are an excellent supervisor. You have a talent in creating a healthy lab environment, and are an effective teacher and mentor, emphasizing the learning experience of grad school both in terms of scientific and personal growth. It was always entertaining to get “Stampfli'd”, as we would call it, during your visits to the lab. I certainly won't forget your many metaphors; the relative value of Asian vs. European gardens comes to mind. Over the past six years I've come to understand the essential value of a good supervisor in fostering budding scientists such as ourselves; thank you for your efforts in this regard.

I would also like to thank my committee, Drs. Dawn Bowdish, Judah Denburg, and Mark Inman, for their years of guidance. Dawn; I remember seeing you in the front row of my first WIP with an encouraging smile, it helped a lot for someone who was a nervous presenter coming into grad school. And it was good fun doing the stair climb for Firestone! Judah; thanks for all of your efforts in reviewing my science and providing excellent feedback; I could always count on you for some solid clinical input and words of encouragement. Mark; thanks for your efforts in teaching MS771 and acting as my comps supervisor. I think almost every one of your emails made me laugh, genuinely. Thanks to all of you for your advice and expertise over the past six years; I really appreciate it.

In addition to my committee, other people have helped mentor me along the way. The late Dr. Mark McDermott, for instance, inspired me to study immunology at Mac and instilled in me a particular interest in mucosal immunology. He also held excellent parties, and will be missed. Dr. Carl Richards taught me in MS716 and provided helpful and detailed insight into experiment planning and cytokine biology, for which I am thankful. We also share an interest in the paintings of Robert Bateman which fostered some good discussion. Dr. Manali Mukherjee served as senior author for my second publication, acting as an excellent and friendly mentor in clinical respiratory science. Finally, toward the end of my PhD Dr. Matthew Miller taught me about the intricacies of influenza, inspiring me to pursue a postdoc in the field and ultimately assisting me in the process of finding one, for which I am very appreciative.

MIRC is an excellent collaborative environment that fosters not only scientific relationships, but personal ones. In particular I am appreciative of friendships I have built with the hilarious duo of Dr. Sam Afkhami and Mike D'Agostino, Dr. Allison Felker, Dr. Puja Bagri, Dr. Joshua Koenig, Hannah Stacey, Jann Ang, Art Marzok, Dr. Pat Schenck, Dr. Olivia Mekhael, Kelly Bruton, Allyssa Phelps, Dr. Jon Mapletoft, Dr. Anna Dvorkin-Gheva, Dr. Rocky Lai, and Dr. Ehab Ayaub. I also want to thank Pritpal Matharu, my math friend, for some good times. He studies turbulence, I think.

I have to extend a special thanks to everyone in my lab. Firstly, to Joanna Kasinska, who has been truly essential in all of my work, and has always been a

friendly face around the lab. Also, to my first lab mentor, Dr. Pamela Shen, who took me under her wing and taught me the basics of microbiological immunology and how to be a good lab citizen. All of my good scientific habits can be attributed to her. Many thanks to Dr. Gilles Vanderstocken, Ashley Beaulieu, Bruce Ly, Rachel Heo, Bomi Park, and Peipei Wang for being awesome companions over the years both in and out of the lab. Special gratitude to Matthew Fantauzzi; thanks for joining our weird bunch of grad students and adding your own flair; it takes a bold man to wear a moustache so proudly but you wore it well. And I was always glad to have another metalhead in the group. Last but not least, Drs. Steven Cass and Danya Thayaparan. Whether it was something as adventurous as hiking through the jungles of Vietnam and exploring the second biggest cave in the world, or as simple as spending an evening having a few drinks and watching movies, I always enjoyed our time together. I cannot understate how much you two along with Matt have helped make this grad school experience a positive one. Thanks for being top-tier friends; I look forward to that being the case for a long time to come.

Finally, I have to thank my family: Mom, Dad, Mitch, Nan Nettie, Nan Irene, Andy – and the pups, Lola and Ruby (fun fact: dog's paws do smell as interesting as the quote above suggests). Grad school was a stressful adventure at times but I always had family around to talk with and spend time with, whether it was Sunday dinner, a trip to South Carolina, fishing at the shoals, hiking in Chutes Provincial Park, going for walks, or any number of other things. I definitely couldn't have done this PhD without the loving support of them, without a doubt.

TABLE OF CONTENTS

LAY ABSTRACT.....	iii
ABSTRACT.....	iv
ACKNOWLEDGEMENTS.....	vii
TABLE OF CONTENTS.....	xi
LIST OF FIGURES AND TABLES.....	xiii
LIST OF ABBREVIATIONS.....	xvi
DECLARATION OF ACADEMIC ACHIEVEMENT.....	xxi
CHAPTER 1 – INTRODUCTION AND OBJECTIVES	1
1.1 – Cigarette Smoke and Human Health	1
1.1.1 – Epidemiology of Tobacco Smoking.....	1
1.1.2 – Broad Health Effects of Tobacco Smoking.....	2
1.1.2.1 – Smoking, COPD, and Infectious Disease.....	3
1.2 – Influenza.....	6
1.2.1 – Burden of Influenza-Associated Disease.....	6
1.2.2 – Virology and Infection.....	7
1.2.3 – Subtypes of Concern.....	9
1.2.4 – Transmission	10
1.2.5 – Immunity and Disease Pathogenesis.....	11
1.2.5.1 – Specific Contribution of Neutrophils.....	14
1.2.5.2 – Specific Contribution of Antibodies.....	16
1.3 – Immunoglobulin A (IgA).....	18
1.3.1 – Structure, Isotype and Valency.....	18
1.3.2 – Effector Functions.....	19
1.3.3 – Induction of IgA Responses in the Upper Airways.....	21
1.3.3.1 – T cell-Dependent Activation.....	21
1.3.3.2 – Antibody-Secreting Cell Homing.....	24
1.3.3.3 – Transepithelial Transcytosis.....	25
1.3.4 – IgA-Oriented Influenza Vaccination.....	25
1.3.5 – Measurement of Antibodies in Mucoid Human Samples.....	27

1.4 – Cigarette Smoke and Antimicrobial Host Defense.....	28
1.4.1 – Mechanisms of Cigarette Smoke-Augmented Influenza.....	28
1.4.2 – Effect of Cigarette Smoke on Antibody Responses.....	30
1.5 – Central Paradigm, Hypotheses and Objectives.....	33
CHAPTER 2 – Cigarette smoke exposure attenuates the induction of antigen-specific IgA in the murine upper respiratory tract.....	37
CHAPTER 3 – Detecting immunoglobulins in processed sputa.....	82
CHAPTER 4 – Cigarette smoke augments CSF3 expression in neutrophils to compromise alveolar-capillary barrier function during influenza infection.....	92
CHAPTER 5 – DISCUSSION	155
5.1 – Summary of Results and General Discussion.....	155
5.1.1 – Cigarette Smoke & IgA Induction in the Upper Airways.....	155
5.1.2 – PBS- vs. DTT-based Sputum Processing for Antibody Detection....	160
5.1.3 – Cigarette Smoke & Pulmonary Influenza Infection.....	161
5.2 – Clinical and Therapeutic Implications.....	167
5.2.1 – Cigarette Smoke & IgA: Implications for Vaccination.....	169
5.2.2 – Cigarette Smoke & Influenza: Therapeutic Implications.....	173
5.3 – Limitations and Future Directions.....	179
5.3.1 – Cigarette Smoke & IgA Induction in the Upper Airways.....	179
5.3.2 – PBS- vs. DTT-based Sputum Processing for Antibody Detection....	184
5.3.3 – Cigarette Smoke & Pulmonary Influenza Infection.....	186
5.4 – Concluding Remarks.....	194
CHAPTER 6 – REFERENCES*	197
<i>*References for each manuscript are included separately at the end of each of their respective Chapters (2-4). References listed in Chapter 6 refer to the Introduction (Chapter 1) and Discussion (Chapter 5) of this thesis only.</i>	
APPENDIX 1 – COPYRIGHT PERMISSIONS TO REPRINT PUBLISHED MATERIAL.....	219

LIST OF FIGURES, TABLES, AND FILES**FIGURES:****Chapter 2:**

Figure 1. Cigarette smoke exposure compromises the induction of nasal and systemic IgA responses following intranasal LPS/OVA immunization.

Figure 2. Cigarette smoke exposure attenuates OVA-specific IgA ASC accumulation in the nasal mucosa after intranasal LPS/OVA immunization.

Figure 3. Cigarette smoke exposure reduces nasal OVA-IgA avidity during the acute post-immunization period while augmenting mutational load in the cognate nasal *Igha* repertoire.

Figure 4. The induction of antigen-specific IgA ASC responses is diminished in the NALT, CLNs and spleen in the context of cigarette smoke exposure.

Figure 5. Cigarette smoke exposure attenuates the transcriptional upregulation of VCAM-1 in the nasal mucosa following immunization.

Figure 6. Cigarette smoke exposure attenuates the upregulation of pIgR in the nasal mucosa following immunization.

Figure 7. Prospective mechanisms of cigarette smoke-mediated IgA inhibition in the upper respiratory tract.

Figure S1. Extended data for Figure 1.

Figure S2. Extended data for Figure 2/3.

Figure S3. Extended data for Figure 4.

Figure S4. Extended data for Figure 6.

Chapter 3:

Figure 1. Schematic of matched sputum processing.

Figure 2. DTT processing moderately improves sputum IgG and IgA recovery, but reduces IgE.

Chapter 4:

Figure 1. Cigarette smoke exposure exacerbates influenza-induced pulmonary edema and hypoxemia in association with PFU-independent vRNA accumulation.

Figure 2. Accumulation of neutrophils in the pulmonary interstitium correlates with disease severity in cigarette smoke-augmented influenza.

Figure 3. Progressive positive dysregulation of CSF3 and IL-6 in the lungs and systemic circulation characterizes cigarette smoke-augmented influenza.

Figure 4. CSF3 supplementation exacerbates morbidity and alveolar-capillary barrier dysfunction during influenza infection.

Figure 5. Systemic CSF3R inhibition improves alveolar-capillary barrier function during smoke-augmented influenza.

Figure 6. Cigarette smoke skews the distribution of *Csf3*-expressing cells towards neutrophils.

Figure 7. Subcluster analysis indicates that cigarette smoke-exposed lungs are enriched for infected, highly inflammatory neutrophils.

Figure 8. Neutrophil gene signatures from smoke-exposed, influenza-infected mice reflect an exacerbated form of typical disease with unique regulatory features.

Figure S1. Extended data for Figure 1.

Figure S2. Extended data for Figure 2.

Figure S3. Extended data for Figure 3.

Figure S4. Extended data for Figure 6.

TABLES:**Chapter 2:**

Table S1. Antibodies and other stains used for flow cytometry in this study.

Table S2. Number of sequencing reads and clones per sample.

Chapter 3:

Table S1. Patient demographics.

Table S2. Spontaneous vs. Induced Sputum Analysis.

FILES:**Chapter 4:**

File S1. Supplementary data. (supplied as an adjunct .xlsx file to this thesis)

Tab number / Content:

1. Reagents – Flow cytometry/Western blot antibodies, RT-qPCR primers
2. Endpoint scoring metrics
3. Lung homogenate cytokine dysregulation scoring
4. Neutrophil DEGs – between subclusters C0/C5
5. Neutrophil DEGs – between subclusters C0/C8
6. Neutrophil DEGs – between subclusters C5/C8
7. STRING analysis of unique subcluster genes
8. Neutrophil DEGs – between samples
9. Neutrophil DEGs – uniquely up/downregulated by CS-FM1

LIST OF ABBREVIATIONS

4-NPP	4-Nitrophenylphosphate
ACK	Ammonium-chloride-potassium
ADCC	Antibody-dependent cell cytotoxicity
ADCP	Antibody-dependent cellular phagocytosis
AECOPD	Acute exacerbation of COPD
AF647	AlexaFluor 647
ALI	Acute lung injury
ANOVA	Analysis of variance
AP	Alkaline phosphatase
ARDS	Acute Respiratory Distress Syndrome
ASC	Antibody-secreting cell
ATN ratio	Airspace-to-tissue neutrophil ratio
BAL	Bronchoalveolar lavage (supernatant + cells)
BALF	BAL fluid (supernatant)
BCR	B cell receptor
BCL	B cell lymphoma
BM	Bone marrow
BSA	Bovine serum albumin
C- (prefix e.g. in “C0”)	Cluster
CBB	Carbonate-bicarbonate buffer
CCL	C–C motif chemokine ligand
CCR	C–C motif chemokine receptor
CD	Cluster of differentiation
cDNA	Complementary DNA
CDR	Complementarity-determining region
cDC	Classical dendritic cell
cfDNA	Cell-free DNA

CLN	Cervical lymph node
COPD	Chronic Obstructive Pulmonary Disease
COVID-19	Coronavirus Disease-19
cRNA	Complementary RNA
CS	Cigarette smoke
CSF	Colony-stimulating factor
CVL	Cervicovaginal lavage
CXCL	C-X-C motif chemokine ligand
CXCR	C-X-C motif chemokine receptor
DAA	Direct-acting antiviral
DAMP	Danger-associated molecular pattern
DEG	Differentially-expressed gene
DNA	Deoxyribonucleic acid
dbp	Days post-boost
dpi	Days post-infection
DTT	Dithiothreitol
DTE	Dithioerythritol
ECMO	Extracorporeal membrane oxygenation
ECP	Eosinophil cationic protein
ELISA	Enzyme-linked immunosorbent assay
EPX	Eosinophil peroxidase
Fab	Antibody antigen-binding fragment
FACS	Fluorescence-activated cell sorting
Fc	Antibody constant fragment
FcR	Fc Receptor
FM1	Influenza A/Fort Monmouth/1/1947-MA (H1N1)
FMO	Fluorescence-minus-one
FWR	Framework region
GCBC	Germinal centre B cell

HA	Hemagglutinin
HAI	Hemagglutination inhibition
H&E	Hematoxylin and eosin
HIF	Hypoxia inducible factor
HRP	Horseradish peroxidase
HPV	Human papillomavirus
IAV	Influenza A virus
IBV	Influenza B virus
ICOSL	Inducible T cell co-stimulator ligand
ICU	Intensive care unit
IFN	Interferon
Ig	Immunoglobulin (e.g. IgA, IgG, IgM, IgE)
IL	Interleukin
ILC	Innate lymphoid cell
IM/MLC	Interstitial macrophage/monocyte-lineage cell
IRF	Interferon response factor
ISG	Interferon-stimulated gene
LAIV	Live attenuated influenza virus
LIF	Leukemia inhibitory factor
LPS	Lipopolysaccharide
MAdCAM	Mucosal addressin cell adhesion molecule
MDA-5	Melanoma differentiation-associated protein
MFI	Median fluorescence intensity
MHC	Major histocompatibility complex
MPO	Myeloperoxidase
NA	Neuraminidase
NAL	Nasal lavage (supernatant + cells)
NALF	NAL fluid (supernatant)
NALT	Nasal-associated lymphoid tissue

NE	Neutrophil elastase
NET	Neutrophil extracellular trap
NF κ B	Nuclear Factor κ B
NK cell	Natural Killer cell
NLR	NOD-like receptor
NM	Nasal mucosa
NOD	Nucleotide-binding oligomerization domain
NP	Nucleoprotein
O.D.	Optical density
O.R.	Odds ratio
OVA	Ovalbumin
PAMP	Pathogen-associated molecular pattern
PBS	Phosphate-buffered saline
PCA	Principal component analysis
PFU	Plaque-forming units
pIgR	Polymeric immunoglobulin receptor
PRR	Pattern recognition receptor
Px	Peroxidase
qPCR	Quantitative polymerase chain reaction
r- (prefix e.g. in “rCSF3”)	Recombinant
r- (prefix e.g. in “rAMs”)	Resident
RA	Room air
RdRp	RNA-dependent RNA polymerase
RIG-I	Retinoic acid-inducible gene I
RLR	RIG-I-like receptor
RNA	Ribonucleic acid
RSV	Respiratory syncytial virus
SARS-CoV-2	Severe acute respiratory syndrome coronavirus 2
SC	Secretory component

scRNA-seq	Single cell RNA sequencing
sIgA	Secretory IgA
SpO ₂	Peripheral arterial blood oxygen saturation
TCR	T cell receptor
TD	T cell-dependent
Tfh	Follicular helper T cell
TGF	Tumour growth factor
Th (e.g. as in “Th1”)	Helper T cell
TI	T cell-independent
TLR	Toll-like receptor
TLT	Tertiary lymphoid tissue
TMA	Tissue microarray
TMB	Tetramethylbenzidine
TNF	Tumour necrosis factor
UMAP	Uniform manifold approximation and projection
UMI	Unique molecular identifier
URT	Upper respiratory tract
VALF	Vaginal lavage (supernatant)
VCAM	Vascular cell adhesion molecule
VE-cadherin	Vascular endothelial cadherin
vRNA	Viral RNA
vRNP	Viral ribonucleoprotein

DECLARATION OF ACADEMIC ACHIEVEMENT**Comprehensive Examination**May 2019: **Pass with Distinction****Graduate Courses**MS771 – Research Methodologies in the Health Sciences Fall 2015: **A+**MS716 – Advanced Immunobiology II Winter 2016: **A+**MS799 – Independent Study: Influenza Summer/Fall 2020: **A+****Research*****First Author***

McGrath JJC*, Vanderstocken G*, Dvorkin-Gheva A, et al. Cigarette smoke augments CSF3 expression in neutrophils to compromise alveolar-capillary barrier function during influenza infection. *Manuscript in review at the European Respiratory Journal*. *Denotes co-first authors.

Cass SP*, **McGrath JJC***, Son K, et al. Detecting immunoglobulins in processed sputa. *Allergy*. doi: 10.1111/all.15049. *Denotes co-first authors.

McGrath JJC, Thayaparan D, Cass SP, et al. (2021). Cigarette smoke exposure attenuates the induction of antigen-specific IgA in the murine upper respiratory tract. *Mucosal Immunology*. 14(5):1067-1076.

McGrath JJC, Stampfli MR. (2018). The immune system as a victim and aggressor in chronic obstructive pulmonary disease. *J Thorac Dis*. 10 (Suppl 17): S2011-S2017.

Co-Author

Cass SP, Mekhael O, Thayaparan D, **McGrath JJC** et al. (2021). Increased monocyte-derived CD11b+ macrophage subpopulations following cigarette smoke exposure are associated with impaired bleomycin-induced tissue remodeling. *Front Immunol*. Online ahead of print.

Cass SP, Dvorkin-Gheva A, Yan Y, **McGrath JJC** et al. (2021). Differential expression of sputum and serum autoantibodies in patients with chronic obstructive pulmonary disease. *Am J Physiol Lung Cell Mol Physiol*. 320(6): L1169-L1182.

Fantauzzi MF, Cass SP, **McGrath JJC** et al. (2021). Development and validation of a mouse model of contemporary cannabis smoke exposure. *ERJ Open Research*. doi: 10.1183/23120541.00107-2021

Schenck LP, **McGrath JJC**, Lamarche D et al. (2020). Nasal tissue extraction is essential for characterization of the murine upper respiratory tract microbiota. *mSphere*. (6):e00562-20.

Bagri P, Ghasemi R, **McGrath JJC**, et al. (2020). Estradiol enhances antiviral CD4+ tissue-resident memory T cell responses following mucosal Herpes Simplex Virus 2 vaccination through an IL-17-mediated pathway. *J Virol*. 95(1):e01206-20.

Cass SP, Yang Y, Xiao J, **McGrath JJC** et al. (2021). Current smoking status is associated with reduced sputum immunoglobulin M and G expression in COPD. *Eur Respir J*. 57(2):1902338.

Shen P, Whelan FJ, Schenck LP, **McGrath JJC** et al. (2017). *Streptococcus pneumoniae* colonization is required to alter the nasal microbiota in cigarette smoke-exposed mice. *Infect Immun*. 85(10):e00434-17.

+ co-author contributions to 3+ other manuscripts in preparation.

Declaration

This dissertation is a ‘sandwich’-style thesis encompassing three studies that I have pursued over the course of my doctoral degree. The first has been published, while the remaining two are in the process of submission/review. I was a principal contributor to most of the work presented herein; however, many colleagues contributed as well, most notably including Dr. Stampfli, as well as Steven Cass and Dr. Gilles Vanderstocken with whom I share co-first author position on Studies 2 and 3, respectively. I have described the relative contributions of myself and each co-author to each publication presented in this thesis at the beginning of each respective chapter (Chapters 2-4).

CHAPTER 1 – INTRODUCTION AND OBJECTIVES

1.1 – Cigarette Smoke and Human Health

1.1.1 – Epidemiology of Tobacco Smoking

Although the earliest estimated cultivation of tobacco dates back to around 6000 B.C.¹, the automation of cigarette rolling and subsequent mass marketing caused an enormous popularization of smoking in the late 19th and early 20th century². Canadian tobacco use prevalence (smokers per capita) peaked in the mid-1900s, with almost 50% of Canadians smoking cigarettes on a regular basis in 1965³. By this time, however, it was also becoming increasingly obvious that smoking was highly detrimental to human health and increased the risk of mortality from various diseases, prominently including lung cancer⁴. Through changes in public perception and anti-smoking efforts/legislature, smoking prevalences have continually declined since that time⁵. However, tobacco addiction still retains a substantial hold on the global population: as of 2019, 32.7% of males and 6.6% of females aged 15 or older continue to smoke, amounting to approximately 1.14 billion individuals worldwide⁵. This furthermore results in the exposure of an estimated one-third of the global population to the harmful effects of second-hand smoke⁶. Critically, although smoking prevalences are indeed shrinking in most countries, the number of daily smokers is actually rising due to population growth, having increased by approximately 150 million individuals between 1990 and 2019⁵. Similarly, the total number of cigarettes consumed per year increased from 4.96 to 6.25 trillion between 1980 and 2012⁷. As of today, tobacco smoke is the leading cause of

preventable death worldwide, being a primary contributor to more than 11.5% of all global deaths, or ~6-8 million individuals, each year^{5,8,9}. In addition, smoking accounts for over 200 million disability-adjusted life years⁵ and more than \$1.8 trillion CAD in health care and economic costs on an annual basis¹⁰. These findings clearly suggest that smoking-related disease and mortality are *growing* issues, not static or diminishing ones⁵. Although smoking cessation strategies are the clearest means with which to reduce this burden¹¹, the addictive and refractory nature of tobacco use starkly warrants research into medical strategies with which to prevent and ameliorate smoking-related disease as well.

1.1.2 – Broad Health Effects of Tobacco Smoking

Tobacco smoke exposure is associated with a wide variety of detrimental health effects. Within the respiratory tract, smoking can cause chronic bronchitis^{12,13}, chronic cough, and asthma¹⁴, as well incite the development of life-threatening conditions such as emphysema, chronic obstructive pulmonary disease (COPD)^{13,15}, pulmonary arterial hypertension (PAH)¹⁶ and idiopathic pulmonary fibrosis (IPF)¹⁷. In the cardiovascular system, smoke exposure can accelerate the development of atherosclerosis¹⁸ and heart failure¹⁹, promote aortic aneurysm development²⁰, and increase the risk of adverse events such as myocardial infarct and stroke²¹. Tobacco use is also well-known to be a primary cause of adenocarcinomas, squamous cell carcinomas and other cancers in the lung²², to an extent that the disease was rare prior to the mass popularization of smoking⁴. Less

well appreciated is that smoking is thought to also contribute to a variety of additional malignancies both within and distal to the respiratory tract, including oral, esophageal, laryngeal, pharyngeal, colorectal, liver, bladder, kidney, pancreas, and lymphatic cancers, to varying degrees²³⁻²⁵. In terms of developmental processes, maternal smoking is a risk factor for low birthweight, miscarriage, stillbirth, and sudden infant death syndrome (SIDS)²⁶⁻³⁰. In surviving children, smoke exposure *in utero* can result increase the risk of a range of psychiatric disorders in adolescence and early adulthood³¹. Finally, smoking is an important risk factor for the development of a wide variety of infectious diseases, both within and beyond the respiratory tract, as discussed below.

1.1.2.1 – Smoking, COPD, and Infectious Disease

Cigarette smoke exposure is well known to increase the risk of various infectious diseases^{32,33}. Smokers are at increased risk of developing clinical ‘colds’, defined by symptoms such as runny nose, sore throat, and myalgia following exposure to viral agents such as rhinovirus, respiratory syncytial virus (RSV) and seasonal coronaviruses³⁴. Alarmingly, smoke exposure also increases the risk of acquiring tuberculosis, as well as developing pneumonia from both bacterial agents, such as *Streptococcus pneumoniae*³⁵⁻⁴⁰, and some viruses. In terms of viral pneumonic agents, influenza is of particular concern: smoke exposure increases the risk of developing influenza-associated illness as determined by microbiological diagnosis (O.R. 5.7)⁴¹, as well as the risk of developing severe disease and the risk of

hospitalization (O.R. 1.5) /intensive-care unit (ICU; O.R. 2.2) admission following infection^{42,43}. Similarly, smoking appears to promote severe Coronavirus Disease (COVID)-19 and adverse outcomes (e.g. ICU admission, death) following severe acute respiratory syndrome coronavirus (SARS-CoV)-2 infection, potentially in a pack-year-dependent fashion (i.e. dependent on prolonged smoking)⁴⁴⁻⁴⁷. However, some studies conversely do not support an increased risk, based on the seemingly low proportion of hospitalized smokers relative to the respective general populations⁴⁸⁻⁵⁰. Further retrospective and experimental analysis will be necessary to clarify this relationship.

Tobacco smoke exposure is known to facilitate infectious disease at sites distal to the respiratory tract as well. Dissemination of bacterial pathogens such as *Streptococcus pneumoniae* and *Neisseria meningitidis* to the inner ear, bloodstream and brain is more prevalent in smokers, causing increased incidences of otitis media, sepsis, and meningitis^{35,39,40,51,52}. In the oral cavity, smoking promotes microbial dysbiosis⁵³ and inflammatory conditions such as periodontitis⁵⁴. Lower in the alimentary tract, smoking increases the risk of protracted intestinal infection by *Clostridium difficile*^{55,56}. Finally, smoking is well known to impair numerous aspects of wound healing throughout the body, thereby potently promoting surgical site infections following invasive procedures⁵⁷⁻⁵⁹.

Patients with COPD, a respiratory disease most frequently attributable to chronic smoking, are also predisposed to infectious disease in the form of pneumonia and acute exacerbations (AECOPD)^{15,60}. An AECOPD is defined as an

acute worsening of lung function beyond an individual's typical daily range to an extent that hospitalization and/or a change in medication is required⁶¹. Although these episodes are considered to be transient, in that symptoms can resolve to an extent with treatment, they are thought to accelerate lung function decline^{62,63} and can result in mortality⁶⁴. Although AECOPD can be infectious or (seemingly) non-infectious (e.g., eosinophilic, "pauci-inflammatory") in nature, the majority appear to be driven by pathogen exposure⁶⁰, with the bacterial species non-typeable *Haemophilus influenzae*, *S. pneumoniae* and *Moraxella catarrhalis* accounting for 40-60% of cases⁶⁵. Viral agents are also commonly implicated; rhinoviruses are detected in 20-25% of exacerbations, and influenza in 5-10%⁶⁵, with upper airway 'cold' symptoms often preceding pulmonary exacerbations⁶⁶. Notably, although influenza vaccination is an effective means with which to reduce influenza-related hospitalizations in COPD patients, deaths from influenza in COPD patients have risen by 19.6% between 2004-2018, seemingly due to decreases in vaccination rates during this period⁶⁷. Given that COPD afflicts over 250 million individuals worldwide and represents the sixth-leading cause of disability-adjusted life-years lost globally⁶⁸, this again suggests that the interaction between smoking-related disease and infection is an imposing and growing concern.

Overall, the relationship between smoking and infectious disease both within and beyond the respiratory tract is substantial. Investigating the mechanisms by which smoking can augment the risk and severity of these diverse infectious diseases is critical to understanding the cross-applicability of therapies developed

for treating and preventing these conditions in both smoking and non-smoking subpopulations. In particular, the stark and unambiguous relationship between cigarette smoke exposure and influenza, one of the most prevalent and burdensome pathogens in existence today, warrants further research in this space.

1.2 – Influenza

1.2.1 – Burden of Influenza-Associated Disease

Most influenza infections are restricted to the upper respiratory tract, and are either asymptomatic or feature only mild symptoms such as sore throat and runny nose^{69,70}. However, dissemination of the virus to the lower respiratory tract can result in more substantial pathologies, ranging from a cough and fever, to bronchitis, and even life-threatening conditions such as pneumonia and acute respiratory distress syndrome (ARDS)^{69,71}. In this manner, influenza virus causes seasonal epidemics that kill over 300 000 people each year⁷², as well as sporadic pandemics (e.g. the 1918 H1N1 ‘Spanish Flu’) which have the potential to elicit a significantly higher death toll⁷³. Notably, even transient (i.e. resolving) viral infection at this site may have long term consequences, in that it can serve to initiate persistent and progressive fibrogenic processes in the lungs in mouse models⁷⁴. Influenza can also affect organ systems beyond the respiratory tract. The virus has been implicated in inciting septic shock, promoting myocarditis and congestive heart failure, triggering cardiovascular events such as myocardial infarct and stroke,

and even instigating neurological diseases such as encephalomyelitis, aseptic meningitis and Guillain-Barré syndrome^{70,75}.

Importantly, certain subsets of the population are at higher risk of influenza virus infection and resultant pathologies, including: young and elderly people, pregnant women, immunocompromised individuals (post-transplant, undergoing chemotherapy), individuals with comorbid conditions (diabetes, various pulmonary and cardiovascular), as well as individuals that are obese, drink excessive amounts of alcohol, or smoke tobacco (as discussed above)^{41,73}. Ultimately, understanding the biology of influenza virus infection and disease pathogenesis is critical in order to develop interventions and strategies with which to prevent and/or treat influenza-associated disease.

1.2.2 – Virology and Infection

Influenza viruses are a group of enveloped, single-stranded, negative-sense RNA viruses belonging to the family *Orthomyxoviridae*⁷⁶. Influenza comprises four types, A, B, C, and D⁶⁹. Among these, types A, B, and C can infect humans: types A (IAV) and B (IBV) cause seasonal epidemics of lower respiratory tract disease, while type C is typically restricted to mild symptomatic illness in the upper airways. Global pandemics are caused by IAV strains alone⁶⁹, making this viral type the most studied.

Each IAV viral particle is comprised of a lipid envelope that surrounds a capsid of matricized viral M1 protein^{76,77}. Embedded in this envelope are two

additional viral glycoproteins, hemagglutinin (HA) and neuraminidase (NA), as well as M2 proton channels. Within the capsid the viral genome is organized into eight segmented viral ribonucleoprotein (vRNP) complexes. Each vRNP consists of single-stranded viral (v)RNA bound by numerous nucleoproteins (NP), as well as an RNA-dependent RNA polymerase (RdRp) complex consisting of PB1, PB2 and PA subunits. The eight genome segments encode the aforementioned RdRp subunits, HA, NA, M1/M2, as well as non-structural (NS) proteins such as NS1 which play important roles in immune evasion^{76,77}.

As with all viruses, influenza particles must infect host cells in order to replicate^{76,77}. To do so, regions of the terminal HA ‘head’ domain interact with sialic acid moieties expressed on the cell surface. This interaction triggers the encapsulation of the particle into a cellular endosome by means of macropinocytosis or clathrin-mediated endocytosis^{76,77}. Following acidification of the endosome by the cell, two processes occur. First, the M2 proton channel permits the acidification of the capsid interior, releasing the vRNPs from the M1 matrix into solution. Second, the change in pH causes HA trimers to undergo a conformational change, bringing the viral and endosome lipid membranes into close proximity and ultimately facilitating their fusion. This releases the viral contents into the cytosol^{76,77}. From here, vRNPs are imported into the nucleus by cellular importins, and each vRNA is both replicated, and transcribed/translated to produce viral proteins^{76,77}. Transcription of positive-sense viral mRNAs requires ‘cap-snatching’, or the excision of 5’ caps from host mRNAs, which is facilitated by the PA

endonuclease of the viral RdRp. Replication of the vRNAs requires the production of positive-sense complementary (c)RNA intermediates^{76,77}. Notably, because these cRNAs are produced only during active replication, they are useful in accurately detecting infected cells by single-cell RNA sequencing technologies. Following the resynthesis of negative-sense vRNAs, new viral particles form through aggregation of vRNPs and viral proteins at the cell membrane. After budding of the virus, NA cleaves sialic acid on the surface of the cell, as well as local mucins, permitting egress and dissemination of the viral particle^{76,77}.

1.2.3 – Subtypes of Concern

Among influenza proteins, HA and NA are highly variable. These glycoproteins are critical to viral fitness in that they facilitate viro-cellular entry and egress respectively (discussed above)^{76,77}. As a result, HA and NA are significant targets for adaptive immune responses aimed at neutralizing viral particles and limiting infection (discussed below)^{69,78}. In response to this immune pressure, influenza rapidly mutates HA and NA glycoproteins relative to other viral components, leading to a substantial diversification of strains over time. This process is known as antigen drift, and is an important contributor to viral immune evasion and the need to revaccinate on an annual basis^{69,73}. Existing influenza A strains can be broadly classified into two groups (1 and 2), each containing numerous viral subtypes based on HA variants (amounting to 18 total) and NA variants (11 total)^{69,73}. Among these subtypes, H1N1 and H3N2 are currently circulating and

causing seasonal epidemics among human populations^{69,73}. Although H3N2 viruses are thought to be associated with greater morbidity/mortality, H1N1 strains have been additionally responsible for two major pandemics in the last century: one in 1918, which is estimated to have killed over 50 million people worldwide, and one in 2009 which was comparatively less severe^{69,73}. Consequently, although it is necessary to understand the virology and immunology across all influenza A variants, much focus to date has been placed on understanding the pathogenesis of H1N1-mediated disease.

1.2.4 – Transmission

Influenza viruses can be spread via airborne or contact-mediated transmission. In terms of airborne spread, the virus can be dispersed by infected individuals largely through sneezing or coughing⁷³. In addition, individuals with high viral loads may shed enough virus by breathing alone to infect individuals in poorly ventilated areas. Viruses shed into the air are contained within large mucous droplets (5-100µm in diameter) or dispersed in fine aerosols (<5µm in diameter); large droplets are more easily filtered by the upper airways upon inhalation, whereas smaller particles may transit directly to the lungs⁷³. Contact-dependent transmission, in comparison, involves touching a contaminated surface (known as a fomite) and subsequent touching of a mucous membrane, typically the nose or mouth, whereafter infection is established⁷³. Importantly, most influenza infections are asymptomatic and resolve without long term consequences, suggesting that a potent

and effective immune response is normally able to engage and control this pathogen in the respiratory tract.

1.2.5 – Immunity and Disease Pathogenesis

If viral particles are able to bypass intrinsic defenses such as the mucous layer, influenza first infects respiratory epithelial cells^{79,80}. The infectious process is described in detail in section 1.2.2 above. Following initial infection of epithelial cells, viral pathogen associated molecular patterns (PAMPs) such as 5' triphosphate moieties on vRNA are detected through pattern-recognition receptors (PRRs) such as Toll-like receptor (TLR)3, TLR7, retinoic acid-inducible gene (RIG)-I, and melanoma differentiation-associated protein (MDA)-5, resulting in the activation of interferon response factors (IRF)-3/7 and nuclear factor (NF) κ B signaling pathways^{79,80}. In addition to stromal cells, hematopoietic cells such as resident macrophages and dendritic cells are also activated. This may occur through the detection of viral PAMPs derived from direct infection of those cells, danger-associated molecular patterns (DAMPs) released during necrotic cell death, or cytokines produced by infected or otherwise activated cells^{79,80}. IRF-3/7 signaling results in the production of type I (IFN- α and - β) and type III (IFN- λ) interferons, which act in an autocrine and paracrine manner to cause the expression of a variety of interferon stimulated genes (ISGs) among local cells. These ISGs, in turn, play various roles in controlling viral replication and infection, including inhibition of envelope-endosome fusion and viral entry, viral nuclear import, transcription of

viral genome, and viral budding, among other processes^{79,80}. IFN- λ is important in precluding dissemination of influenza from the upper to the lower airways⁸¹. Concurrently, activation of the NF κ B pathway results in the secretion of various pro-inflammatory cytokines, such as interleukin (IL)-6, colony-stimulating factor (CSF)3 (granulocyte (G)-CSF), C-C motif chemokine ligand (CCL)2, tumour necrosis factor (TNF)- α , and IL-1 family cytokines, among others⁷⁹⁻⁸². One important consequence of type I IFN and pro-inflammatory cytokine production is the recruitment of additional hematopoietic cells, including neutrophils, natural killer cells, monocyte-derived macrophages, and dendritic cells, into the lungs^{79,83}. In turn, these cells can amplify cytokine release and cellular recruitment, directly promote viral clearance, and initiate the activation of downstream adaptive immune responses. Aside from acting as a sentinel cell and orchestrating inflammatory processes, the primary functional role of macrophages is to phagocytose viral particles and debris generated from apoptotic/necrotic cell death^{79,80}. The complex and diverse role of neutrophils in both resolving and severe influenza are discussed in detail below (section 1.2.5.1).

Dendritic cells (DCs) are key orchestrators of adaptive immune processes that are initiated after infection⁸⁴. Following antigen acquisition and activation by detection of PAMPs/DAMPs/cytokines in the local microenvironment, dendritic cells migrate to draining lymphoid tissues and activate T and B cells responses⁸⁴. In terms of T cell immunity, DCs activate CD4⁺ and CD8⁺ T cells through presentation of peptides in the context of Major Histocompatibility Complex

(MHC) class II and class I, respectively⁸⁴. Through variations in microenvironmental cytokine exposure during this process, CD4⁺ T cells polarize into helper T cell subsets: follicular helper T(fh) cells assist in B cell activation and thereby antibody production⁸⁵, while T helper (Th)1 cells assist in cytotoxic CD8⁺ T cell activation⁸⁶. Following migration from draining lymph nodes to the respiratory submucosa, CD8⁺ T cells contribute by surveying local cells for influenza antigen presented in the context of MHC class I, and elicit apoptosis in infected cells through the release of perforin and granzyme, among other mechanisms⁸⁶. The contribution of antibodies to anti-influenza immunity⁷⁸ is discussed in detail in section 1.2.5.2 below.

Under normal circumstances, the aforementioned immune responses effectively clear the virus and themselves diminish in a self-limiting manner⁷⁹. In these cases, M2 polarized macrophages and CD8⁺/regulatory T cells produce anti-inflammatory cytokines such as IL-10 to quell the potent antiviral responses, and innate lymphoid cells (ILCs) contribute to the repair of damaged tissues via the production of IL-22 and amphiregulin⁷⁹. However, in some circumstances, such as is often observed in high-risk individuals (discussed above), initial immune responses to the virus are insufficient. Consequently, the virus continues to replicate, and aspects of the immune response auto-amplify. In particular, severe influenza-associated disease is characterized by the excessive recruitment of neutrophils and monocyte-derived macrophages to the airways, activation of coagulation cascades within the pulmonary vasculature, and destruction of

parenchymal tissue⁷⁹. One critical consequence of these ongoing inflammatory processes is a loss of alveolar-capillary barrier function, permitting fluid accumulation in the airways⁷⁹. As a result of this edema, gas exchange may be compromised, leading to pneumonia associated with blood oxygen desaturation and systemic shock. This pathological condition is a form of acute lung injury (ALI), which can result in ARDS^{79,80}.

1.2.5.1 – Specific Contribution of Neutrophils

Neutrophils have been associated with both protective and detrimental roles in the context of influenza. Complete depletion of neutrophils has been shown by multiple studies to exacerbate weight loss and mortality during influenza infection⁸⁷⁻⁸⁹, suggesting that these cells are important in viral clearance and/or tissue homeostasis. Neutrophils, along with macrophages, have been implicated in phagocytosis of surfactant D-opsonized viral particles and apoptotic debris⁹⁰. Protection may also be partly conferred by neutrophil-mediated T cell chemoattraction, given that acute neutrophil depletion was demonstrated to delay CD8⁺ effector T cell accumulation in the lungs⁹¹, although other studies have implicated neutrophils in constraining harmful T cell-mediated immunopathology⁹². In humans, neutropenia was found to be a significant risk factor for death among influenza-infected hematopoietic stem cell transplant recipients⁹³. In aggregate, these data clearly suggest that neutrophils can play an important role in the effective mitigation of influenza-associated illness.

Alternatively, other studies have demonstrated a detrimental impact for neutrophils in the context of severe disease. In mice, neutrophil-associated transcriptional signatures have been associated with lethal outcome in H1N1-infected mice, and partial reduction of neutrophilia was able to improve survival outcomes⁸⁹. In support of this finding, individuals with severe influenza infection had a significantly greater neutrophil gene signature compared to individuals with moderate infection⁹⁴. Similarly, patients that died of influenza had a greater neutrophil density in the blood and an increase in the expression of transcripts encoding CD177, a neutrophil activation marker involved in endothelial adhesion⁹⁴. Thus, despite contributing to the normal resolution of infection, neutrophils appear to play a role in promoting negative outcomes during severe influenza.

Mechanistically, neutrophils may propagate disease pathogenesis in a variety of ways. For instance, they may undergo NETosis, releasing neutrophil extracellular traps (NETs) - decondensed DNA comprised of citrullinated histones bound with neutrophil elastase (NE), α -defensin, myeloperoxidase (MPO), and other antimicrobial molecules⁹⁵. In a beneficial context, NETs have been shown to physically ensnare microbes to prevent their dissemination and provide direct protection against diverse viral pathogens⁹⁵. However, NETs have also been observed to be elevated in plasma samples from individuals with severe H1N1 and H7N9 infection, and correlate with negative disease outcome⁹⁶. Similar observations have been made in mice, with NETs appearing to augment ALI by causing endothelial damage⁹⁷. Mechanistically, histones in cell-free (cf)DNA in the

airways may act as a DAMP, compounding inflammatory processes following detection by PRR-expressing cells⁹⁵. In the systemic circulation, NETs appear to have pro-coagulant properties, potentially through the ability of histones to activate platelets and promote thrombosis⁹⁸. Deposition of NETs and thrombi within organs is thought to contribute to organ failure during sepsis⁹⁹. MPO, a component of NETs that is also released from azurophilic granules through degranulation, has been implicated in promoting edema by modulating claudin function at the alveolar-capillary barrier following H1N1 infection in mice¹⁰⁰.

Overall, there is clear evidence that neutrophils play a protective role during influenza infection⁸⁷⁻⁸⁹. At the same time, severe influenza is associated with exacerbated neutrophilic inflammation^{89,94}, and partial inhibition of the neutrophil recruitment cascade can ameliorate disease progression in experimental models⁸⁹. This suggests that a balanced neutrophil response is optimal; too many neutrophils is associated with negative outcome, while with too few cells viral replication proceeds uncontrolled and alternate immunopathological cascades ensue. Ultimately, these findings highlight neutrophils as a target in modulating influenza severity, but warn of the need for a refined approach in promoting a balanced neutrophilia as opposed to an unregulated augmentation or inhibition.

1.2.5.2 – Specific Contribution of Antibodies

Influenza exposure is capable of generating antibody responses that, collectively, play a critical role in protecting the upper and lower respiratory tract upon

secondary exposure; systemic IgG and mucosal IgA responses are known to be of particular importance^{78,101-105}. Typically, IgG antibodies afford protection by facilitating a range of effector functions. One of the most important is neutralization, wherein antibodies inhibit processes related to viral entry or egress. Neutralization is classically thought of as the inhibition of viro-cellular contact, in precluding contact between the HA receptor-binding site and sialic acid on host cells⁷⁸. This is the method by which antibodies raised by seasonal influenza vaccines are typically thought to function⁷⁸. Depending on the epitope specificity, however, neutralization may also occur through the inhibition of HA conformational changes necessary for membrane fusion¹⁰⁶, blockade of NA enzymatic function to prevent viral budding¹⁰⁷, or other processes. In addition, IgG has several other functions which are Fc receptor (FcR)-dependent. These include complement activation, opsonization (antibody-dependent cellular phagocytosis; ADCP) and antibody-dependent cellular cytotoxicity (ADCC)^{78,108}. This latter process involves the identification of infected cells for apoptotic cell death by natural killer (NK) cells. Systemic influenza-specific antibodies such as IgG have been described to play an important role in protecting the lungs from viral infection, and are therefore a critical correlate of protection against the development of clinical influenza^{78,103,104}. In humans, IgG1 and IgG3 are dominant contributors to antiviral immunity, while IgG2 and IgG4 are negligible in this regard⁷⁸. In contrast, the role of systemic antibodies such as IgG in protecting the upper airways from influenza infection is limited^{101,103,104}, and thus it is likely that even IgG-bearing

individuals may become reinfected at this site, as has been observed in recent cases assessing infection in SARS-CoV-2 mRNA vaccinees¹⁰⁹. This is a significant potential drawback for existing peripheral vaccines, in that they may induce protective, but not sterilizing, immunity¹¹⁰. In comparison to IgG, influenza-specific mucosal IgA responses are thought to be the dominant isotype involved in protecting the upper respiratory tract^{101,103,104}. Activation of an IgA response at this site therefore holds the potential to prevent/limit asymptomatic carriage of the virus and promote sterilizing immunity. The specific contribution of IgA is discussed in more detail in section 1.3 below. Overall, IgA and IgG antibodies play diverse and important roles in the defense against influenza virus in the respiratory tract.

1.3 – Immunoglobulin A (IgA)

1.3.1 – Structure, Isotype and Valency

Immunoglobulin A (IgA) is the classical, mucosa-associated antibody isotype. In humans, two subtypes exist, IgA1 and IgA2, while in mice a single variant exists that is more similar to IgA2¹¹¹. The major structural difference between human subtypes is that IgA1 has longer hinge regions bridging the antigen-binding (Fab) and constant (Fc) fragment domains; this facilitates an increased conformational flexibility¹¹¹, but also decreases stability and confers a susceptibility to degradation by bacterial proteases¹¹². The majority of IgA in human serum is IgA1 (~90%), with the remainder being IgA2¹¹¹. At mucosal surfaces, the relative representation varies – for instance, in the nasal lumen IgA1 again dominates by a similar magnitude,

while IgA2 is more prevalent in intestinal secretions¹¹¹. In terms of valency, most IgA present in the human sera is monomeric, while IgA produced at mucosal surfaces is mostly dimeric¹¹¹. For mice, serum IgA is largely dimeric as well¹¹³. Interestingly, it has been reported that some higher-order (e.g. trimeric, tetrameric, pentameric) IgA are produced at mucosal surfaces, although at a lower frequency^{102,111,114,115}. These high-order IgA polymers were shown to be induced in the nasal mucosa following intranasal influenza vaccination in humans, and have a greater neutralizing potential against influenza than IgA dimers¹⁰². Similarly, recent work has demonstrated dimeric IgA to be more effective at neutralizing SARS-CoV-2 than monomeric IgA¹¹⁶. Regardless of valency, the polymerization of IgA is mediated by interactions between the Fc domains of individual IgA monomers with a ‘J chain’ subunit within the secreting cell^{111,117}.

1.3.2 – Effector Functions

The primary effector function attributed to secretory IgA at mucosal surfaces is neutralization¹¹⁸. IgA specific for critical pathogen-associated ligands can effectively preclude infection or colonization of mucosal surfaces. For example, IgA specific for influenza HA is known to be induced in the nasal mucosa by influenza, and can prevent infection of epithelial cells in the airways^{101–103} as well as the local dissemination of newly shed viral particles¹¹⁹. Such secretory (s)IgA responses can provide protection against influenza-associated illness^{105,120,121}. In the case of bacterial pathogens, IgA binding can lead to agglutination through

stochastic means (random co-binding of multiple bacteria) or through enchainment growth (enchainment of clonal lineages of dividing bacteria by bound IgA, independent of stochastic agglutination)¹²². Alternatively, sIgA may bind and entangle bacterial flagella to impair motility¹²². Ultimately, in contrast to IgG, sIgA effector functions are largely prophylactic in that they protect the host by precluding host-pathogen interactions, a process known as ‘immune exclusion’^{123,124}, generally without eliciting overt inflammatory responses. In comparison, monomeric IgA in the serum has a wider array of effector capabilities. In humans, IgA can interact with the Fc α RI (CD89)¹¹¹ on neutrophils, monocytes and monocyte-lineage cells (macrophages, DCs), among other cell types to facilitate opsonophagocytosis, ADCC¹¹¹, and netosis¹²⁵. No homologous receptor has been described in mice to date, however. Notably, both monomeric and polymeric IgA demonstrate binding to Fc α RI¹²⁶, suggesting that the propensity of sIgA to neutralize without eliciting inflammation is not due to steric hinderance caused by J chain-associated polymerization. Rather, the ‘anti-inflammatory’ capacity may occur as a result of the anatomical context – in areas where cells expressing the Fc α RI are sparse, FcR-mediated effector functions will be limited. Finally, of importance is the fact that IgA backbones appear to confer advantage in terms of neutralizing heterotypic influenza viruses over IgG backbones^{101,127}.

Ultimately, although IgG antibodies have been more studied in the influenza field due to their protective efficacy in the lungs and induction following systemic vaccination, it is becoming increasingly clear that mucosal IgA responses represent

an additional immunological arm with which to enhance vaccination strategies^{110,116,128}. Currently, IgG-oriented intramuscular influenza vaccination strategies are not considered to be sterilizing, in that they can protect against influenza-associated illness but not necessarily upper respiratory tract infection. This may allow even protected individuals to be viral carriers, as has been observed in the case of COVID-19 vaccines^{109,110}. Inducing IgA in the upper airways via vaccination has the potential to promote sterilizing, in addition to protective, immunity and thus reduce viral transmission within human populations¹¹⁰.

1.3.3 – Induction of IgA Responses in the Upper Airways

IgA induction in the upper airways is a complex process involving several phases^{129,130}. First, IgA-producing antibody secreting cells (ASCs) must be activated either locally or in distal nasal-draining lymphoid tissues. These cells must then home to the nasal submucosa and secrete the antibody. Finally, IgA molecules must be transcytosed from the basolateral to the apical surface of epithelial cells. Each of these processes is critical to producing a pool of sIgA in the nasal lumen that can neutralize inhaled pathogens^{129,130}.

1.3.3.1 – T cell-Dependent Antibody-Secreting Cell (ASC) Activation

IgA responses can be generated in both T cell-dependent (TD) and - independent (TI) manners following antigen acquisition at mucosal surfaces¹³¹.

However, TD processes are thought to be responsible for the generation of high-affinity antibodies¹³². This occurs through the induction of germinal centre reactions, during which B cells undergo affinity maturation by introducing point mutations into the B cell receptor (BCR) variable region in an attempt to increase the antigen-binding affinity¹³². Notably, the resultant affinity-matured antibodies are thought to have an increased ability to neutralize pathogens such as IAV^{133–135}, as well as facilitate bactericidal defense against *Streptococcus pneumoniae*¹³⁶ and *Haemophilus influenzae*^{137,138}. Therefore, TD B cell responses represent an important aspect of humoral immunity against mucosal pathogens.

In the upper airways, TD antibody responses typically occur within local lymphoid tissues, such as the tonsils/adenoids in humans, the nasal-associated lymphoid tissue (NALT) in mice, as well as the cervical lymph nodes (CLNs) and spleen that drain the nasal mucosa in both species^{130,139,140}. Notably, the ability to induce influenza-specific IgA levels remains unchanged following NALT removal in mice, suggesting that additional lymphoid tissues or TI processes redundantly contribute to local immunity as well¹⁴¹. The initiation of TD immunity requires dendritic cell-mediated activation of follicular helper Tfh cells, which in turn provide activating signals to naïve B cells displaying cognate major histocompatibility complex (MHC)-II-peptide complexes¹³². To initiate this process, dendritic cells must acquire antigen. This may occur via transfer of antigen from the nasal lumen directly into the NALT or nasal mucosa via microfold cells, where it is acquired by submucosal dendritic cells¹³⁰. In order for downstream Tfh

activation to occur, dendritic cells must become activated during the course of antigen acquisition. This may occur through the sensing of inflammatory stimuli, including pathogen-/danger-associated molecular patterns (PAMPs/DAMPs) and/or inflammatory cytokines. Dendritic cell maturation entails the upregulation of MHC-II (to enhance antigen presentation) as well as the co-stimulatory molecules CD80 and CD86^{142,143}. Concurrently, dendritic cells upregulate specific chemokine receptors. C-C motif receptor (CCR)7, for instance, facilitates mucosal dendritic cell migration to the T cell zone within draining lymph nodes¹⁴⁴, such as the CLNs¹⁴⁵. Subsequently, it is thought that migratory dendritic cells upregulate C-X-C motif receptor (CXCR)5 to migrate into the lymph node interfollicular zone, where they facilitate Tfh activation¹⁴⁶⁻¹⁴⁸.

Dendritic cell-mediated polarization of naïve T cells into Tfh cells requires several molecular interactions, including: peptide-loaded MHC-II on dendritic cells with a cognate T cell receptor (TCR); DC-expressed CD80/86 with T cell-expressed CD28¹³¹; dendritic cell-expressed inducible T cell co-stimulator ligand (ICOSL) with T cell-expressed ICOS receptor¹⁴⁹. In this process, these T cells must also be polarized in a manner that stimulates them to produce tumour growth factor (TGF)- β 1, a molecule important to downstream IgA class-switch recombination¹⁵⁰. Upon receiving these signals, Tfh cells upregulate the transcription factor B cell lymphoma (BCL)6, and form stable interactions with naïve IgM⁺ IgD⁺ B cells expressing cognate peptide-MHC-II complexes¹⁴⁸. In addition to this interaction, T cells ligate CD40 on the surface of B cells with CD40L, and secrete IL-21 and TGF-

β 1 to activate these cognate B cells and facilitate IgA class-switch recombination¹⁵⁰. Following this initial activation process, B cells may either develop directly into ASCs (plasmablasts) or migrate into the B cell follicle to enter a germinal centre reaction^{132,148,151}. This process involves the somatic hypermutation of complementarity-determining regions (CDRs) within heavy- and light-chain variable regions in an attempt to increase the binding affinity of individual antibody clones for their cognate antigen (affinity maturation)¹³². Upon exiting the follicle, these germinal centre B cells may develop either into ASCs or memory cells prepared for reactivation upon secondary exposure¹³².

1.3.3.2 – Antibody-Secreting Cell (ASC) Homing

Following activation, ASCs induced in lymphoid tissues home back to the nasal mucosa¹²⁹. Following egress of these cells into the bloodstream, this process is regulated by two molecular axes. In order for cells to home to the correct mucosal surface they must follow a specific chemokine gradient. In the case of the nasal mucosa, IgA ASCs detect CCL28 produced by nasal epithelial cells via CCR10 receptor on their cell surface^{129,152–154}. In contrast, gut-homing ASCs detect a gradient of CCL25 via CCR9 expression. Once in the vasculature, these cells must undergo extravasation, a process regulated by tissue-specific expression of adherins and cell-specific expression of integrins. For the nose, α 4 β 1 integrin on ASCs interacts with vascular cell adhesion molecule (VCAM)-1 on local endothelial cells, whereas gut-homing ASCs utilize an α 4 β 7-mucosal addressin cell adhesion

molecule (MAdCAM-1) interaction¹²⁹. Importantly, cell-adhesion molecules such as VCAM-1 are upregulated by endothelial cells and other stromal cells during local inflammatory processes in order to facilitate extravasation^{155,156}.

1.3.3.3 – Transepithelial Transcytosis

Finally, once IgA ASCs have extravasated into the nasal submucosa, the antibody they secrete must be transported across the epithelial barrier into the lumen. This is a non-redundant process mediated by the polyimmunoglobulin receptor (pIgR), which is expressed on the basolateral surface of these cells¹⁵⁷. For this to occur, the IgA J chain interacts with the pIgR, and the complex is transcytosed to the apical surface¹⁵⁸. Here, endogenous proteases in the lumen cleave the pIgR, releasing the secretory IgA bound with a pIgR-derived fragment known as the secretory component (SC)¹¹¹. From here, the IgA is free to mediate its effector functions in neutralizing inhaled pathogens.

1.3.4 – IgA-Oriented Influenza Vaccination

Notably, vaccine development has attempted to capitalize on antibody induction processes in the upper respiratory tract. Although systemic immunization consistently induces antibody responses in the circulation, responses at mucosal sites, although sometimes observed, are inconsistent and often weak¹⁵⁹. In the case of systemic vaccines against viral pathogens, such scenarios are considered to be

insufficient to protect the upper airways¹¹⁰. Consequently, these vaccines are not thought to provide sterilizing immunity, but instead focus primarily on interrupting the link between the initial infection and the establishment of infectious disease. In contrast, intranasal vaccination represents a promising approach with which to induce mucosal IgA that can neutralize pathogens in the upper respiratory tract and prevent the initial stages of infection^{105,120,121,140,160}. In this regard, an intranasally-delivered live-attenuated influenza vaccine (LAIV) is currently produced and available for public use in Canada on an annual basis¹⁶¹. This vaccine specifically targets the upper respiratory tract through the genetic attenuation of viral particles such that they can replicate only at temperatures observed in the upper respiratory tract, but not the lungs¹⁶². In addition, other efforts to develop intranasal, IgA-producing vaccines against influenza virus, *S. pneumoniae*^{105,128,163–165} and SARS-CoV-2 (e.g. NCT04751682, NCT04798001, NCT04816019; ^{166,167}) are underway. Thus, although the majority of vaccines for respiratory pathogens are currently systemic in nature, the development of efficacious IgA-producing intranasal vaccine formulations has clearly been made a priority by the immunological community^{128,163}. Ultimately, such mucosal vaccination may prevent upper respiratory tract infection through neutralization, thus precluding viral carriage and promoting sterilizing immunity.

1.3.5 – Measurement of Antibodies in Mucoïd Human Samples

In order to assess the induction of antibody responses following intranasal vaccination, sampling and analysis of mucosal samples is critical. Relevant samples may include nasal lavage (NAL), saliva, sputum (matter expectorated from the lungs), bronchoalveolar lavage (BAL), and perhaps cervicovaginal lavage (CVL) if the intranasal vaccine targets a urogenital pathogen. Notably, the mucous content of these samples varies; those generated with little or no fluid instillation, such as saliva and sputum, will have a greater proportion of mucous than those that do, such as NAL, BAL, and CVL. However, even BAL can contain considerable mucous when patients have chronic respiratory conditions such as cystic fibrosis (CF)¹⁶⁸. Mucous can retain cells and soluble mediators such as eosinophil cationic protein (ECP) and DNA^{169,170} which may theoretically interfere with the detection of often-sparse antigen-specific antibody clones. To date, it is unclear whether clinical protocols used for mucolysis of mucosal respiratory samples such as sputum affect antibody recovery. Dithiothreitol (DTT), a mucolytic agent frequently used for this purpose¹⁷⁰, does so through its ability to reduce disulfide bonds, chemical linkages that are also notably present in antibodies^{171,172}. Thus, studies assessing the relative impact of DTT-based mucolysis on total and antigen-specific antibody detection in human mucoïd samples are warranted in order to optimize future studies of intranasal immunization and smoking-related disease.

1.4 – Cigarette Smoke and Antimicrobial Host Defense

1.4.1 – Mechanisms of Cigarette Smoke-Augmented Influenza

Numerous studies have investigated the ways in which cigarette smoke exposure can augment influenza infection. For instance, smoke-exposed, infected mice demonstrate increased weight loss¹⁷³, apoptosis¹⁷⁴, tissue fibrosis⁷⁴, and mortality¹⁷⁵ compared to room air controls. Mechanistically, early work from our group found that cigarette smoke exacerbated neutrophilic and mononuclear airway infiltrates following high dose (2.5×10^5 plaque-forming units (PFUs); A/FM/1/47) H1N1 infection¹⁷⁶. Although myeloperoxidase activity was unchanged in lung homogenates of smoke-exposed, infected mice relative to infected controls, neutrophils were also observed to be elevated in the bloodstream throughout infection. In contrast, smoke exposure attenuated the accumulation of activated CD69⁺ CD4⁺ T cells in the lungs. At 3 days post-infection (dpi), around the time of peak viral replication, no difference in replication-competent viral load was observed between room air and smoke-exposed controls, while at 7dpi smoke-exposed animals exhibited slight reductions in this regard. These findings were observed in association with higher interferon activity, as determined by plaque-reduction assays¹⁷⁶. Notably, infection with a mouse-adapted variant (A/FM/1/47-MA) phenocopied high-dose infection with the parent strain in most aspects¹⁷⁷. In particular, exacerbated pulmonary neutrophilia is consistently observed in studies using similar model systems^{173,178,179}. Given the known association between neutrophils and negative outcomes in influenza infection^{89,94}, it seems likely that

excess neutrophilia may play a role in the exacerbated morbidity observed following cigarette smoke exposure.

Although smoke exposure appears to enhance interferon responses and reduce/minimally change viral burden during the course of pulmonary *in vivo* infection, smoke components may have distinct effects within different cellular compartments. In lung epithelial and fibroblast cultures, smoke-conditioned media was observed to impair polyI:C-induced antiviral signaling, including interferon secretion and ISG upregulation, in association with excessive viral replication¹⁸⁰. Similar observations of elevated viral burden have been made in cultured airway epithelial cells infected with influenza¹⁸¹ and human rhinovirus¹⁸². In addition, smokers demonstrated higher viral RNA in nasal lavage fluid cells (the majority of which are epithelial¹⁸³) and longer shedding duration than non-smokers following intranasal vaccination with LAIV¹⁸⁴. In aggregate, these data suggest smoke exposure consistently inhibits antiviral defense to promote excess viral replication in airway structural cells. When considered in tandem with *in vivo* work, these findings also implicate non-structural, haematopoietic cells in overproducing type I interferon following viral stimulation in the context of smoke. However, this dichotomy has not been conclusively demonstrated and requires further research.

Mechanistically, specific cytokines have been implicated in exacerbating neutrophil recruitment and morbidity in cigarette smoke-exposed, influenza-infected mice, including IL-17¹⁷⁹ and IL-33¹⁷³. Interruption of IL-1 α signaling has also been shown to reduce excess neutrophilia in this context¹⁷⁸, while antagonism

of C-X-C motif chemokine receptor (CXCR)1/2, receptors for the classical neutrophilic chemokines C-X-C motif chemokine ligands (CXCL)1/2, has been shown to ameliorate morbidity due to influenza alone¹⁸⁵. However, despite having identified these targets, there is still a critical paucity of host-directed therapies for use in the later stages of influenza infection. Understanding the molecular mechanisms which contribute to negative outcomes in influenza is critical to supporting the development of these host-acting treatments. Notably, models which utilize concurrent influenza infection and cigarette smoke exposure may be useful in identifying molecular targets which are applicable to both smoking and non-smoking patient subpopulations.

1.4.2 – Effect of Cigarette Smoke on Antibody Responses

The effect of smoking on antibody responses varies depending on the specific immunizing agent and site of exposure. For instance, responses to peripheral vaccination are variable. Several studies have indicated that smoking has no effect on peripheral influenza vaccine protective efficacy^{186–189}. However, one investigation found that, among individuals with low pre-vaccination haemagglutination inhibition (HAI) titres, although initial titres were similar smokers demonstrated a reduced longevity of serum HAI at 50 weeks post-subunit vaccination compared to non-smokers¹⁸⁶. This suggests that smoke exposure may compromise the activation of long-lived plasma cells, which are thought to be responsible for maintaining serum antibody levels. Another study demonstrated that

although total human papillomavirus (HPV)-specific antibodies induction was comparable between smoking and non-smoking women following vaccination, smokers developed low-avidity antibodies more frequently than non-smokers¹⁹⁰. In contrast, smokers did not seroconvert as frequently as non-smokers following hepatitis B vaccination¹⁹¹. Overall, results are variable but suggest that systemic vaccine efficacy should be assessed in smokers on a case-by-case basis.

Numerous studies have assessed the impact of smoke exposure on antibody responses in the lower respiratory tract. For instance, previous work from our laboratory has demonstrated that cigarette smoke is capable of impairing IgG1 and IgG2a responses, but not IgA, in the serum following the intranasal delivery of replication-deficient adenovirus to mice¹⁹². Other groups have found that influenza-specific IgA and IgG induction are compromised following pulmonary infection in cigarette smoke-exposed mice^{179,193}, although our work using a similar influenza model indicated no difference in this regard¹⁷⁶. In terms of baseline immunoglobulins, our group recently demonstrated that smoking does not impact total IgG, IgM or IgA levels in sputum among individuals with normal lung function¹⁹⁴. Overall, data currently indicates that smoke exposure may have the potential to reduce antibody induction in the lower respiratory tract, although reports are conflicting in this regard.

In comparison to the lungs, little research has been conducted regarding the effect of cigarette smoke on mucosal immune responses in the upper airways. This is of importance, given that antibody isotypes show differential utility in protecting

against influenza between these two sites^{103,104}. In terms of total IgA, several groups have reported decreased salivary IgA levels in smokers¹⁹⁵⁻¹⁹⁸, while other groups have indicated that smoking increases salivary IgA^{199,200}. Another study found no difference in nasal wash IgA levels between COPD patients and healthy controls²⁰¹. However, total IgA levels are not directly indicative of the ability to induce an IgA response, which requires analysis of antibodies of determined specificity pre- and post-induction. In 1982 one study reported that smoking individuals exhibited lower levels of IgA specific for the lipopolysaccharide (LPS) of *Pantoea agglomerans* and *Pseudomonas syringae* in nasal secretions compared to non-smokers²⁰², suggesting that antigen-specific IgA induction may be impaired. In terms of induction, another study (as mentioned above) determined that there were no differences between smokers and non-smokers in terms of seroconversion or serum hemagglutination-inhibiting titres following intranasal LAIV immunization¹⁸⁶. However, this study did not assess antigen-specific immunoglobulin responses of any kind in the upper airways. Consequently, prior to the initiation of this thesis no study to our knowledge had addressed the effect of smoke exposure on the induction of antigen-specific IgA responses in the upper respiratory tract. This represented a significant knowledge gap; understanding whether cigarette smoke compromises IgA responses may inform the efficacious design and implementation of intranasal vaccination strategies in our highly smoke-exposed population.

1.5 – Central Paradigm, Hypotheses & Aims

Although smoking-related disease is abstractly preventable through cessation, tobacco use is highly addictive and refractory in nature. As a consequence of this, and its numerous detrimental health effects, smoking takes an enormous toll on health care systems around the globe and is the leading cause of preventable death worldwide^{8,10}. In addition to further smoking cessation measures, this fact warrants investigation into the mechanisms by which smoke exposure affects human health so as to gain a better understanding of potential unique medical requirements in this subpopulation. The relationship between cigarette smoke and host antimicrobial immunity in particular has been a focus of our laboratory over the past two decades given the well known predisposition of smokers to a variety of infectious diseases, including influenza.

This thesis builds upon the laboratory's previous work by investigating the impact of cigarette smoke on select aspects of antimicrobial host defense. Summarized here is our work in assessing the impact of cigarette smoke exposure on IgA responses in the upper respiratory tract, as well as mechanisms underpinning smoke-augmented influenza. In addition, we conducted a methodological study to optimize antibody detection in mucoid human respiratory samples as a precursor to future investigations of intranasal vaccine efficacy, and other studies in smoke-exposed individuals. Below are listed the specific hypotheses and objectives for each study.

Study 1 (Chapter 2) – Investigating the impact of cigarette smoke on IgA responses in the murine upper respiratory tract.

To date, it is unclear whether cigarette smoke affects the induction of antigen-specific IgA responses in the upper airways. This information has important implications for the effective design, testing and implementation of intranasal vaccines that are intended for use in smoke-exposed individuals. Given previous reports of attenuated reduced salivary IgA¹⁹⁵⁻¹⁹⁸ and LPS-specific nasal IgA²⁰² in smokers, *we hypothesized that cigarette smoke that cigarette smoke exposure would attenuate the induction of antigen-specific IgA following intranasal immunization. In addition, we anticipated that this IgA would be of reduced antigen-binding avidity.*

Objective 1: Investigate the impact of smoke exposure on antigen-specific antibody induction in the upper airways of mice following intranasal immunization.

Objective 2: Investigate the antigen-binding avidity of nasal secretory IgA produced in the context of cigarette smoke relative to room air.

Objective 3: Investigate mechanisms underpinning any observed deficits.

Study 2 (Chapter 3) – Comparing clinical processing methods for the optimal analysis of immunoglobulins in human sputum.

Currently, two methods are used clinically to process human sputum for the assessment of immune cells and mediators in respiratory disease. These feature the use of either PBS or the mucolytic agent DTT. However, the relative detection and stability of antibodies has not been systematically compared between these methods. Such an analysis is a critical step in optimizing methods with which to assess IgA (and other antibody) responses in future studies of smoking-related disease in both the upper and lower airways. Because of the known ability of mucous to retain IgA molecules, but also to denature antibodies, *we hypothesized that DTT-based sputum processing would increase the yield of sputum IgA, while decreasing the yield of IgM/IgG/IgE.*

Objective 1: Investigate the impact of PBS- and DTT-based processing on antibody (IgG, IgA, IgM, IgE) recovery from human sputum samples.

Objective 2: Compare the stability of each antibody isotype in PBS- and DTT-processed sputum over several freeze-thaw cycles.

Study 3 (Chapter 4) – Investigating immune mechanisms underpinning cigarette smoke-augmented influenza in mice.

Cigarette smoke is well known to increase the risk of acquiring influenza, progressing to severe disease and being admitted to hospital/ICU following infection^{41,42}. However, the mechanisms underpinning this relationship have not been fully elucidated. Understanding the immunopathology of smoke-augmented influenza may unveil novel therapeutic strategies for use in smoke-exposed individuals and provide insight into pathogenic principles governing influenza viral pneumonia. With this in mind, *we hypothesized that cigarette smoke would exacerbate pulmonary neutrophilia, edema and hypoxemia through exacerbated CSF3-CSF3R signaling. In addition, we anticipated that cigarette smoke would alter the distribution of Csf3-expressing cells in the context of influenza.*

Objective 1: Investigate the impact of smoke exposure on morbidity, mortality, immunopathology and viral burden following influenza infection in mice.

Objective 2: Investigate to what extent cigarette smoke dysregulates cellular (e.g. neutrophils) and molecular mediators (e.g. cytokines) of disease during influenza, and the functional role of identified cytokines of interest.

Objective 3: Assess the distribution of infected and cytokine-expressing cells in the context of smoke exposure and influenza using single cell RNA sequencing.

CHAPTER 2 – Cigarette smoke exposure attenuates the induction of antigen-specific IgA in the murine upper respiratory tract

Joshua J.C. McGrath, Danya Thayaparan, Steven P. Cass, Jonathan P. Mapletoft, Peter Y.F. Zeng, Joshua F.E. Koenig, Matthew F. Fantauzzi, Puja Bagri, Bruce Ly, Rachel Heo, L. Patrick Schenck, Pamela Shen, Matthew S. Miller, Martin R. Stämpfli

Manuscript Status: Published; *Mucosal Immunology*, Springer Nature.

Copyright © 2021 The Authors. Reprinted with permission (see Appendix 1).

Citation: McGrath JJC, Thayaparan D, Cass SP, et al. (2021). Cigarette smoke exposure attenuates the induction of antigen-specific IgA in the murine upper respiratory tract. *Mucosal Immunol.* 14(5):1067-1076.

Contributions: JJCM, PS and MRS conceived the study. JJCM and MRS designed the experiments. JJCM, DT, SPC, JPM, MF, PB, BL, RH and JFEK conducted experiments. PYFZ conducted bioinformatic analysis of raw sequencing data, and JJCM performed all other analysis including compilation of sequencing data. JJCM, DT, SPC, MSM and MRS were involved in data interpretation. JJCM and MRS wrote the manuscript with feedback from all authors. MSM and MRS secured funding for the study.

Abstract

The upper respiratory tract is highly exposed to airborne pathogens and serves as an important inductive site for protective antibody responses, including mucosal IgA and systemic IgG. However, it is currently unknown to what extent inhaled environmental toxins, such as a cigarette smoke, affect the ability to induce antibody-mediated immunity at this site. Using a murine model of intranasal lipopolysaccharide and ovalbumin (LPS/OVA) immunization, we show that cigarette smoke exposure compromises the induction of antigen-specific IgA in the upper airways and systemic circulation. Deficits in OVA-IgA were observed in conjunction with a reduced accumulation of OVA-specific IgA antibody-secreting cells (ASCs) in the nasal mucosa, inductive tissues (NALT, cervical lymph nodes, spleen) and the blood. Nasal OVA-IgA from smoke-exposed mice also demonstrated reduced avidity during the acute post-immunization period in association with an enhanced mutational burden in the cognate nasal *Igha* repertoire. Mechanistically, smoke exposure attenuated the ability of the nasal mucosa to upregulate VCAM-1 and pIgR, suggesting that cigarette smoke may inhibit both nasal ASC homing and IgA transepithelial transport. Overall, these findings demonstrate the immunosuppressive nature of tobacco smoke and illustrate the diversity of mechanisms through which this noxious stimulus can interfere with IgA-mediated immunity in the upper airways.

Introduction

The upper respiratory tract (URT), including the nasal, oral, and pharyngeal mucosae, serves as an important node of control for inhaled pathogens. Immune responses in the URT are critical to combat infectious agents and prevent them from spreading to fragile sites such as the lungs, an organ in which pathogen exposure may compromise gas exchange and cause life-threatening tissue pathologies.

Immunity in the upper airways is multifactorial, encompassing both innate and adaptive components. Among the adaptive components, secretory sIgA antibody responses induced within the upper airway lumen provide protection upon exposure to respiratory pathogens, such as influenza virus^{1,2}. sIgA antibodies mediate their protective effects at mucosal surfaces by exclusion and neutralization of inhaled pathogens, thereby precluding the colonization or infection of local epithelial cells without eliciting overt inflammatory responses³. In addition, recent evidence suggests that sIgA may also prevent the local dissemination of viral particles⁴. Through these mechanisms, sIgA-mediated defense in the URT provides an initial barrier to infection, complementing IgG- and cytotoxic T cell-mediated defenses that protect the lungs against harmful infectious agents.

Cigarette smoke is a noxious inhaled stimulus that is known to compromise or alter the function of the immune system, both in the respiratory tract and at distal sites⁵. While it is well documented that smokers are at increased risk of various infectious diseases⁶, including influenza⁷, the mechanisms by which smoke exposure causes this predisposition have not been fully elucidated. With regards to

sIgA responses in the URT, the reported effects of cigarette smoke exposure are controversial. For instance, Rylander *et al* reported that smokers exhibited lower levels of IgA specific for the lipopolysaccharides (LPS) of the Gram-negative bacteria *Pantoea agglomerans* and *Pseudomonas syringae* in nasal secretions compared to non-smokers within cohorts of wood- and cotton-mill workers⁸. Similarly, a number of groups have reported decreased baseline sIgA levels in the saliva of cigarette smokers⁹⁻¹², while still others have indicated that smoking increases salivary IgA^{13,14}. In mouse models, cigarette smoke has been reported to inhibit IgA induction in the lungs following influenza virus infection¹⁵; however, IgA is thought to play a minimal role in directly protecting the lower respiratory tract from disease pathogenesis in this context¹. Overall, to what extent cigarette smoke modulates the induction of novel sIgA responses in the upper airways, where this isotype is a potent contributor to host defense, remains unclear. This is an important knowledge gap, given that infectious diseases represent a significant source of excess mortality in the 1.1 billion individuals worldwide that continue to smoke tobacco^{16,17}.

To address this question, we studied the effect of cigarette smoke exposure on the induction of antigen-specific sIgA responses in the URT of mice. We found that tobacco smoke inhibited IgA induction in the systemic circulation and nasal lumen, in part by attenuating the accumulation of antibody-secreting cell (ASC)s in the underlying nasal mucosa and draining lymphoid tissues. In addition to being decreased in quantity, we provide evidence that IgA generated in smoke-exposed

animals possesses a lower antigen-binding avidity, but paradoxically, a greater mutational load than observed in room air controls. Furthermore, smoke exposure compromises the upregulation of molecules critical to nasal ASC homing and transepithelial IgA transport in the nasal mucosa. Overall, our findings clearly indicate that cigarette smoke compromises multiple mechanisms involved in effective sIgA induction in the URT and associated lymphoid tissues.

Results

Cigarette smoke compromises the induction of IgA responses in the upper respiratory tract following intranasal LPS/OVA administration.

To investigate whether cigarette smoke compromises IgA induction in the upper airways, we exposed mice to either room air (RA) or cigarette smoke (CS) for one week, and subsequently intranasally immunized these mice with a mixture of LPS, a prototypical pathogen-associated molecular pattern, and ovalbumin (OVA), a well-described model antigen, using a multidose prime/boost schedule (**Figure 1A**). Smoke exposure was continuous during this protocol. We observed consistently decreased OVA-IgA in both the nasal lavage fluid (NALF; **Figures 1B, S1A**) and serum (**Figures 1C, S1A**) at 3, 7, 14 and 28 days post-boost (dpb). In a similar manner, LPS-specific IgA was induced in the serum of room air-exposed, but not smoke-exposed mice (**Figure 1D**). Notably, despite observing concurrent reductions in OVA-IgA in the NALF and serum at 3dpb, no significant correlation was observed between these two parameters within room air- and

cigarette smoke-exposed groups (RA: $r=0.2385$, $p=0.5069$ and CS: $r=0.1036$, $p=0.7758$; **Figure 1E**). Deficits in total IgA were also observed in the NALF, while no significant changes were observed in the serum (**Figures 1F, S1B/C**). OVA-IgA and total IgA levels in the NALF correlated strongly within smoke-exposed mice at 3dpb ($r=0.8402$, $p=0.0023$), while room air-exposed mice exhibited a moderate but non-significant positive correlation ($r=0.4956$, $p=0.1452$; **Figure S1D**). NALF and serum OVA-IgA were similarly decreased at 3dpb in mice exposed to cigarette smoke for 10 and 32 weeks prior to immunization (**Figure S1E**), as well as in mice administered 1 or 7 booster doses (**Figure S1F**). OVA-IgA induction was also attenuated in the vaginal lavage fluid (VALF; **Figure 1G**). In contrast to IgA, OVA-specific IgM and IgG1 levels in the serum were unchanged between groups (**Figure 1H**), and OVA-IgM, which can also be secreted across mucosal surfaces in a manner similar to IgA, was not detectable in the NALF (data not shown). Finally, when cigarette smoke-exposed mice were alternatively immunized with a mixture of OVA and polyI:C, a TLR-3 agonist and viral nucleic acid mimic, we found that the induction of OVA-IgA responses was similarly impaired (**Figure 1I**). These findings suggest that acute and chronic cigarette smoke exposure compromises the host's ability to induce IgA responses against antigens in the upper airways, and that such inhibition is observed in the context of diverse pathogen-associated molecular patterns.

Cigarette smoke exposure attenuates OVA-specific ASC accumulation in the nasal mucosa after intranasal LPS/OVA immunization

IgA antibodies secreted into the upper airway lumen are produced by antibody-secreting cells (ASCs; plasma cells) within the nasal mucosa¹⁸. To determine whether the observed reduction in nasal OVA-IgA was associated with changes in ASC populations, we next quantified the presence of OVA-specific ASCs (IgD⁻B220^{lo}CD138⁺IgG1⁻IgA⁺OVA⁺; **Figure 2A**, FMO controls presented in **Figure S2A**) in the nasal mucosa by flow cytometry. OVA-specific ASCs were quantified by intracellular staining with AlexaFluor (AF)647-conjugated OVA. We observed reductions in the number of both total and OVA-specific IgA ASCs (represented in **Figure 2B**) in the nasal mucosa of cigarette smoke-exposed mice at both 3dpb and 7dpb (**Figures 2C/D, S2B/C**). Notably, these differences were not caused by changes in the total cellularity of the nasal mucosa (**Figures S2D**). OVA-specific ASCs comprised more than 50% of total IgA ASCs at 3dpb, with smoke-exposed mice exhibiting a small but significant reduction in this proportion compared to RA controls (**Figure 2E**). Similar to antibody titres, deficits in OVA-IgA ASCs were also observed in mice exposed to cigarette smoke for either 10 or 32 weeks prior to immunization (**Figure S2C**). In contrast, OVA-IgA ASCs in the bone marrow were not significantly reduced in the context of smoke exposure at either 3 or 28dpb (**Figures 2F, S2E**). These data demonstrate that the deficit in nasal antigen-specific IgA observed in the context of cigarette smoke exposure occurs, at least in part, as a result of reduced ASC accumulation in the underlying mucosa.

Cigarette smoke exposure reduces nasal OVA-IgA avidity during the acute post-immunization period while augmenting nasal *Igha* mutational load.

In addition to quantity, the antigen-binding affinity of antibodies plays an integral role in their effector capacity. IgA responses induced in upper airway-associated lymphoid tissues are able to undergo somatic hypermutation (SHM) of their variable regions in order to promote antibody affinity maturation¹⁹. In light of this, we sought to assess metrics of antibody antigen-binding capacity. Initially, we quantified the ability of intracellular IgA to retain Alexa Fluor (AF)647-conjugated OVA by examining the ratio of IgA and OVA median fluorescence intensities (MFIs) within nasal OVA-IgA ASCs following intracellular staining. At 3dpb, we observed that there was no significant difference in IgA MFI between OVA-IgA ASCs generated in room air- and cigarette smoke-exposed mice (**Figure 3A**), suggesting that antibody production rate is likely similar between ASCs induced under either condition. In contrast, OVA MFI displayed a strong trend towards being reduced in the context of cigarette smoke. When quantified as a ratio, smoke-exposed mice demonstrated a significant reduction in OVA:IgA within ASCs compared to room air controls (**Figure 3B**). A similar trend was observed at 7dpb, but by 14dpb no differences were observed. Notably, during this timeframe the MFI ratio remained stable for smoke-exposed mice but contracted for room air-exposed mice. These early differences in MFI ratio suggest that, despite the same amount of total IgA per OVA-specific IgA ASC, there is a differential ability of smoke-

exposed ASCs to retain cognate antigen and thus an attenuated antigen-binding affinity.

Although similar measures of antigen retention by B cell receptors have been demonstrated to correlate with avidity²⁰, we sought to confirm these findings through direct analysis of NALF OVA-IgA antibodies. To do so, we used avidity ELISAs, which feature an antibody dissociation step via the transient addition of chaotropic urea after sample incubation. Using this approach, we determined that OVA-IgA in the NALF of smoke-exposed animals demonstrated a lower avidity index than that of room air controls at 3dpb (**Figure 3C**). Similar to ASC MFI data, avidity indices normalized by 28dpb, suggesting delays but ultimately does not permanently compromise the affinity maturation of OVA-IgA responses following immunization.

Next, we assessed whether cigarette smoke exposure alters the extent to which the IgA ASCs induced in the upper airways undergo SHM. To do so, we performed high-throughput sequencing to quantify mutational load within the heavy chain variable region of nasal IgA transcripts as described by Turchaninova *et al.*²¹. Specifically, we assessed the mean frequency of replacement mutations within combined complementarity-determining regions (CDRs 1/2), which comprise the antigen-binding paratope, and framework regions (FWRs 1/2/3; **Figure 3D**), which are also reportedly also able to alter antibody effector capacity²². Through clonal clustering²³, we found that room air- and smoke-exposed, immunized mice exhibited a similar predicted number of unique IgA clones per

sample (**Figure S2F**). In terms of mutational load, we observed a significant increase in the frequency of replacement mutations within CDR1/2 and FWR1/2/3 regions of smoke-exposed, immunized mice compared to room air controls (**Figure 3D**). Overall, these data suggest that IgA from the nasal mucosa of smoke-exposed, immunized mice possesses a greater mutational burden than room air controls, despite demonstrating a reduced polyclonal avidity at this timepoint.

Cigarette smoke exposure attenuates the induction of OVA-IgA ASCs in nasal-draining lymphoid tissues.

ASCs that populate the upper airways are typically induced within secondary lymphoid tissues that drain the nasal mucosa, such as the nasal-associated lymphoid tissue (NALT), cervical lymph nodes (CLNs) and spleen. To assess whether the observed reduction in nasal ASCs results from attenuated ASC induction, we next quantified OVA-IgA ASCs at these sites (IgD⁻B220^{lo}CD138⁺IgG1⁻IgA⁺OVA⁺; **Figure S3A**). At 3dpb, a timepoint at which we observe a large attenuation of IgA induction, we also observed that cigarette smoke attenuated the expansion of both total (**Figure 4A/B**) and OVA-IgA ASCs (**Figure 4C, S3G**) in the NALT. In room air-exposed mice, LPS/OVA immunization caused the physical expansion of CLNs as measured by cellularity and weight (**Figures 4D, S3B**). In contrast, smoke-exposed naïve mice had smaller CLNs at baseline, which did not expand to the same size as room air controls following immunization. Notably, this difference in

baseline CLN weight could not be explained by differences in mouse weight, which were minimal (**Figure S3F**). Within the CLNs, we observed a reduction in the absolute number of OVA-IgA ASCs, as well as the proportion of OVA-IgA ASCs within total ASCs (**Figure 4E, S3C**). Similarly, although the spleen did not expand with immunization, spleens from smoke-exposed mice were significantly smaller than those of room air controls at baseline (**Figures 4F, S3D**), and fewer OVA-IgA ASCs were present (**Figures 4G, S3E**). Lastly, we analyzed the blood at this timepoint, and found fewer OVA-IgA ASCs in the blood of cigarette smoke-exposed mice compared to room air controls (**Figure 4H**). Overall, these data suggest that cigarette smoke compromises the induction of OVA-IgA ASCs in nasal-draining lymphoid tissues, including the NALT, CLNs, and spleen, and ultimately reduces the output of these cells into the circulation.

In light of the observed changes in IgA antigen-binding capacity and mutational frequency in the context of smoke exposure, we also sought to assess whether smoke-exposed mice exhibited any differences in the number of germinal centre B cells (GCBCs; $\text{IgD}^- \text{B220}^+ \text{CD138}^- \text{GL7}^+ \text{CD95}^+$; **Figure S3A**), the B cell stage in which SHM and affinity maturation occur. Interestingly, at baseline, cigarette smoke-exposed control mice exhibited an increase in the proportion of GCBCs in the NALT compared to room air controls (**Figure 4I**). However, at 3dpb, smoke-exposed mice exhibited fewer total (**Figure 4I/J**) and OVA-IgA GCBCs (**Figures 4K, S3H**). Ultimately, these data suggest that cigarette smoke-exposed mice exhibit elevated basal NALT germinal center activity but feature reduced

antigen-specific IgA germinal centre induction relative to room air controls following intranasal immunization.

Cigarette smoke reduces basal CCL28 and VCAM-1 levels in the nasal mucosa and interferes with the transcriptional upregulation of VCAM-1 following intranasal immunization.

Following their generation in secondary lymphoid tissues, newly-formed ASCs migrate to the nasal mucosa²⁴. Homing of ASCs to respiratory surfaces is thought to be mediated by two molecular axes: a) the interaction between CCL28 produced at the mucosa and the CCR10 receptor on the surface of ASCs, and; b) the interaction between VCAM-1 expressed by local endothelial cells and $\alpha 4\beta 1$ integrin (VLA-4) on ASCs²⁴. To assess whether cigarette smoke compromises ASC homing, we first assessed baseline expression of tissue-derived factors CCL28 and VCAM-1. Cigarette smoke exposure reduced baseline expression of CCL28 and VCAM-1 in nasal homogenates following both 2 and 8 weeks of exposure. In contrast, no significant differences were observed in either CCL28 or VCAM-1 expression in lung homogenates or serum (**Figure 5A/B**). In addition, we observed that the upregulation of VCAM-1, but not CCL28, was impaired at 3dpb in nasal homogenates of cigarette smoke-exposed mice (**Figure 5C**). *Vcam1* transcript upregulation was similarly diminished in smoke-exposed mice that were administered 10 μ g of LPS alone for 1 hour (**Figure 5D**). Next, we assessed the

expression of $\alpha 4\beta 1$ integrin, the VCAM-1 binding partner. In this regard, we observed a marginal but significant reduction in the proportion of $\alpha 4\beta 1^+$ OVA-IgA ASCs within the CLNs of smoke-exposed mice, while no difference was observed on cells in the bloodstream or nasal mucosa (**Figure 5E**). In the CLNs, more substantial reductions were observed in the MFIs of both $\alpha 4$ and $\beta 1$ integrin subunits (**Figure 5F**). Again, however, $\alpha 4\beta 1$ expression in the bloodstream was equivalent, and no differences were observed in the effector tissue. Overall, these data suggest that cigarette smoke interferes with the transcriptional upregulation of VCAM-1 in the nasal mucosa, likely impairing the extravasation of ASCs into the submucosa following immunization.

Cigarette smoke attenuates the upregulation of pIgR in the nasal mucosa following intranasal immunization.

In addition to impaired induction and homing of ASCs to the nasal mucosa, quantities of IgA in the nasal lumen may be affected by the efficiency of transepithelial transport. IgA is transported from the submucosa across epithelial barriers with the assistance of the polymeric immunoglobulin receptor (pIgR)²⁴. Using Western blots, we found that cigarette smoke exposure attenuated the upregulation of pIgR and its post-transport cleavage product secretory component (SC) in the nasal mucosa following LPS/OVA administration (**Figure 6; Figure S4**). This impairment in pIgR upregulation may further explain the reduced OVA-

IgA levels observed in the nasal lumen of smoke-exposed mice, given the non-redundant role of this receptor in IgA transcytosis.

Discussion

IgA-mediated immunity has been implicated in providing protection against viral agents in the upper airways¹, and is thought to be an important component of existing and novel vaccination strategies against influenza and other mucosal pathogens²⁵⁻²⁸. As a result, it is important to understand how common inhaled environmental factors such as cigarette smoke can impact IgA induction in the upper airways in order to identify circumstances in which IgA-mediated defense, elicited by either natural infection or intranasal vaccination, may be ineffective.

In our studies using LPS/OVA as a model immunogen, we observed that both acute and long-term cigarette smoke exposure attenuated the induction of antigen-specific IgA responses in the URT and systemic circulation. Nasal and serum antigen-specific IgA responses did not correlate well with one another, which support previous findings in humans², and studies in mice suggesting differential mechanisms of mucosal and systemic IgA induction²⁹. In contrast, OVA-IgA correlated well with total IgA in the nasal lumen, which suggests that the OVA-specific response comprised the major proportion of total nasal IgA antibodies in our model. Interestingly, cigarette smoke exposure also attenuated IgA responses at the vaginal mucosa. The common mucosal immune system is known to facilitate

the dissemination of lymphocytes between distal mucosal sites³⁰, with antigen-specific responses induced in the URT being able to provide protection at the female reproductive tract. These findings imply that tobacco smoke may compromise the efficacy of intranasal vaccination strategies intended to elicit protective IgA responses in the genital tract³¹⁻³³. Notably, we observed an attenuation of OVA-IgA responses in the URT and circulation even when polyI:C was used as an adjuvant instead of LPS, suggesting that mechanistically, smoke exposure attenuates conserved elements of both TLR-4- and TLR-3/RIG-I-dependent IgA inductive pathways.

Cigarette smoke exposure impaired the generation of short-lived mucosal OVA-IgA ASCs in the nose, but not ASCs that populated the bone marrow. This reduction in nasal ASCs notably corresponded with a reduced number of these cells within inductive sites that drain the nasal mucosa, including the NALT, CLNs, and spleen. Evidence of reduced IgA ASCs in these secondary lymphoid organs suggests that the activation of T cell-dependent B cell responses at these sites is compromised. This may constitute deficits in the activation or polarization of nasal dendritic cells^{34,35}, follicular helper Tfh cells³⁶, or B cells. Further investigation is required to understand which of these pathways may be affected. Overall, however, our findings suggest that IgA ASC expansion is differentially modulated by cigarette smoke at different effector sites, but is consistently impaired within inductive tissues.

The reduced VCAM-1 upregulation we observe is reflective of previous observations in cigarette smoke extract/TNF- α -treated human coronary artery endothelial cells³⁷, suggesting that circulating ASCs may be unable to extravasate into the nasal mucosa though an inefficient ability to attach to local endothelial cells. In addition, our baseline CCL28 and VCAM-1 data are in line with previous clinical reports; in human smokers, *CCL28* gene expression has been observed to be attenuated in nasal epithelium, but not bronchial epithelium, and VCAM-1 protein expression is unchanged in the pulmonary vasculature relative to controls^{38,39}. Similarly, findings of impaired pIgR expression strongly indicate that IgA produced in the nasal submucosa may not be efficiently transcytosed to the nasal lumen following immunization. pIgR expression and sIgA levels have been reported to be attenuated in the airways of patients with severe COPD^{40,41}, an effect that is thought to be caused by extensive epithelial remodelling during disease progression⁴⁰. In contrast, the attenuation of nasal pIgR upregulation we observed occurs following an acute duration of smoke exposure, and thus likely occurs via an alternate mechanism. Overall, however, the data presented here demonstrate a refractory capacity of stromal cells within nasal mucosa to upregulate inflammatory molecules in response to immunogenic stimulation following cigarette smoke exposure.

Importantly, we also observed differences in antibody affinity and mutational load between room air- and smoke-exposed mice. Nasal OVA-IgA ASCs from smoke-exposed mice exhibited lower antigen retention despite

expressing similar total levels of IgA during the acute post-immunization period. These findings firstly demonstrate that IgA production on a per-cell basis is similar between groups, and thus that the observed deficit in NALF OVA-IgA likely does not occur as a result of changes in antibody production rate by individual ASCs. In addition, they provide evidence that antigen-specific IgA produced in smoke-exposed mice is of lower avidity than that produced by room air controls, a finding confirmed by chaotropic ELISA analysis of NALF OVA-IgA. Notably, these data are in line with clinical observations that smokers more frequently produce low-avidity antibodies in response to human papillomavirus (HPV) vaccination compared to non-smokers⁴². However, to our knowledge such an observation has not been previously reported for sIgA.

Strikingly, mutational data seem at first to contradict avidity findings, in that a greater level of mutation occurred within CDRs and FWRs as a result of immunization in smoke-exposed mice compared to room air controls. However, it is possible that smoke exposure facilitates these mutations, either directly or indirectly, in a manner that precludes them from undergoing rigorous affinity-based selection against the immunization antigen. In turn, these mutations could have potentially detrimental effects on affinity, explaining the observed differences in antigen-binding capacity. Notably, one limitation of our sequencing approach is that it comprised the entire IgA repertoire rather than OVA-IgA ASCs specifically. However, OVA-specific IgA ASCs comprised more than 50% of the total IgA compartment in both room air- and smoke-exposed mice at this timepoint,

suggesting that the mutational burden we observe is reflective of the antigen-specific compartment.

In assessing NALT germinal center activity, we also observed that smoke exposure upregulated the proportion of GCBCs at baseline, but attenuated the induction OVA-IgA GCBCs compared to room air controls. This suggests that the elevated mutational load observed in smoke-exposed immunized mice occurs either as a result of augmented germinal center activity at an earlier timeframe following primary immunization doses, or alternatively, does not occur as a result of events occurring after immunization. In this regard, cigarette smoke may promote SHM of B cells specific for smoke-associated antigens, which also demonstrate or develop cross-reactivity to OVA antigen, prior to immunization. Ultimately, further investigations are required to understand the manner in which cigarette smoke exposure dysregulates antigen-specific SHM and affinity maturation of sIgA responses in the URT.

In summary, our findings demonstrate for the first time that cigarette smoke exposure has the capacity to attenuate antigen-specific IgA responses induced in the upper airways of mice. Importantly, the mechanisms by which smoke exposure inhibits antigen-specific IgA induction in the upper airways are multifactorial, seemingly comprising deficits in ASC induction, homing, and transepithelial IgA transport (Figure 7). These findings are of importance, as sIgA has been implicated in providing a first line of defense in precluding acquisition and carriage of respiratory viruses, and preventing the cellular release and local dissemination of

viral particles⁴. Although one investigation demonstrated that intranasal live-attenuated influenza virus (LAIIV) vaccination was similarly effective at generating protective serum haemagglutination-inhibiting antibodies in smoking individuals as compared to non-smokers⁴³, it may be that cigarette smoke exposure specifically inhibits IgA-mediated defense against early asymptomatic upper airway infection, but not pulmonary defense mediated by IgG and cellular immune responses. In support of this notion, a recent study demonstrated that both cigarette smokers and e-cigarette users had a diminished IgA response to LAIV vaccination in the upper airways⁴⁴, providing evidence that our findings are relevant to humans. Ultimately, understanding mechanisms by which cigarette smoke compromises antigen-specific IgA responses in the upper respiratory tract may provide valuable insight into why smokers are predisposed to infectious disease, and aid in identifying potential challenges for the design and implementation of intranasal vaccination strategies.

Methods

Animals. 6-10 week old female C57BL/6 mice were purchased from Charles River Laboratories (Montreal, QC, Canada), and housed in the McMaster Central Animal Facility. Mice were given *ad libitum* access to food and water, and subject to 12 hour light/dark cycling. All experiments were approved by the Animal Research Ethic Board at McMaster University.

Cigarette smoke exposure. Mice were exposed to mainstream cigarette smoke of 12 3R4F research cigarettes (University of Kentucky; filters removed) over 50 minutes, twice per day, 5 days per week in a whole-body smoke exposure system (SIU48, Promech; Sweden). Details of the protocol were reported previously⁴⁵. Duration of smoke exposure is detailed in the text. Control mice were exposed to room air only.

Intranasal Immunizations. Unanaesthetized mice were restrained, and a mixture of either purified *Escherichia coli* O111:B4 LPS or polyI:C (10µg; Sigma Aldrich) and ovalbumin (OVA) (100µg) in a combined volume of 10µl was pipetted into the URT via the nares. This administration protocol has been shown to restrict delivery to the upper airways as opposed to the lungs⁴⁶. Control mice received phosphate-buffered saline (PBS) vehicle alone. Specific experimental administration schedules are described in the text.

Sample Collection and Processing. At the timepoints described in the text, mice were anaesthetized with isoflurane and blood was collected via cardiac puncture. To collect nasal samples, mice were culled by exsanguination, and decapitated. The lower mandible was removed and nasal lavage (NAL) was performed by cannulating the nasopharynx and retrograde flushing the nasal passages with 300µl of sterile PBS. After removing the cranial skin and the palate, the nasal-associated lymphoid tissue (NALT) was excised using a dissection microscope. Subsequently,

the external nose was removed, and the skull bisected with scissors. The nasal mucosa (NM) was then excised with fine forceps. Cervical lymph nodes (CLNs; mandibular, accessory mandibular LNs) were extracted using a dissection microscope. Vaginal lavage (VAL) was performed pipetting 150µl of PBS in and out of the vaginal opening, repeated twice.

Unheparinized blood was incubated at 37°C for 1h, microcentrifuged at 13,000rpm for 10 minutes, and serum was collected. NAL, BAL, and VAL were microcentrifuged at 2500rpm for 10 minutes to pellet cells. Serum, as well as nasal, bronchoalveolar, and vaginal lavage supernatant fluid samples (NALF, BALF, VALF) were stored at -80°C for future analysis. Nasal mucosae and spleens were mechanically dissociated by abrasion against a 40µm filter. NALT and CLNs were mechanically dissociated by abrasion between glass slides. NALT cells were pooled within each group for staining and flow cytometry analysis due to low cellular yield. Bone marrow (BM) was extracted by removing the ends of one femur and flushing with sterile PBS. All samples were refiltered using 40µm filters, centrifuged at 1400rpm for 5 minutes, and resuspended in PBS. Spleen and BM cells were further treated with ACK lysis buffer. Total cells were counted for each sample using a haemocytometer or Countess™ Automated Cell Counter (Invitrogen).

ELISAs. To detect OVA-specific IgA, NUNC Maxi-Sorp 96-well plates (ThermoFisher Scientific) were coated with goat anti-mouse IgA (Southern

Biotech) in carbonate-bicarbonate buffer (CBB; Sigma). Subsequently, plates were blocked with 1% bovine serum albumin (BSA; Sigma Aldrich; in PBS), and incubated with sample diluted in 1% BSA. All reagents herein were diluted in 1% BSA unless otherwise indicated. Adherent OVA-specific antibodies were detected using digoxigenated OVA (300 ng/ml), followed by anti-digoxigenin-POD (poly) Fab fragments (Roche). ELISAs were developed using tetramethylbenzidine (TMB; SurModics), and stopped with 2 N H₂SO₄. To detect OVA-specific IgG1 and IgM antibodies by ELISA, plates were coated with 4 µg/ml of purified OVA (Sigma Aldrich) in PBS. Following blocking and sample incubation as above, wells were incubated with biotinylated antibodies specific for the indicated isotype heavy chains (Southern Biotech) and detected using streptavidin-alkaline phosphatase (ThermoFisher) and 4-NPP (Sigma). To detect LPS- specific IgA, plates were coated with 50 µg/ml of purified Escherichia coli O111:B4 LPS in CBB, blocked and incubated with samples. Bound antibodies were detected with biotinylated anti-IgA, streptavidin-AP, and 4-NPP. Background from empty control wells was subtracted to acquire final O.D. values for all antigen- specific antibody ELISAs. To detect total IgA, plates were coated with anti-mouse IgA (Southern Biotech), blocked, and incubated with sample as above. Subsequently, wells were incubated with biotinylated anti-mouse IgA (Southern Biotech) followed by development with streptavidin-HRP and TMB. Concentrations were interpolated using a standard curve of purified mouse IgA (Southern Biotech). To generate avidity indices, we performed avidity ELISAs^{47,48}. ELISA plates were coated with OVA,

blocked, and incubated with sample as above for 2h. After washing, samples were treated with 50µl of 4M urea in PBS, or PBS alone, at room temperature under constant agitation for exactly 15 min. Urea was washed off and bound antibodies were detected using biotinylated anti-IgA, streptavidin-HRP and TMB. Avidity indices were calculated as $(\text{O.D.450 Urea} / \text{O.D.450 No Urea} * 100)$ for each sample.

To detect CCL28 and VCAM-1, nasal mucosa and lungs were homogenized in 400µl of RIPA buffer containing protease inhibitors. Bradford assay was used to determine the total protein content of each sample. Subsequently, samples were normalized to 0.25µg/ml total protein, and assessed for CCL28 and VCAM-1 using commercial ELISAs (Biolegend and R&D, respectively) as per the manufacturer's instructions.

Flow Cytometry. For flow cytometry, single cell suspensions were transferred to a 96-well plate. Cells were stained for viability using LIVE/DEAD[®] Fixable Yellow Dead Cell Stain (Molecular Probes; 1:400 in PBS), and blocked with anti-CD16/32 (Biolegend; 1:100 in fluorescence-activated cell sorting (FACS) buffer (0.5% BSA, 2mM EDTA in PBS)). Subsequently, cells were stained with fluorophore-conjugated antibodies targeting specific antigens (Table S1) diluted in FACS buffer. Cells were next fixed and permeabilized using Cytofix/Cytoperm (BD Biosciences), and intracellular staining was performed using antibody cocktails and other stains diluted in Perm/Wash Buffer (BD Biosciences; Table 1). Fluorescence-

minus-one (FMO) controls were used to determine thresholds for gating strategies. Data was collected using a BD LSRFortessa (BD Biosciences), and data analysis performed using FlowJo software (V10; TreeStar, Inc.). Absolute cell number quantification was performed by multiplying the frequency of the given population with regards to live singlet events by the total cell count for that sample.

IgA Sequencing. To quantify mutational load within the nasal IgA repertoire, high-throughput sequencing was performed. Briefly, at 3dpb the nasal mucosae were removed and homogenized in buffer RLT (Qiagen) containing β -mercaptoethanol. After centrifugation to remove cellular debris, RNA was isolated from lysates using an RNeasy kit (Qiagen) as per manufacturer's instructions. 700ng of total RNA per sample was used for the sequencing analysis, which was performed as per Turchaninova *et al.*²¹. Illumina adapters (NEBNext DNA Library Prep Set; NEB E6040) were added to the resulting cDNA products as per the manufacturer's instructions. All DNA cleanup steps were performed using Monarch PCR & DNA Cleanup Kits (NEB T1030L). Asymmetric 400+200nt paired-end sequencing was performed on an Illumina Mi-Seq platform (v3). Sample demultiplexing and unique molecular identifier (UMI)-based assembly of full-length variable regions was performed using MIGEC software. V(D)J alignment against reference and clonal clustering was performed using Change-O package²³ with default settings. Mutations were quantified within the full variable region using the R package ShazaM (version 0.2.0)⁴⁹. Overall, following all processing steps we reconstructed

a median of 69751 full length IgA reads and that were clustered into a median of 4484 IgA clones (Table S2).

RT-qPCR Analysis. To assess *Vcam1* expression, the upper airways were lavaged with RLT buffer, and RNA was extracted from the resulting mucosal lysate as above. Subsequently, RNA was reverse transcribed into cDNA using Superscript II (Invitrogen), as per manufacturer's instructions. cDNA was then quantified by qPCR using Taqman primers and probes (*Vcam1* Mm01320970_m1; ThermoFisher Scientific) in a StepOnePlus real-time PCR system (Life Technologies Inc., Burlington, ON, Canada). Gene expression was determined using the $\Delta\Delta CT$ method. *Vcam1* gene expression was normalized to that of the housekeeping gene *Gapdh* (Mm99999915_g1), and expressed as a fold change relative to the indicated control group.

Western Blotting. Nasal mucosae were homogenized in RIPA buffer (0.1% SDS, 0.5% sodium deoxycholate, 1% Igepal CA-630 in PBS) containing protease inhibitors (Roche, Complete Mini Protease Inhibitor Cocktail, 11836153001), and a Bradford assay was used to quantify total protein. 20 μ g of protein per sample was loaded per well, and a 10% gel was used to resolve the proteins. Following resolution and transfer to nitrocellulose membrane, total protein was assessed using LICOR REVERT Total Protein Stain as per manufacturer's instructions. After imaging the total protein stain, and blocking, the membrane was incubated with a

primary monoclonal antibody specific for pIgR (AF2800, R&D), and, subsequently, a secondary detection antibody. Following imaging of pIgR bands, densitometry scores were determined using ImageStudio Lite. Scores from pIgR (~115kDa) and secretory component (SC; ~95kDa) bands were normalized to total protein stain bands.

Statistical Analysis. GraphPad Prism 8 (GraphPad Software, Inc.) was used for statistical analyses. Two-group, single-variable comparisons were assessed by unpaired Student's T-test. Mutational load data were assessed by Mann–Whitney U test with Bonferroni post-hoc analysis. Two-way ANOVAs adjusted for multiple comparisons using Tukey's post-hoc test were used to assess all other multi-variable comparisons. Significance (*) is defined as $p < 0.05$.

References

1. Renegar, K. B., Small, P. A., Boykins, L. G. & Wright, P. F. Role of IgA versus IgG in the control of influenza viral infection in the murine respiratory tract. *J. Immunol.* **173**, 1978–1986 (2004).
2. Gould, V. M. W. *et al.* Nasal IgA provides protection against human influenza challenge in volunteers with low serum influenza antibody titre. *Front. Microbiol.* **8**, 1–9 (2017).
3. Corthésy, B. Multi-faceted functions of secretory IgA at mucosal surfaces. *Front. Immunol.* **4**, 1–11 (2013).
4. Okuya, K. *et al.* A potential role of non-neutralizing IgA antibodies in cross-protective immunity against influenza A viruses of multiple hemagglutinin subtypes. *J. Virol.* (2020).doi:10.1128/jvi.00408-20
5. Stämpfli, M. R. & Anderson, G. P. How cigarette smoke skews immune responses to promote infection, lung disease and cancer. *Nat. Rev. Immunol.* **9**, 377–384 (2009).
6. Arcavi, L. & Benowitz, N. L. Cigarette Smoking and Infection. *Arch. Intern. Med.* **164**, 2206–2216 (2004).
7. Lawrence, H., Hunter, A., Murray, R., Lim, W. S. & McKeever, T. Cigarette smoking and the occurrence of influenza – Systematic review. *J. Infect.* **79**, 401–406 (2019).
8. Rylander, R., Wold, A. & Haglind, P. Nasal antibodies against gram-negative bacteria in cotton-mill workers. *Int. Arch. Allergy Appl. Immunol.* **69**, 330–4 (1982).
9. Barton, J. R., Riad, M. A., Gaze, M. N., Maran, A. G. D. & Ferguson, A. Mucosal immunodeficiency in smokers, and in patients with epithelial head and neck tumours. *Gut* **31**, 378–382 (1990).

10. Giuca, M. R., Pasini, M., Tecco, S., Giuca, G. & Marzo, G. Levels of salivary immunoglobulins and periodontal evaluation in smoking patients. *BMC Immunol.* **15**, 1–5 (2014).
11. Bennet, K. R. & Reade, P. C. Salivary immunoglobulin A levels in normal subjects, tobacco smokers, and patients with minor aphthous ulceration. *Oral Surgery, Oral Med. Oral Pathol. Oral Radiol.* **53**, 461–465 (1982).
12. Agarwal, A., Rao, S. ., Sowmya, S. ., Augustine, D. & Patil, S. Estimation of Salivary Immunoglobulin A and Serum Immunoglobulin A in Smokers and Nonsmokers : A Comparative Study. *J. Int. Oral Heal.* **8**, 1008–1011 (2016).
13. Norhagen Engström, G. & Engström, P. E. Effects of tobacco smoking on salivary immunoglobulin levels in immunodeficiency. *Eur. J. Oral Sci.* **106**, 986–91 (1998).
14. Mandel, M. A., Dvorak, K. & Decosse, J. J. Salivary Immunoglobulins In Patients with Oropharyngeal and Bronchopulmonary Carcinoma. *Cancer* **31**, 1408–1413 (1973).
15. Wang, J., Li, Q., Xie, J. & Xu, Y. Cigarette smoke inhibits BAFF expression and mucosal immunoglobulin A responses in the lung during influenza virus infection. *Respir. Res.* **16**, 1–12 (2015).
16. World Health Organization *WHO Report on the Global Tobacco Epidemic, 2015.* (2015).at <www.who.int/tobacco>
17. Carter, B. D. *et al.* Smoking and Mortality-Beyond Established Causes. *N. Engl. J. Med.* **372**, 631–640 (2015).
18. Kiyono, H. & Fukuyama, S. NALT- versus Peyer's-Patch-mediated mucosal immunity. *Nat. Rev. Immunol.* **4**, 699–710 (2004).
19. Shimoda, M. *et al.* Isotype-specific selection of high affinity memory B cells in nasal-associated lymphoid tissue. *J. Exp. Med.* **194**, 1597–1607 (2001).

20. Frank, G. M. *et al.* A simple flow-cytometric method measuring B cell surface immunoglobulin avidity enables characterization of affinity maturation to influenza a virus. *MBio* **6**, 1–11 (2015).
21. Turchaninova, M. A. *et al.* High-quality full-length immunoglobulin profiling with unique molecular barcoding. *Nat. Protoc.* **11**, 1599–1616 (2016).
22. Klein, F. *et al.* Somatic mutations of the immunoglobulin framework are generally required for broad and potent HIV-1 neutralization. *Cell* **153**, 126–138 (2013).
23. Gupta, N. T. *et al.* Change-O: A toolkit for analyzing large-scale B cell immunoglobulin repertoire sequencing data. *Bioinformatics* **31**, 3356–3358 (2015).
24. Macpherson, A. J., McCoy, K. D., Johansen, F.-E. & Brandtzaeg, P. The immune geography of IgA induction and function. *Mucosal Immunol.* **1**, 11–22 (2008).
25. Ambrose, C. S., Wu, X., Jones, T. & Mallory, R. M. The role of nasal IgA in children vaccinated with live attenuated influenza vaccine. *Vaccine* **30**, 6794–6801 (2012).
26. Terauchi, Y. *et al.* IgA polymerization contributes to efficient virus neutralization on human upper respiratory mucosa after intranasal inactivated influenza vaccine administration. *Hum. Vaccines Immunother.* **14**, 1351–1361 (2018).
27. Amorij, J. P., Hinrichs, W. L. J., Frijlink, H. W., Wilschut, J. C. & Huckriede, A. Needle-free influenza vaccination. *Lancet Infect. Dis.* **10**, 699–711 (2010).
28. Lycke, N. Recent progress in mucosal vaccine development: potential and limitations. *Nat. Rev. Immunol.* **12**, 592–605 (2012).

29. Gärdby, E. *et al.* Strong Differential Regulation of Serum and Mucosal IgA Responses as Revealed in CD28-Deficient Mice Using Cholera Toxin Adjuvant. *J. Immunol.* **170**, 55–63 (2003).
30. McDermott, M. R. & Bienenstock, J. Evidence for a common mucosal immunologic system. I. Migration of B immunoblasts into intestinal, respiratory, and genital tissues. *J. Immunol.* **122**, 1892–8 (1979).
31. Johansson, E. L., Wassén, L., Holmgren, J., Jertborn, M. & Rudin, A. Nasal and vaginal vaccinations have differential effects on antibody responses in vaginal and cervical secretions in humans. *Infect. Immun.* **69**, 7481–7486 (2001).
32. Wern, J. E., Sorensen, M. R., Olsen, A. W., Andersen, P. & Follmann, F. Simultaneous subcutaneous and intranasal administration of a CAF01- adjuvanted Chlamydia vaccine elicits elevated IgA and protective Th1/Th17 responses in the genital tract. *Front. Immunol.* **8**, 1–11 (2017).
33. Mestecky, J., Raska, M., Novak, J., Alexander, R. C. & Moldoveanu, Z. Antibody-mediated Protection and the Mucosal Immune System of the Genital Tract: Relevance to Vaccine Design. *J. Reprod. Immunol.* **85**, 81–85 (2010).
34. Lee, H. *et al.* Phenotype and function of nasal dendritic cells. *Mucosal Immunol.* **8**, 1–16 (2015).
35. Takaki, H. *et al.* Toll-like receptor 3 in nasal CD103+ dendritic cells is involved in immunoglobulin A production. *Mucosal Immunol.* **11**, 82–96 (2018).
36. Dullaers, M. *et al.* A T Cell-Dependent Mechanism for the Induction of Human Mucosal Homing Immunoglobulin A-Secreting Plasmablasts. *Immunity* **30**, 120–129 (2009).
37. Teasdale, J. E. *et al.* Cigarette smoke extract profoundly suppresses TNF α -mediated proinflammatory gene expression through upregulation of ATF3 in human coronary artery endothelial cells. *Sci. Rep.* **7**, 1–10 (2017).

38. Zhang, X. *et al.* Similarities and differences between smoking-related gene expression in nasal and bronchial epithelium. *Physiol. Genomics* **41**, 1–8 (2010).
39. Schaberg, T. *et al.* Expression of adhesion molecules in peripheral pulmonary vessels from smokers and nonsmokers. *Lung* **174**, 71–81 (1996).
40. Gohy, S. T. *et al.* Polymeric immunoglobulin receptor down-regulation in chronic obstructive pulmonary disease: Persistence in the cultured epithelium and role of transforming growth factor- β . *Am. J. Respir. Crit. Care Med.* **190**, 509–521 (2014).
41. Polosukhin, V. V. *et al.* Secretory IgA Deficiency in Individual Small Airways Is Associated with Persistent Inflammation and Remodeling. *Am. J. Respir. Crit. Care Med.* **195**, 1010–1021 (2017).
42. Namujju, P. B. *et al.* Impact of smoking on the quantity and quality of antibodies induced by human papillomavirus type 16 and 18 AS04-adjuvanted virus-like-particle vaccine - A pilot study. *BMC Res. Notes* **7**, 2–7 (2014).
43. MacKenzie, J. S. *et al.* The effect of cigarette smoking on susceptibility to epidemic influenza and on serological responses to live attenuated and killed subunit influenza vaccines. *J Hyg (Lond)*. **77**, 409-417 (1976).
44. Rebuli, M. E. *et al.* Electronic-cigarette use alters nasal mucosal immune response to live-attenuated influenza virus: A clinical trial. *Am. J. Respir. Cell Mol. Biol.* **64**, 126–137 (2021).
45. Shen, P. *et al.* Streptococcus pneumoniae colonization is required to alter the nasal microbiota in cigarette smoke-exposed mice. *Infect. Immun.* **85**, 1–14 (2017).

46. Southam, D. S., Dolovich, M., O'Byrne, P. M. & Inman, M. D. Distribution of intranasal instillations in mice: effects of volume, time, body position, and anesthesia. *Am. J. Physiol. - Lung Cell. Mol. Physiol.* **282**, L833–L839 (2002).
47. Keating, R. *et al.* Broadly Reactive Influenza Antibodies Are Not Limited by Germinal Center Competition with High-Affinity Antibodies Rachael. *MBio* **11**, 1–13 (2020).
48. Tennant, R. K., Holzer, B., Love, J., Tchilian, E. & White, H. N. Higher levels of B-cell mutation in the early germinal centres of an inefficient secondary antibody response to a variant influenza haemagglutinin. *Immunology* **157**, 86–91 (2019).
49. Cui, A. *et al.* A Model of Somatic Hypermutation Targeting in Mice Based on High-Throughput Ig Sequencing Data. *J. Immunol.* **197**, 3566–3574 (2016).

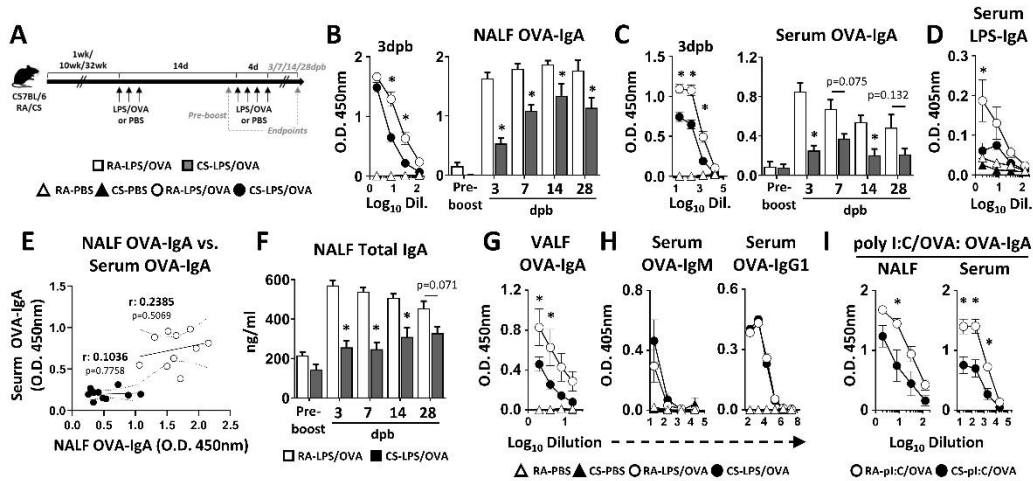


Figure 1. Cigarette smoke exposure compromises the induction of nasal and systemic IgA responses following intranasal LPS/OVA immunization. (A) C57BL/6 mice were exposed to room air (RA) or cigarette smoke (CS) for the indicated durations. Subsequently, three doses of LPS/OVA or PBS vehicle were administered intranasally to the upper respiratory tract, once daily. After two weeks of continued exposure, mice received four booster doses of LPS/OVA or vehicle. Animals were culled and samples collected at the indicated timepoints. OVA-specific or LPS-specific antibodies of the indicated isotypes were measured in the indicated samples by ELISA at (B, C) the indicated timepoints or (D-E, G-I) 3dpb. (B-C) Data represent n=3-10 mice per group from three independent experiments. (D, G, H) Data represent n=3-7 mice per group. (E) Data represent n=10 mice per group from two independent experiments. (F) Total IgA was measured by ELISA at the indicated timepoints. Data represent 5-10 mice per group from two independent experiments. (I) Mice were exposed to room air or cigarette smoke for 1 week and immunized with polyI:C/OVA as per the schedule in panel A. Data represent n=4-5 mice per group. (E) Linear regression and Pearson’s correlation, dotted lines represent 95% confidence bands. All others two-way ANOVA with Tukey’s post-hoc test. Mean ± SEM. *p<0.05.

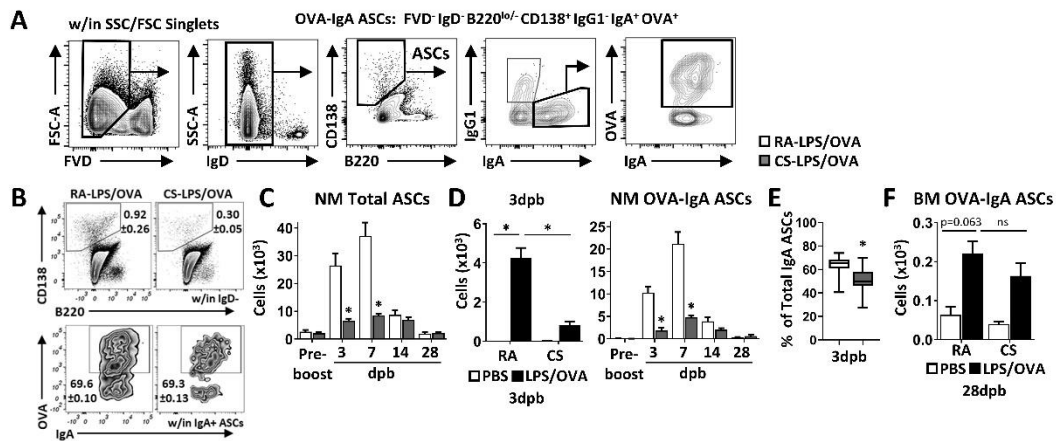


Figure 2. Cigarette smoke exposure attenuates OVA-specific IgA ASC accumulation in the nasal mucosa after intranasal LPS/OVA immunization. Mice exposed to room air (RA) or cigarette smoke (CS) for one week were intranasally immunized with LPS/OVA, and mice were analyzed at the indicated timepoints. (A) Nasal OVA-IgA ASC gating strategy (IgD⁻B220^{lo/-}CD138⁺IgG1⁻IgA⁺OVA⁺). (B) Flow cytometry plots demonstrating total ASCs (top), and OVA-IgA ASCs within IgA ASCs (bottom) in the nasal mucosa at 7dpb. Frequencies presented are mean \pm SD. (C-D) Absolute numbers of (C) total and (D) OVA-specific IgA ASCs were quantified in the nasal mucosa (NM) at the indicated timepoints. Data represent (C) n=3-7 mice per group from two independent experiments, (D) n=3-7 mice per group from three independent experiments. (E) Nasal OVA-IgA ASCs were quantified as a proportion of total IgA ASCs at 3dpb. Data represent n=12 mice per group from two independent experiments. (F) Absolute number of OVA-IgA ASCs in the bone marrow quantified at 3dpb. Data represent n=3-10 per group. FVD: fixable viability dye. (E) Student's unpaired t-test, all others two-way ANOVA with Tukey's post-hoc test. Mean \pm SEM. *p<0.05.

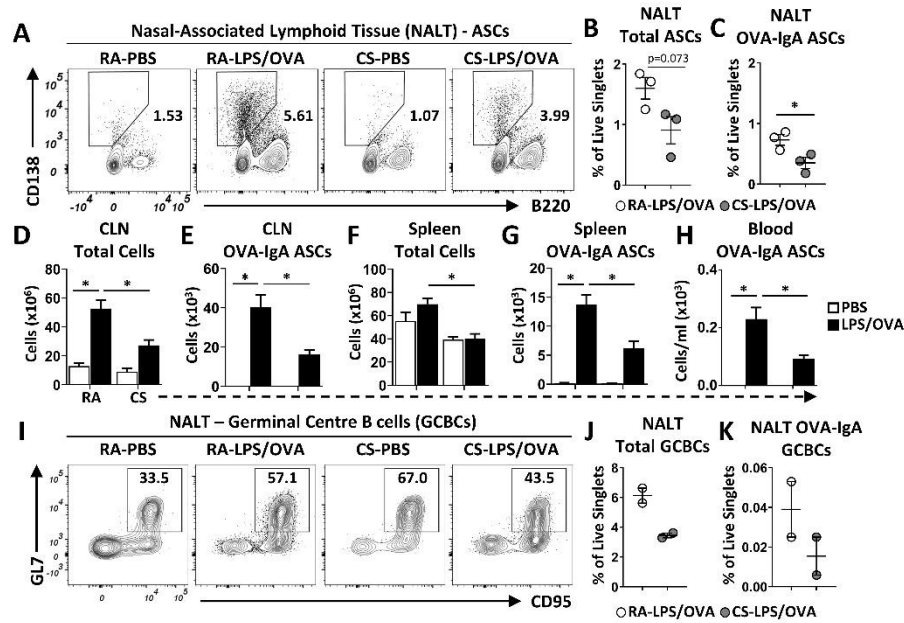


Figure 4. The induction of antigen-specific IgA ASC responses is diminished in the NALT, CLNs and spleen in the context of cigarette smoke exposure. Mice exposed to room air (RA) or cigarette smoke (CS) for one week were intranasally immunized with LPS/OVA as described in Figure 1, and NALTs, CLNs, spleen, and blood were assessed by flow cytometry at 3dpb. (A,B) Total NALT ASCs are (A) visualized as flow cytometry plots within the parent gate (IgD⁻ live singlets) and (B) quantified. (C) NALT OVA-IgA ASCs quantified as a percentage of total ASCs. NALT data points represent the means of pooled samples (n=5-7 mice per group per experiment) from three independent experiments. (D) Pooled CLN cell count per mouse. (E) Absolute number of CLN OVA-IgA ASCs. (F) Spleen cell counts per mouse. (G,H) Absolute number of OVA-IgA ASCs in the (G) spleen and (H) whole blood. Data represent: (D-G) n=3-12 mice per group from two independent experiments, (H) n=3-10 mice per group, one of two representative experiments is shown. (I,J) Total NALT GCBCs are (I) visualized as flow cytometry plots within the parent gate (CD138⁻B220⁺) and (J) quantified. (K) NALT OVA-IgA GCBCs quantified as a percentage of total GCBCs. NALT data points represent the means of pooled samples (n=5-7 mice per group per experiment) from two independent experiments. (B,C,J,K) Student's unpaired t-tests, (D-H) two-way ANOVA with Tukey's post-hoc test. Mean ± SEM. *p<0.05.

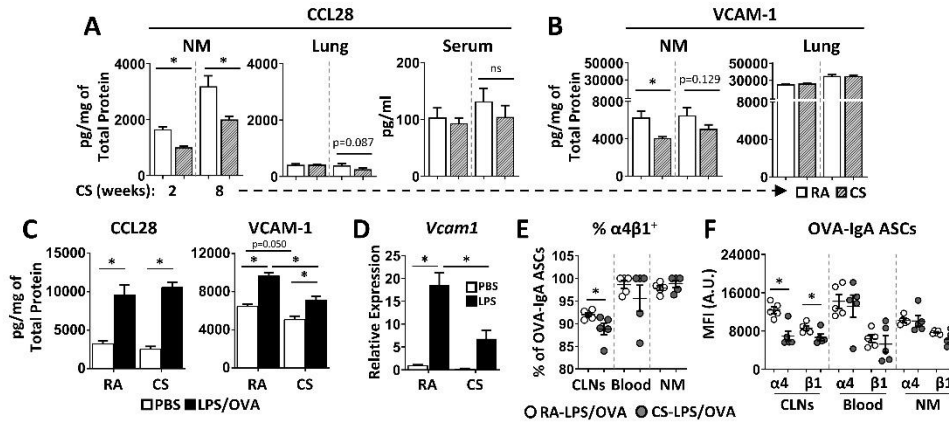


Figure 5. Cigarette smoke exposure attenuates the transcriptional upregulation of VCAM-1 in the nasal mucosa following immunization. (A,B) Mice were exposed to room air (RA) or cigarette smoke (CS) for 2 or 8 weeks. Serum, NM homogenates and lung homogenates were assessed for (A) CCL28 and (B) VCAM-1 expression by ELISA. Data represent n=5-7 mice per group from two independent experiments. (C) Mice were exposed to room air or cigarette smoke for 1 week and intranasally immunized with LPS/OVA as described in Figure 1A. At 3dpb, nasal homogenates were assessed for CCL28 and VCAM-1 expression by ELISA. Data represent n=5 mice per group. (D) Mice were exposed to room air or cigarette smoke for 2 weeks and intranasally administered 10 μ g of LPS alone. *Vcam1* gene expression was quantified in nasal lysates 1 hour post-administration. Data in each group are normalized to the mean of the RA-PBS group. Data represent n=5 mice per group. (E,F) Mice were treated as in (C), at which point (E) the proportion of $\alpha 4^+ \beta 1^+$ integrin OVA-IgA ASCs and (F) the MFI of each integrin was quantified. Data represent n=5 mice per group. A.U.: arbitrary units. (A,B,E,F) Student's unpaired t-tests, (C-D) two-way ANOVA with Tukey's post-hoc test. Mean \pm SEM. *p<0.05.

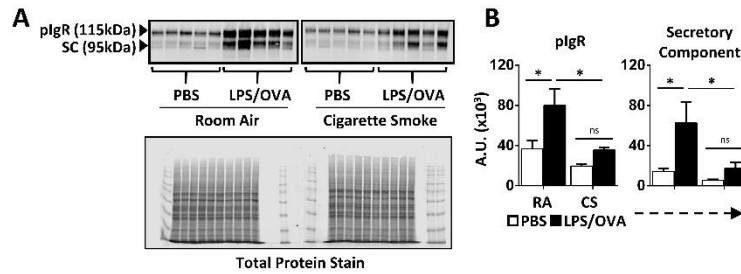


Figure 6. Cigarette smoke exposure attenuates the upregulation of pIgR in the nasal mucosa following immunization. Room air (RA) and cigarette smoke (CS)-exposed mice were immunized with LPS/OVA as per Figure 1. At 3dpb, nasal mucosa was extracted. (A) Western blots for pIgR/secretory component (SC) were performed. An uncropped version of pIgR/SC blots is presented in Figure S4. (B) pIgR and SC expression was quantified by densitometry. Data represent n=5 mice per group. A.U.: arbitrary units. Two-way ANOVA with Tukey's post-hoc test. Mean \pm SEM. *p<0.05.

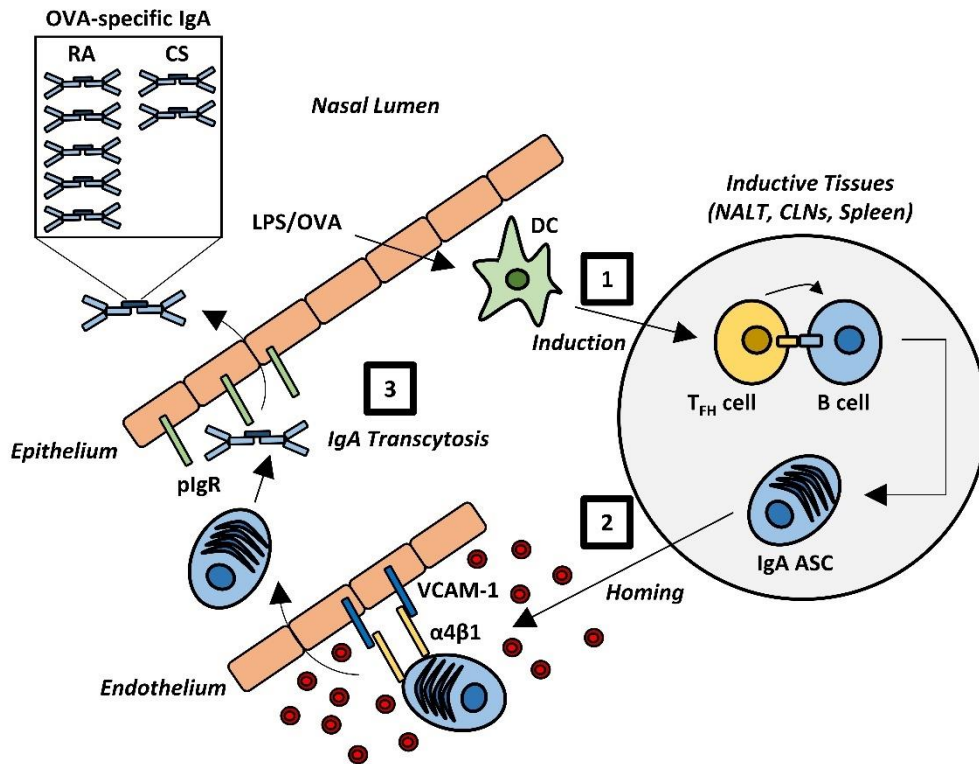


Figure 7. Prospective mechanisms of cigarette smoke-mediated IgA inhibition in the upper respiratory tract. Mice exposed to cigarette smoke during the course of intranasal immunization with LPS/OVA demonstrated reduced induction of antigen (OVA)-specific IgA antibodies in the nasal and systemic circulation. These antibodies demonstrate reduced polyclonal avidity during the acute post-immunization period. [1] Evidence of impaired OVA-IgA ASC accumulation in the nasal mucosa, secondary lymphoid tissues, and bloodstream suggest an impairment in the activation these cells. Nasal OVA-IgA ASCs from smoke-exposed mice also demonstrate reduced OVA-binding capacity, suggesting that they possess a reduced antigen-binding affinity compared to room air controls. [2] Data also demonstrate that cigarette smoke exposure compromises the upregulation of VCAM-1 in the nasal mucosa following LPS exposure, suggesting that following generation in secondary lymphoid tissues, these cells may not be able to efficiently extravasate back into the nasal mucosa. [3] Finally, pIgR expression in the nasal mucosa was similarly impaired following immunization, strongly suggesting that IgA transepithelial transport may also be attenuated.

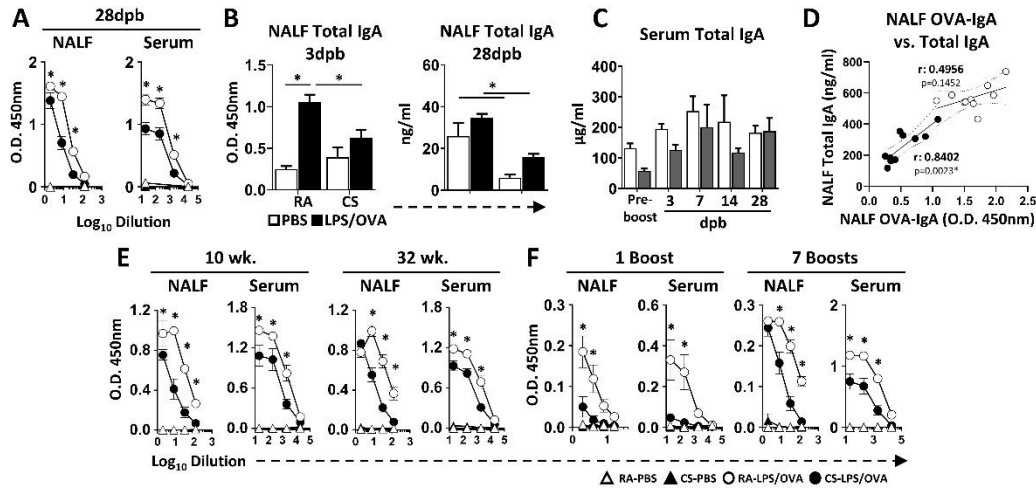


Figure S1. Extended data for Figure 1. Mice exposed to room air (RA) or cigarette smoke (CS) for one week were intranasally immunized with LPS/OVA as described in Figure 1. (A) OVA-specific or (B/C) total IgA antibodies measured in the indicated sample(s) at the indicated timepoint(s) or (D) at 3dpb. (D) Linear regression and Pearson's correlation analyses were performed between NALF-OVA IgA and serum OVA-IgA. Dotted lines represent 95% confidence bands. Data represent n=10 mice per group from two independent experiments. (E) Mice were immunized with LPS/OVA as described in Figure 1 after 10 or 32 weeks of room air/smoke exposure, and OVA-IgA was quantified in the NALF and serum by ELISA. Data represent n=5 (10wk) and n=5-10 (32wk) mice per group. (F) Mice exposed to room air or cigarette smoke for one week were intranasally immunized with LPS/OVA as described in Figure 1, with the exception that animals were administered one or seven, rather than four, booster doses. At 3dpb, OVA-IgA was quantified in the NALF and serum by ELISA. Data represent n=3-7 mice per group. (D) Linear regression and Pearson's correlation, dotted lines represent 95% confidence bands. All others two-way ANOVA with Tukey's post-hoc test. Mean \pm SEM. *p<0.05.

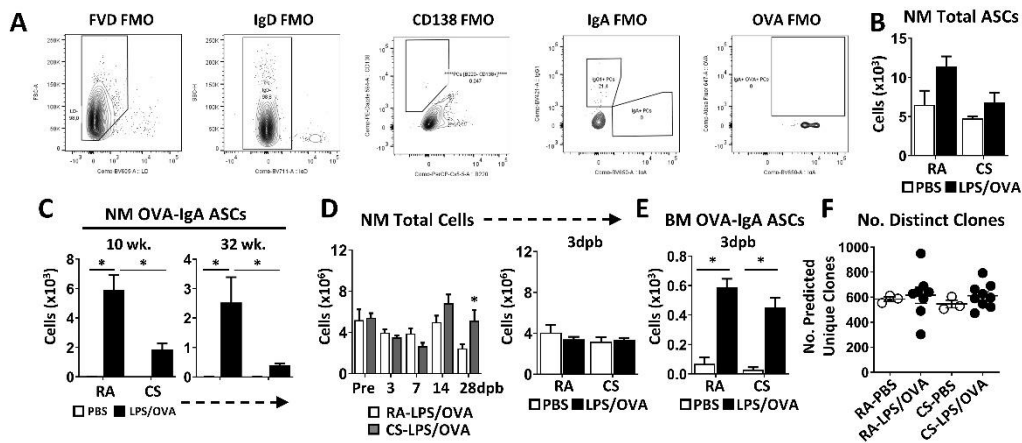


Figure S2. Extended data for Figures 2 and 3. (A) Fluorescence-minus one (FMOs) for gating nasal ASCs. (B,C) Mice exposed to room air (RA) or cigarette smoke (CS) for one week were intranasally immunized with LPS/OVA. (B) Total and ASCs were quantified in the NM at 3dpb. (C) Mice were immunized with LPS/OVA as described in Figure 1 after 10 or 32 weeks of room air/smoke exposure, and OVA-IgA ASCs were quantified in the NM by flow cytometry. Data represent $n=5$ (10wk) and $n=5-10$ (32wk) mice per group. (D) Total cells from nasal single cell suspensions were counted at the indicated timepoints. Data represent $n=5$ mice per group from three independent experiments. (E) Animals were treated as in (B) and OVA-IgA ASCs were quantified in the BM. Data represent $n=3-7$ mice per group. (F) Nasal IgA mRNA transcripts were analyzed at 3dpb by high-throughput immunoglobulin sequencing, and the number of distinct clones was predicted based on sequence similarity. Data represent $n=3-9$ mice per group. Two-way ANOVA with Tukey's post-hoc test. Mean \pm SEM. * $p<0.05$.

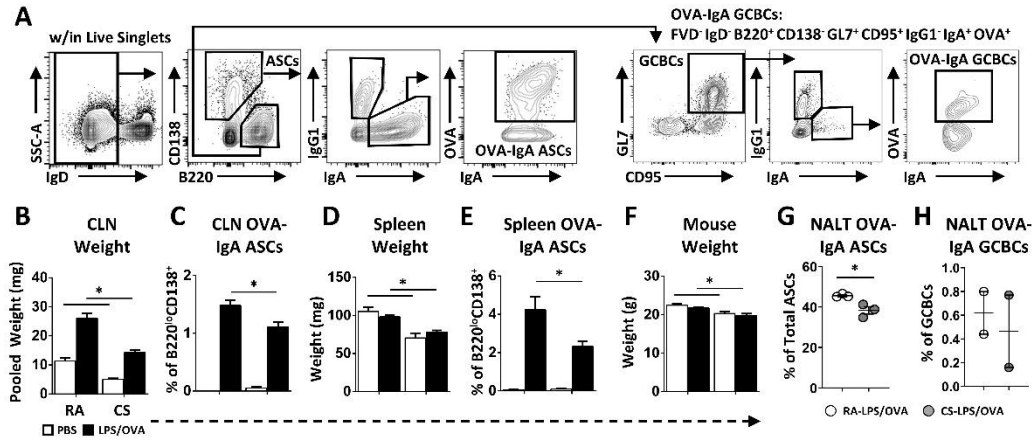


Figure S3. Extended data for Figure 4. (A) Gating strategies for ASCs and germinal centre B cells (GCBCs) in the draining lymphoid tissues. Mice exposed to room air (RA) or cigarette smoke (CS) for one week were intranasally immunized with LPS/OVA as described in Figure 1, and the NALT, CLNs and spleen were assessed by flow cytometry at 3dpb. (B) Pooled CLN weight per mouse. (C) CLN OVA-IgA ASCs were quantified by flow cytometry, and are represented as proportion of total ASCs. (D) Spleen weight per mouse. (E) Spleen OVA-IgA ASCs represented as proportion of total ASCs. (F) Mouse weight (grams) at endpoint. (G) NALT OVA-IgA ASCs and (H) OVA-IgA GCBCs represented as a proportion of total ASCs. NALT data points represent the means of pooled samples (n=5-7 mice per group per experiment) from (G) three and (H) two independent experiments. (G,H) Student's unpaired t-test, all others two-way ANOVA with Tukey's post-hoc test. Mean \pm SEM. * <0.05 .

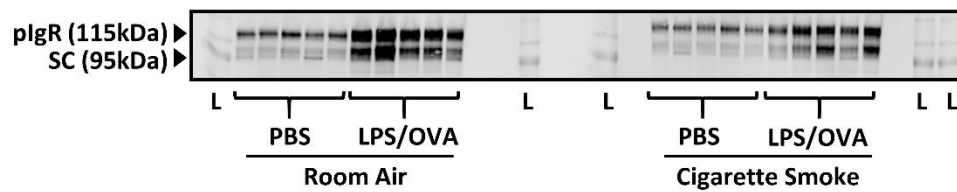


Figure S4. Extended data for Figure 6. The uncropped version of the blots in Figure 6 is presented above. pIgR: polyimmunoglobulin receptor; SC: secretory component; L: molecular weight ladder.

Table S1. Antibodies and other stains used for flow cytometry in this study.

Flow Cytometry Antibodies					
Target	Conjugate	Clone	Company	Catalog No.	Dilution
CD16/32 (Block)	None	93	Biologend	101302	100
IgD	BV711	11-26c.2a	Biologend	405731	400
B220	PerCPCy5.5	RA3-6B2	Biologend	103236	100
CD138/Syndecan-1	PEDazzle594	281-2	Biologend	142528	100
GL7	AF488	GL7	eBioscience	53-5902-82	400
CD95	PECy7	Jo2	BD Biosciences	557653	100
IgG1	BV421	RMG1-1	Biologend	406616	100
IgA	BV650	C10-1	BD Biosciences	743296	100
Integrin α 4/CD49d	AF488	R1-2	Biologend	103611	100
Integrin β 1/CD29	PECy7	HM β 1-1	Biologend	102222	100
Other Flow Cytometry Stains					
Name	Fluorophore	Clone	Company	Catalog No.	Dilution
OVA	AF647	n/a	Molecular Probes	O34784	100
LIVE/DEAD Fixable Yellow Stain	n/a	n/a	Molecular Probes	L34967	400

Table S2. Number of sequencing reads and clones per sample.

Sample	Reads/Sample	Clones/Sample
ra_ctrl1	61210	3116
ra_ctrl2	64785	4917
ra_ctrl3	69751	4812
ra_imm4	81378	9830
ra_imm5	65909	6340
ra_imm6	87709	7263
ra_imm7	58549	604
ra_imm8	87136	7192
ra_imm9	91280	12288
ra_imm11	34245	4484
ra_imm12	44466	4108
cs_ctrl14	82346	2763
cs_ctrl15	41990	2130
cs_ctrl16	67601	3245
cs_imm17	144540	4695
cs_imm18	26723	2386
cs_imm19	74726	2758
cs_imm21	84191	5862
cs_imm22	87236	5624
cs_imm23	68375	3052
cs_imm24	28861	2222
cs_imm25	72845	3983
cs_imm26	81085	5750

CHAPTER 3 – Detecting Immunoglobulins in Processed Sputa

Steven P. Cass*, Joshua J.C. McGrath*, Kiho Son, Katherine Radford,
Nicola LaVigne, Ditte K. Klein, Sisse B. Ditlev, Celeste Porsbjerg,
Parameswaran Nair, Martin R. Stämpfli, Manali Mukherjee

**co-first author*

Manuscript Status: Published; *Allergy*, John Wiley and Sons, Ltd.

Copyright © 2021 The Authors. Reprinted with permission (see Appendix 1).

Citation: Cass SP*, **McGrath JJC***, Son K, et al. Detecting immunoglobulins in processed sputa. *Allergy*. doi: 10.1111/all.15049. *Denotes co-first authors.

Co-First Author Contributions: Steven Cass and I contributed equally to all aspects of the study as described below.

Contributions: SPC, MM, MRS, PN conceived the study design. JJCM, SPC, DKK, SBD, KR, MM conducted experiments. SPC, JJCM analysed the data. KS contributed to manuscript development. NL, KR collected sputum samples. JJCM, SPC and MM wrote the manuscript with input from all authors. MRS secured funding for the study.

Study Overview: In this study, we assess the effect of PBS- vs DTT-based sputum processing on antibody (IgA, IgG, IgM, IgE) recovery and stability. We find that DTT improves the recovery of total IgA and a specific IgG autoantibody from sputum, while reducing IgE yield.

To the editor,

Induced sputum is regarded as a gold standard for the assessment of airway inflammation in asthma; in addition to a standard differential cell count, a range of inflammatory markers can be assessed. Two sputum processing methods are routinely employed, which use either a dithiothreitol (**DTT**)¹ or phosphate-buffered saline (**PBS**)² disbursement step. This step is crucial for effective mucous dispersal and analyte recovery. Immunoglobulins (**Igs**) are commonly investigated analytes in respiratory research due to their importance in humoral protection against respiratory pathogens and potential autoimmune functions. However, the differential impact of PBS/DTT processing on Ig detection has not been investigated.

For this purpose, excess sputum plugs (100-300mg, post-clinical processing) were successively collected from 22 clinically-indicated patients with severe asthma (n=19/22), eosinophilic granulomatosis with polyangiitis (EGPA; n=4/22) (**Table S1**) on varying treatments (median 64.5 years [34-80]). To note, 5/22 sputum samples were produced spontaneously, while the remaining were induced following the protocol outlined by Pizzichini *et al.*¹. Selected sputum plugs were split equally and processed concurrently using either PBS (8:1v/v)² or DTT (0.1%; 4:1v/v, followed by 4:1v/v PBS)¹ and processed within 2-hours of expectoration (**Figure 1**).

After processing, the resultant matched cell-free supernatants were initially assessed for total IgM, IgA and IgG using previously described ELISAs developed in-house³ (**Online Supplement**). The processing buffer used did not affect IgM or IgG yields; however, DTT increased IgA yield compared to PBS (**Figure 2A**). Recoverable Ig strongly correlated post-PBS and DTT processing (**IgM**: $r=0.68$, $p=0.0004$; **IgG**: $r=0.89$, $p<0.0001$; **IgA**: $r=0.72$, $p=0.0002$) and showed modest agreement on Bland-Altman analysis, except IgA which demonstrated a clear bias towards DTT (**Figure 2A**). Of note, the induction method (spontaneous or induced), was not associated with any trends in Ig recovery (**Table S2**). No difference in spiked Ig recovery was observed between buffers (**IgM**: PBS: $51.7\pm 14.8\%$, DTT: $48.3\pm 13.9\%$; **IgG**: PBS: $40.2\pm 6.8\%$, DTT: $42.7\pm 6.6\%$; **IgA**: PBS: $35.3\pm 8.5\%$, DTT: $37.2\pm 6.2\%$). Lastly, due to the low abundance of IgE in sputum⁴ we assessed IgE using a validated bead assay system, finding that DTT decreased IgE recovery (**Figure 2B**). Overall, although IgM and IgG yields were comparable, DTT processing was associated with a moderate improvement in recoverable IgA and decreased IgE.

For freeze-thaw (**FT**) analysis, individual aliquots were freeze-thawed up to four times on ice on consecutive days. In PBS-treated samples, an increase in IgM was observed following FT2/3 compared to FT1 (**Figure 2C**) potentially resulting from a breakdown in pentameric structure and increased monomer detection. In DTT-treated samples, a modest decrease in IgG was observed between FT2 and FT3. No other significant changes were observed. Overall, these data show that

serial freeze-thaw cycles only marginally reduce sputum Ig recovery, with neither PBS nor DTT providing a clear benefit to stability.

We next assessed the impact of processing buffers on the recovery of total antibodies and anti-eosinophil peroxidase (**EPX**) IgG following immunoprecipitation, as described previously³. The recovery of Ig was less than 20% of neat supernatants, independent of processing buffer (**Figure 2D**). We observed a significant increase in IgA recovery, and a trend to increase for IgG, in immunoprecipitated fractions from DTT-processed sputa (**Figure 2D**). This difference was further evident in the increased detection of anti-EPX IgG in an independent group of severe asthma patients (n=62, from the SATS cohort⁵) (**Figure 2E**). In summary, DTT processing improved the recovery of IgA and enhanced detection of a disease-relevant IgG autoantibody³ following immunoprecipitation.

DTT is a mucolytic agent that reduces glycoprotein disulphide bonds, improving the recovery of cytokines and cells from sputum⁶. The optical isomer of DTT, dithioerythritol, has previously been reported to increase IgA recovery in sputum⁷. Being a mucolytic agent, DTT offers greater consistency in mucus plug dispersal to release soluble components such as Ig. In this regard, we found that mucus plug disbursement was occasionally incomplete when using PBS (observational data on bench, not shown) which may interfere with immunoprecipitation processing. Notably, the reductive activity of DTT responsible for mucolysis is also proposed to degrade IgM and IgE at high

concentrations^{8,9}. Using the protocol defined by Pizzichini *et al*¹, we did not observe decreased IgA, IgG or IgM recovery, or vast differences in the freeze-thaw stability of these isotypes between buffers. However, sputum IgE was sensitive to denaturation in this context.

In summary, we report that PBS/DTT sputum processing buffers are largely comparable in terms of IgG and IgM recovery; however, DTT increased total IgA and immunoprecipitated IgG/A recovery but decreased total IgE. Without any apparent risk to Ig stability, we recommend DTT as the preferential processing buffer for total and specific IgM/A/G analysis, and PBS processing for total IgE analysis in sputum.

Ethics: Ethical approval was received from Hospital Research Ethics Board, St Joseph's Hospital, Hamilton (Project #12-371) and the local Ethics Committee, Region H, Copenhagen (H-1-2014-047).

References

1. Pizzichini, E., Pizzichini, M. M., Efthimiadis, A., Hargreave, F. E. & Dolovich, J. Measurement of inflammatory indices in induced sputum: effects of selection of sputum to minimize salivary contamination. *Eur. Respir. J.* **9**, 1174–80 (1996).
2. Bafadhel, M. *et al.* Profiling of sputum inflammatory mediators in asthma and chronic obstructive pulmonary disease. *Respiration* **83**, 36–44 (2012).
3. Mukherjee, M. *et al.* Sputum autoantibodies in patients with severe eosinophilic asthma. *J. Allergy Clin. Immunol.* **141**, 1269–1279 (2018).
4. Mukherjee, M. *et al.* Airway autoimmune responses in severe eosinophilic asthma following low - dose Mepolizumab therapy. *Allergy, Asthma Clin. Immunol.* (2017) doi:10.1186/s13223-016-0174-5.
5. Von Bülow, A. *et al.* Differentiation of adult severe asthma from difficult-to-treat asthma – Outcomes of a systematic assessment protocol. *Respir. Med.* 41–47 (2018) doi:10.1016/j.rmed.2018.10.020.
6. Efthimiadis, A., Pizzichini, M. M. M., Pizzichini, E., Dolovich, J. & Hargreave, F. E. Induced sputum cell and fluid-phase indices of inflammation: Comparison of treatment with dithiothreitol vs phosphate-buffered saline. *Eur. Respir. J.* **10**, 1336–1340 (1997).
7. Louis, R. *et al.* The effect of processing on inflammatory markers in induced sputum. *Eur. Respir. J.* **13**, 660–667 (1999).
8. Okuno, T. & Kondelis, N. Evaluation of dithiothreitol (DTT) for inactivation of IgM antibodies. *J. Clin. Pathol.* **31**, 1152–1155 (1978).
9. Rousseaux-Prévost, R., Rousseaux, J., Bazin, H. & Biserte, G. Differential reduction of the inter-chain disulfide bonds of rat immunoglobulin E: Relation to biological activity. *Mol. Immunol.* **21**, 233–241 (1984)

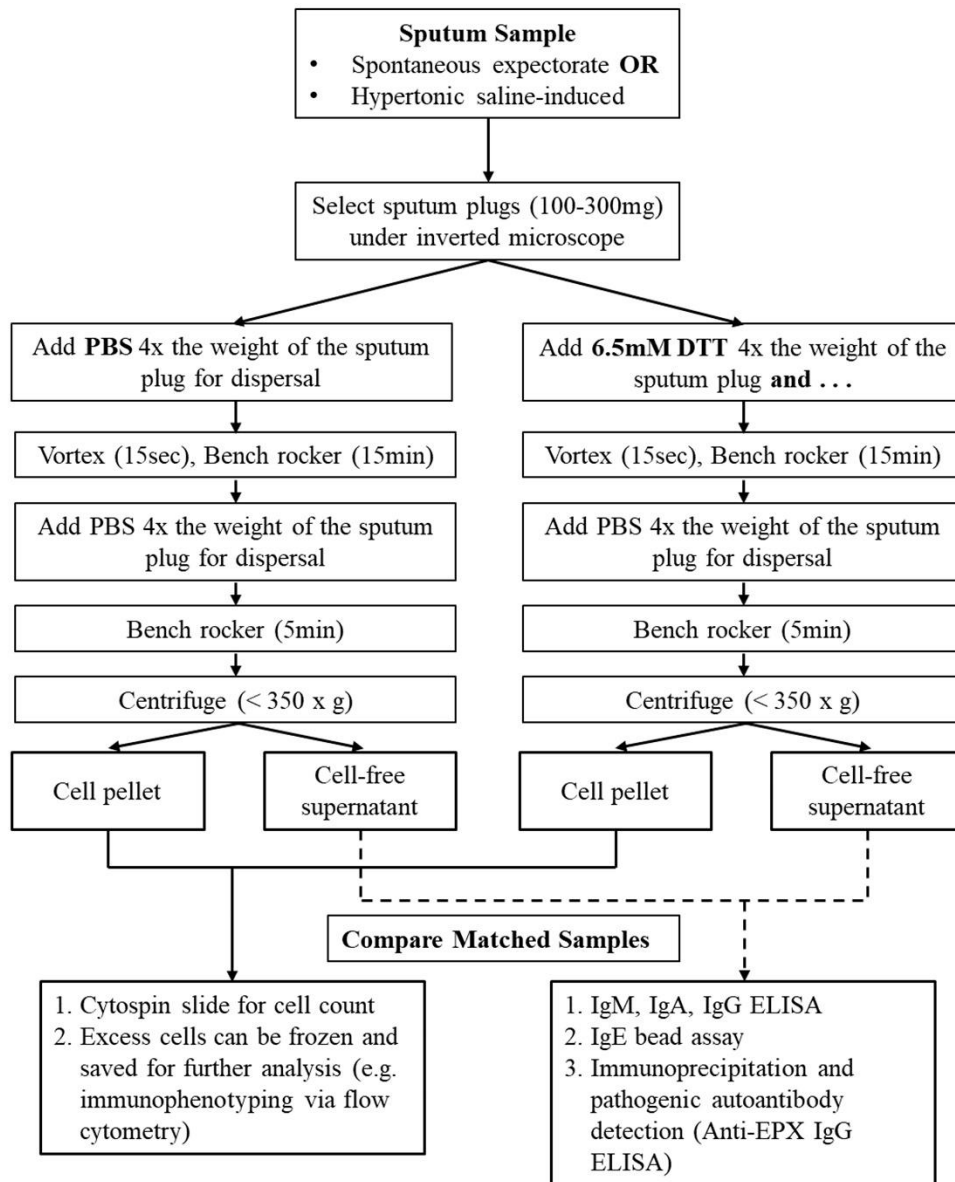


Figure 1. Schematic of matched sputum processing. Sputum samples were split and processed with (i) PBS equal to eight times the weight², or (ii) with 6.5mM DTT equal to four times the initial weight followed by PBS equal to four times the initial weight¹. Each processing method resulted in matched samples with equal dilutions normalized to the weight of the selected plug. 10 μ l of protease inhibitor cocktail was added to all processed supernatants.

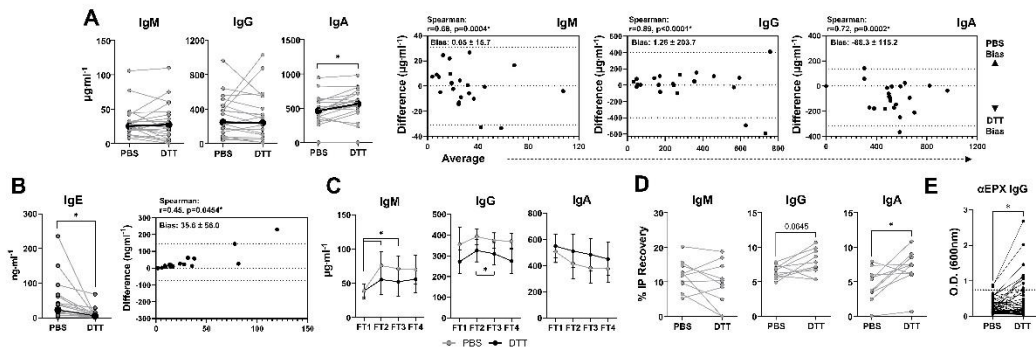


Figure 2. DTT processing moderately improves sputum IgG and IgA recovery, but reduces IgE. (A) Total IgM, IgG and IgA were measured by ELISA in matched PBS- or DTT-processed neat sputum supernatants. Bolded dots represent medians. Bland Altman analysis plots for each Ig subtype are given, with dotted lines as the confidence intervals. (B) IgE was measured by bead assay. Bolded dots represent medians. (C) Serial freeze-thaw (FT) analysis in neat sputum. Data represents mean \pm SEM. (D) Total IgM, IgG and IgA were measured in immunoprecipitated (IP) sputum fractions. (E) Anti-eosinophil peroxidase (EPX) IgG was measured in IP sputum fractions from an external cohort (SATs) using the exact sputum processing methods. Paired t-test with Wilcoxon paired-rank correction (A,B,D,E). Two-way repeated measures ANOVA with Tukey's multiple comparisons (C). * $p<0.05$, GraphPad Prism 9.1 (GraphPad Software, Inc).

Table S1. Patient Demographics.

Patient	Age	Gender	Diagnosis	Airway inflammation	IP	FT	Induced/ Spontaneous
1	53	M	Asthma	Eosinophilic			Induced
2	80	M	Asthma	Eosinophilic			Induced
3	60	M	Asthma	Eosinophilic		Y	Induced
4	55	F	Asthma	No Inflammation		Y	Induced
5	57	F	Asthma	Neutrophilic	Y	Y	Induced
6	56	F	Asthma	No Inflammation	Y	Y	Induced
7	76	F	EGPA	No Inflammation	Y	Y	Spont.
8	64	M	Asthma	No Inflammation	Y		Spont.
9	70	F	Asthma	Eosinophilic	Y	Y	Induced
10	50	M	Asthma	No Inflammation			Induced
11	74	M	Asthma	No Inflammation	Y	Y	Spont.
12	77	F	Asthma	Eosinophilic	Y		Induced
13	34	F	EGPA	Eosinophilic			Induced
14	77	M	Asthma	No Inflammation			Induced
15	78	F	EGPA	Eosinophilic			Induced
16	59	F	Asthma	Eosinophilic	Y	Y	Induced
17	65	F	Asthma	Eosinophilic	Y	Y	Spont.
18	70	M	Asthma	No Inflammation	Y		Spont.
19	76	M	Asthma, EGPA	No Inflammation		Y	Induced
20	66	M	Asthma	Eosinophilic			Induced
21	47	M	Asthma	Eosinophilic			Induced
22	57	F	Asthma	Neutrophilic			Induced
*IP/FT - Inclusion of patient in immunoprecipitation / freeze-thaw analysis (Y: yes)							
EGPA - Eosinophilic granulomatosis with polyangiitis							

Table S2. Spontaneous vs. Induced Sputum Analysis

	IgG				IgA			
	PBS		DTT		PBS		DTT	
	Induced	Spont	Induced	Spont	Induced	Spont	Induced	Spont
Mean ± SD	300.5 ± 227.8	331.6 ± 249.7	309.8 ± 283.3	294.7 ± 247.8	448.4 ± 182.8	572.4 ± 209.7	549.2 ± 217.2	618.1 ± 204.3
p-value	0.811		0.911		0.278		0.534	
	IgM				IgE			
	PBS		DTT		PBS		DTT	
	Induced	Spont	Induced	Spont	Induced	Spont	Induced	Spont
Mean ± SD	32.6 ± 25.3	24.8 ± 10.5	32.5 ± 26.6	25.0 ± 30.4	53.2 ± 64.1	34.0 ± 27.6	12.8 ± 17.3	11.0 ± 6.5
p-value	0.331		0.636		0.391		0.747	

Supplementary Methods

Total Ig ELISAs

Briefly, 50µl of ChromPure Ig (IgM/A/G) (Jackson ImmunoResearch, USA) standard or sample was diluted in PBS (IgM (1:100), IgA/G (1:500)) and incubated for 90 minutes at 37°C using 96 well Maxisorp Nunc plates (#44-2404-21, ThermoFisher Scientific). For Ig spiked assays, a fixed concentration of each ChromPure Ig standards were added to matched DTT and PBS-treated samples. All wells were stringently washed (#5150-0011 KPL wash buffer, LGC sera-care), blocked for one hour at room temperature (KPL blocking buffer #5440-0001) and probed with 50µl/well secondary antibody (1:2000, Biotin Mouse Anti-Human IgG/IgA/IgM, BD Biosciences #555785, 555884, 555781). After a one-hour incubation, all sample wells were developed using alkaline phosphatase based-detection reagents (BluePhos #5120-0061, Stop solution #5150-0026 KPL) and read at 595 nm (SpectraMax i3x, Molecular Devices). IgE was detected in undiluted samples using a bead assay conducted by Eve Technologies (Calgary, AB, Canada).

CHAPTER 4 – Cigarette smoke augments CSF3 expression in neutrophils to compromise alveolar-capillary barrier function during influenza infection

Joshua J.C. McGrath*, Gilles Vanderstocken*, Anna Dvorkin-Gheva,
Steven P. Cass, Sam Afkhami, Matthew F. Fantauzzi, Danya Thayaparan,
Amir Reihani, Peiyao Wang, Ashley Beaulieu, Pamela Shen, Mathieu Morissette,
Rodrigo Jimenez-Saiz, Arata Tabuchi, Diana Zabini, Warren L. Lee,
Carl D. Richards, Matthew S. Miller, Kjetil Ask, Wolfgang Kuebler,
Jeremy A. Simpson, Martin R. Stämpfli

**co-first authors*

Manuscript Status: Under Review, *European Respiratory Journal*

Co-First Author Contributions: This study was initiated by Dr. Gilles Vanderstocken and continued by myself after his departure. **Ultimately, I generated data amounting to all of Figures 2-8 and S2-S4 and an equal part of Figures 1/S1. In addition, I wrote the manuscript and am performing revisions.** Dr. Vanderstocken established the model, defined a number of the key experimental readouts, and contributed data amounting to an equal part of Figures 1/S1.

Contributions: JJCM, GV and MRS conceived the study and designed the experiments. JJCM, GV, SPC, SA, MFF, DT, PW, AB, RJS, PS, MM, AT, DZ conducted experiments. ADG conducted bioinformatic analysis of scRNAseq data, while JJCM compiled scRNAseq data. AR performed HALO analysis. WLL, KA, WK, CDR, MSM and JAS provided technical insights for experimental design. JJCM and MRS wrote the manuscript with feedback from all authors. MRS secured funding for the study.

Abstract

Background: Cigarette smokers are at increased risk of acquiring influenza, developing severe disease, and requiring hospitalization/ICU admission following infection. However, immune mechanisms underlying this predisposition are incompletely understood, and therapeutic strategies for influenza are limited.

Methods: We used a mouse model of concurrent cigarette smoke exposure and influenza (A/FM/1/47-MA) infection, colony-stimulating factor (CSF)3 supplementation/receptor (CSF3R) blockade, and single-cell RNA sequencing (scRNA-seq) to elucidate mechanisms underpinning this relationship.

Results: Cigarette smoke exposure exacerbated features of viral pneumonia such as edema, hypoxemia, and pulmonary neutrophilia. Smoke-exposed, infected mice demonstrated an increase in viral (v)RNA, but not replication-competent viral particles, relative to infection-only controls. Interstitial rather than airspace neutrophilia positively predicted morbidity in smoke-exposed, infected mice. Screening of pulmonary cytokines using a novel dysregulation score identified an exacerbated expression of CSF3 and interleukin (IL)-6 in the context of smoke exposure and influenza. Recombinant (r)CSF3 supplementation during influenza aggravated morbidity, hypothermia, and edema, while anti-CSF3R treatment of smoke-exposed infected mice improved alveolar-capillary barrier function. scRNA-seq delineated a shift in the distribution of *Csf3*⁺ cells towards neutrophils in the context of cigarette smoke and influenza. However, although smoke-exposed lungs were enriched for infected, highly-activated neutrophils, gene signatures of

these cells largely reflected an exacerbated form of typical influenza with select unique regulatory features.

Conclusion: This work provides novel insight into the mechanisms by which cigarette smoke exacerbates influenza infection, unveiling potential therapeutic targets (CSF3R blockade, excess vRNA accumulation) for use in this context and clinical limitations to rCSF3 therapy for neutropenia during viral infectious disease.

Introduction

The ongoing tobacco-related disease pandemic represents the leading cause of preventable death worldwide[1]. Significant contributors to this excess mortality include smoking-induced cardiovascular disease, chronic obstructive pulmonary disease (COPD), numerous cancers, as well as infectious diseases such as pneumonia[2]. Within the spectrum of pneumonic microbial agents, one that is of particular concern to smokers is the influenza virus. Individuals that smoke are at a significantly greater risk of developing laboratory-confirmed influenza[3], progressing to severe disease[4], and being admitted to hospital/ICU following infection[5]. Influenza is furthermore a prominent cause of acute exacerbations in patients with COPD[6], a disease caused primarily by smoking, and is an actively growing contributor to mortality in this patient population[7]. Ultimately, the relationship between smoking and influenza represents a serious global health concern given that over 1.1 billion people continue to smoke tobacco worldwide[8].

To date, mechanisms by which cigarette smoke aggravates influenza are incompletely defined. In mice, concurrent smoke exposure exacerbates influenza-induced weight loss[9], pulmonary apoptosis[10], fibrosis[11], and mortality[12]. These effects are accompanied by an exaggerated production of inflammatory cytokines, and an enhanced infiltration of leukocytes such as neutrophils into the lungs[9, 13, 14]. Although there is evidence indicating that neutrophils are important to influenza resolution[15–17], severe disease is frequently associated with excess neutrophilia[18, 19] and partial neutrophil depletion reduces mortality in mice[19]. Overall, this suggests that neutrophils can contribute to negative outcomes during severe influenza[20]. In this regard, neutrophils produce factors such as extracellular traps (NETs), decondensed chromatin strands coated with myeloperoxidase and neutrophil elastase, which may compromise alveolar-capillary barrier function and potentiate inflammation[21–23]. However, although numerous neutrophilic chemokines have been identified, none have been unambiguously implicated in the pathogenesis of severe influenza to date, thus precluding the development of neutrophil-oriented chemokine blockade therapies for viral infectious disease.

In the current study, we conducted a comprehensive investigation of physiological, edematous, and inflammatory sequelae in a clinically-relevant mouse model of concurrent cigarette smoke exposure and influenza infection. We observed key features of viral pneumonia that were exacerbated by cigarette smoke, including edema and hypoxemia, and determined that infiltration of neutrophils in

the pulmonary interstitium rather than airspaces positively correlates with disease severity. Viral (v)RNA load was elevated in the context of smoke exposure independent of replicating viral particles. Furthermore, through a novel dysregulation scoring approach we identified interleukin (IL)-6 and colony stimulating factor (CSF)3 expression as being exacerbated in smoke-exposed, infected lungs. Functionally, CSF3 supplementation during influenza enhanced morbidity, hypothermia, and edema, while anti-CSF3 receptor (CSF3R) treatment improved alveolar-capillary barrier function. Using single cell RNA sequencing (scRNA-seq), we identified neutrophils as a novel source of *Csf3* in the lungs and defined a skew in the distribution of *Csf3*-expressing cells towards neutrophils in the context of smoke exposure and infection. Finally, by comparing transcriptional patterns between groups we demonstrate that gene signatures from cigarette smoke-exposed neutrophils resemble exacerbated influenza-typical responses with unique regulatory features.

Results

Cigarette smoke exacerbates influenza-induced morbidity, edema and hypoxemia in mice.

To assess the effect of smoke exposure on influenza infection, BALB/c mice were exposed to room air (RA) or cigarette smoke (CS) for two weeks and intranasally infected with 50 plaque-forming units (PFUs) of mouse-adapted influenza A/Fort Monmouth/1/1947 (H1N1; “FM1”). After a two-day rest, smoke exposure was

continued until 7dpi at which time animals were euthanized (**Figure 1a**). Influenza infection induced significant weight loss (**Figure 1b**) and hypothermia (**Figure 1c**) which were exacerbated by concurrent cigarette smoke exposure. Core body temperature strongly correlated with weight loss (**Figure S1a**), supporting previous work that has defined hypothermia as a reliable predictor of morbidity and mortality in mouse models of influenza infection[24]. CS-FM1 animals also exhibited significant reductions in peripheral blood O₂ saturation (SpO₂) as measured by pulse oximetry; oxygen levels were quantitatively reduced, and a greater number of smoke-exposed (13/15, 86.7%) than room air-exposed animals (4/15, 26.7%) had desaturated below 92% (a clinical threshold for hypoxemia) following infection (**Figure 1d**). These mice also demonstrated a higher symptom score at 7dpi (**Figure 1e**). CS-FM1 animals reached endpoint (based on predetermined symptom score thresholds) between 7dpi and 9dpi (**Figure 1f**), while RA-FM1 mice did not. In terms of viral burden, CS-FM1 mice demonstrated no difference in PFUs in lung homogenates at 7dpi (**Figure 1g**), although an increased expression of hemagglutinin (*HA*) mRNA was observed relative to RA-FM1 controls (**Figure 1h**). *HA* expression showed a significant negative correlation with core temperature in both groups (**Figure 1i**), while PFUs exhibited no relationship (**Figure S1b**). Overall, these data demonstrate that cigarette smoke exposure exacerbates the severity of influenza in association with a PFU-independent accumulation of vRNA in the lungs.

Severe cases of influenza are characterized by the loss of alveolar-capillary barrier integrity and leakage of hematogenous fluids into the airspaces to an extent that compromises gas exchange. In this regard, smoke-exposed, infected mice exhibited an increased lung wet-to-dry weight ratio compared to all controls (**Figure 1j**) and areas of significant fluid accumulation around peri-bronchial blood vessels (**Figure S1c**). Moreover, levels of the high-molecular weight serum protein albumin were significantly elevated in the bronchoalveolar lavage fluid (BALF) of CS-FM1 animals relative to all other groups (**Figure 1k**). Evidence of pulmonary edema was associated with an elevated hematocrit (**Figure 1l**), consistent with hypoxic conditions and potential fluid translocation from the systemic compartment into the lungs. Mechanistically, we observed a reduced expression of vascular endothelial (VE)-cadherin, a molecule critically involved in maintaining endothelial adherens junctions, in the lung tissue of CS-FM1 animals relative to controls (**Figure 1m**). Overall, these data provide evidence that cigarette smoke-augmented influenza is characterized by exacerbated pulmonary edema and arterial hypoxemia in association with excessive impairment of the alveolar-capillary barrier.

Accumulation of neutrophils in the pulmonary interstitium rather than airspaces correlates with disease severity in influenza.

In our model, concurrent smoke exposure promoted morbidity and mortality following influenza infection. Given that excess neutrophilia has been frequently associated with severe disease[18, 19], we next performed a flow cytometric analysis of cells in the bronchoalveolar lavage (BAL), lungs, and blood (gating strategy in **Figure S2a**). Total cellularity in the lungs and BAL increased following infection but was similar between infected groups (**Figure S2b**). However, smoke exposure significantly increased the number of neutrophils in the BAL and lung in CS-FM1 mice compared to all controls (**Figure 2a/b/d**). In the blood, CS-FM1 mice exhibited an increase in the proportion, but not absolute number, of neutrophils relative to infection-only controls (**Figure 2e**). In contrast to neutrophils, monocyte/macrophage-lineage cells were either reduced or unchanged by smoke exposure in all compartments relative to infection alone, and both total and activated ($CD44^{hi}CD69^{+}$) $CD4^{+}/CD8^{+}$ T cells were consistently reduced in CS-FM1 relative to RA-FM1 lungs (**Figure S2c**). In line with the observed neutrophilia, peroxidase activity, which may be attributed to neutrophil myeloperoxidase, was elevated in the BAL fluid (BALF; **Figure 2c**). Overall, cigarette smoke exposure skewed the nature of cellular infiltrates induced by influenza towards a neutrophil-dominant state with reduced monocyte-lineage cells and T cells.

The elevated neutrophilia in highly morbid CS-FM1 animals prompted us to hypothesize that mice with lower core temperature would demonstrate a greater airspace neutrophilia. However, we found a positive correlation indicating that CS-FM1 animals with lower body temperature had lower BAL neutrophils (**Figure 2f**). RA-FM1 mice demonstrated no significant relationship. This was not due to differences in BAL recovery efficiency (**Figure S2d**). To explain this finding, we evaluated metrics of neutrophil death in CS-FM1 airspaces. In this regard we detected increases in cell-free (cf)DNA in the BALF of CS-FM1 animals relative to controls (**Figure 2g**). However, cfDNA levels did not significantly correlate with core temperature (**Figure S2e**). In addition, flow cytometry data showed fewer dead neutrophils in CS-FM1 airspaces (**Figure 2h**), which again demonstrated no relationship with hypothermia (**Figure S2f**). Next, we developed an airspace-to-tissue neutrophil (ATN) ratio, which indicated that a differential accumulation of neutrophils in the interstitium relative to the airspaces may correlate with negative outcome (**Figure S2g/h**; refer to **Supplementary Results**). To elaborate on this finding, we quantified interstitial neutrophils in lung tissue microarrays by histology and found that CS-FM1 mice had significantly more Ly6G⁺ cells in the interstitium relative to controls (**Figure 2i, S2i**). Furthermore, there was a positive correlation between the number of interstitial neutrophils and weight loss in infected animals as a whole (**Figure 2j**). Overall, these data show that the distribution of recruited neutrophils across pulmonary niches provides critical

information about prognosis, with interstitial rather than airspace neutrophilia being the positive predictor of morbidity.

Progressive positive dysregulation of CSF3 and IL-6 in the lungs and systemic circulation characterizes cigarette smoke-augmented influenza.

Because neutrophils were elevated in CS-FM1 lungs, we next sought to broadly assess the effect of cigarette smoke on cytokine responses following influenza infection. Lung homogenates were generated at both 5dpi and 7dpi and analysed using a 31-plex bead array (**Figure 3a/d, S3**). To determine the extent to which cigarette smoke dysregulates each cytokine, we developed a “dysregulation score” which quantifies changes in expression in CS-FM1 mice relative to CS-PBS and RA-FM1 control groups (**Figure 3b left**, validation in **Figure S3a; Supplementary Methods**). Using this approach, we identified several cytokines that were highly dysregulated in the context of cigarette smoke exposure at 7dpi, including IL-6, leukemia inhibitory factor (LIF), CSF3, and CCL2 (**Figure 3b middle, File S1**). Scores were consistent across experimental replicates (**Figure 3b right**). Globally, mean dysregulation scores increased significantly between 5dpi and 7dpi (**Figure 3c**). Moreover, when individual cytokines were binned according to their change in dysregulation score between these timepoints (**Figure 3c, File S1**), 59.4% (e.g. IL-6, CSF3, CCL2 and LIF; **Figure 3d**) were positively dysregulated, as compared to the 31.3% and 9.4% which demonstrated progressive normalization (e.g. TNF- α)

and negative dysregulation (e.g. IL-4) respectively. qPCR analysis of whole lung tissue confirmed that differences in IL-6, CSF3, and LIF were related to increased transcriptional activity (**Figure 3e**). Interestingly, although IL-6 protein dominated in lung homogenates, CSF3 levels were highest in the plasma, while LIF was largely undetectable (**Figure 3f**). In terms of morbidity, a significant negative correlation was observed between plasma CSF3 levels and core temperature in CS-FM1 mice (**Figure 3g**), while IL-6 demonstrated a similar but non-significant trend. Overall, these data suggest that CSF3 and IL-6 are progressively dysregulated in the lungs and circulation during the late stages of cigarette smoke-augmented influenza, with plasma CSF3 levels positively predicting disease severity.

CSF3 exacerbates morbidity and alveolar-capillary barrier dysfunction during influenza infection.

Given that CSF3 and IL-6 were two of the most dysregulated neutrophil-related cytokines in our system, we next sought to assess the effect of recombinant (r)CSF3 or rIL-6 supplementation over the background of influenza infection. Between 4-6dpi, four doses of either cytokine or PBS vehicle were administered intranasally to infected mice. Animals were culled at 6dpi, three hours after the last dose (**Figure 4a**). Relative to FM1+PBS controls, mice receiving rCSF3 demonstrated greater symptom scores than those receiving vehicle or rIL-6 (**Figure 4b**). While rCSF3 supplementation did not modify weight loss (**Figure 4c**), an exacerbated

hypothermia was observed (**Figure 4d**). In comparison, rIL-6-treated animals exhibited a modest additional decrease in weight, and a near-significant increase in temperature, relative to PBS-treated controls. Hypoxemia was noted only sporadically in all influenza-infected groups (**Figure 4e**). Interestingly, supplementation with rCSF3 increased BALF albumin levels over infection plus PBS vehicle, while rIL-6 substantially reduced them (**Figure 4f**). rCSF3 produced a marked increase in neutrophils in both whole lung tissue and blood, but not the airspaces (**Figure 4g**). Notably, lung neutrophils recruited by rCSF3 expressed lower levels of surface Ly6G (**Figure 4h**), indicative of a young/immature cell state[25]. In comparison, although rIL-6 increased blood neutrophil levels it did not elicit any additional neutrophilia in the lungs over the background of influenza. In summary, these data demonstrate that excess CSF3 can promote alveolar-capillary barrier dysfunction and exacerbate morbidity during influenza infection.

CSF3R blockade improves alveolar-capillary barrier function during smoke-augmented influenza

Because CSF3 supplementation appeared to promote excess morbidity and edema, we next assessed whether CSF3R blockade could ameliorate negative outcomes in our model. To do so, CS-FM1 mice were treated intraperitoneally with an anti-CSF3R antibody or isotype control at 2, 4, and 6dpi, and culled at 7dpi (**Figure 5a**). Despite substantially reducing neutrophils in the whole lung tissue and blood (but

not airspaces; **Figure 5b**), CSF3R blockade did not alter endpoint symptom score (**Figure 5c**), weight loss (**Figure 5d**), core temperature (**Figure 5e**), or oxygen saturation (**Figure 5f**). However, reciprocal to supplementation experiments anti-CSF3R reduced BALF albumin relative to isotype control (**Figure 5g**). Thus, CSF3R blockade was able to improve alveolar-capillary barrier function during smoke-augmented influenza.

scRNAseq identifies neutrophils as a dominant expressor of *Csf3* and reveals a skew in the distribution of *Csf3*-producing cells in CS-FM1 mice.

After finding a significant dysregulation of CSF3 and IL-6 in CS-FM1 mice, we next assessed whether cigarette smoke altered the distribution of cytokine-expressing cells relative to infection alone. Single cell suspensions generated from the lungs of RA-PBS (n=5 mice pooled, 1899 cells), RA-FM1 (n=5 mice pooled, 2307 cells) and CS-FM1 mice (n=4 mice pooled, 2308 cells) at 7dpi were analysed (**Figure 6a left**). Linear dimensionality reduction via principal component analysis (PCA) followed by UMAP clustering yielded 15 cell clusters which were grouped into 9 different cell identities based on their expression of *a priori* established canonical genes (**Figure 6a top-right, S4a**). In line with flow cytometry data, neutrophils expanded with influenza infection and further still in the context of smoke, while macrophage and T cell populations remained stable and contracted, respectively, between infection groups (**Figure 6a bottom-right**). Both *Csf3* and

Il6 were detectable in our dataset (**Figure 6b**); the overall total number of *Csf3*⁺ and *Il6*⁺ cells increased with influenza infection alone and more so with exposure to cigarette smoke (**Figure 6c**). In terms of distribution, interstitial macrophages/monocyte-lineage cells (IM/MLCs) comprised the largest fraction of cell types expressing each cytokine, and were the largest inducible population following infection. Neutrophils were also significant expressors of *Csf3*, with some transcripts being additionally observed in resident alveolar macrophages (rAMs), endothelial cells and classical DC (cDC)1s. For *Il6* T cells were the next most populous expressors after IM/MLCs, although this population contracted with infection. Additional transcripts were detected in cDC1s, endothelial cells, neutrophils, B cells, rAMs and epithelial cells (**Figure 6c**).

Because functional experiments indicated a detrimental role for CSF3 during influenza infection, we focused further on this molecule. Although there was no significant difference in *Csf3* expression between groups/cell types, *Csf3*⁺ neutrophils expressed approximately 2.9-fold higher levels of the transcript than IM/MLCs (**Figure 6d**). Neutrophils and IM/MLCs were also the major expressors of *Csf3r* (**Figure 6c**), although neutrophils again expressed it at much higher levels (**Figure 6e**). Reciprocally, IM/MLCs comprised most of the cells expressing the cognate receptors for IL-6 (*Il6ra*⁺*Il6st*⁺; **Figure 6c**). Influenza expression alone reduced *Csf3r* expression in neutrophils, while concurrent smoke exposure and influenza infection reduced it further in both neutrophil and IM/MLC populations (**Figure 6e**). To approximate an absolute number of *Csf3*⁺ cells of each dominant

cell type (**Figures 6f**), we multiplied the frequency of each (**Figure 6c**) by the mean cell count of the pooled input samples (**Figure S4b**). In RA-FM1 mice, increases in IM/MLCs dominated the *Csf3* response, with little contribution by neutrophils over baseline. In CS-FM1 mice, however, *Csf3*⁺ IM/MLCs were reduced relative to RA-FM1 levels, while *Csf3*⁺ neutrophils were increased, suggesting that smoke exposure skews the distribution of *Csf3*-expressing cells away from monocyte/macrophage-lineage cells towards neutrophils.

Next, we sought to determine to what extent cytokine expression correlated with infection status within individual cells. To do so, we mapped scRNA-seq reads to the eight FM1-MA complimentary (c)RNA sequences and summed their expression per cell to generate an *FMI* composite score (**Figure 6g**). Within infected samples, 28.3% of cells were positive for FM1 cRNAs, with infected cells (*FMI*⁺) being enriched in CS-FM1 (40.1% of total) relative to RA-FM1 (16.6%) cells. Notably, *HA* single-cell transcript data (**Figure S4d**) reflected observations in whole lung tissue (**Figure 1h**). Refer to **Supplementary Results** for further details about cRNA distributions. In correlating the expression of individual cytokines with *FMI*, we found a significant but very weak positive association with *Il6* in RA-FM1 mice ($r=0.066$, $p=0.0013$; **Figure 6h**), but no relationship in CS-FM1 mice or with *Csf3* in either group. Within *Csf3*⁺ neutrophils specifically, *FMI* transcripts were detected only in a subset (33.3%) of CS-FM1 cells (**Figure 6i**). Overall, our findings identify neutrophils as a novel source of *Csf3*, and indicate

that smoke exposure skews the distribution of *Csf3*-expressing cells in favour of both infected and bystander neutrophils during the course of influenza infection.

Cigarette smoke-exposed lungs are enriched for infected, highly-activated neutrophils

In light of their known association with severe disease[18, 19], we next assessed transcriptional diversity within neutrophils specifically. Three neutrophil subclusters were algorithmically identified (C8/C0/C5; **Figure 7a left**). C8 was comprised almost entirely of RA-PBS-derived cells, and consequently was almost entirely deficient of *FMI* transcripts. This naïve cluster was enriched for genes such as *Slc7a11*, *Thbs1*, *Lst1* and *Lyz2* (**Figure 7b top left**). In comparison, C0 and C5 contained cells from both infected groups, with C5 demonstrating a greater proportion of *FMI*⁺ cells (36.5% of total C5 cells) compared to C0 (16.6% of total C0). CS-FM1 neutrophils were slightly enriched for C5 cells (C5/C0: 35.1/64.7%) relative to RA-FM1 neutrophils (22.3/73.8%; **Figure 7a, right**). Transcriptionally, C5 was enriched for genes such as *Ccl4*, *Ccl3*, *Tnf* and *Il1a*, while C0 uniquely expressed *Ngp*, *Lrg1*, *Mmp8*, and *Rnasel*, among others. Expression of *Cd274* (PD-L1), a molecule previously reported to identify influenza-infected, high inflammatory neutrophils[26], was upregulated in C5 relative to C0/8 (**File S1**). Unsupervised neutrophil-restricted Monocle analysis[27] identified a multilinear pseudotime trajectory between infected neutrophil subclusters with RA-FM1-

(bottom) and CS-FM1-biased (top) arms (**Figure 7b bottom left**). Across this trajectory, C0-specific genes such as *Mmp8* and *Rnasel* were downregulated across a clear gradient, while genes such as *Ccl4* and *Ctsb* were gradually upregulated (**Figure 7b right**), suggesting that these subclusters are transcriptionally related rather than entirely distinct. To assess putative functions for each subset, unique differentially-expressed genes (DEGs) for each subcluster were probed using KEGG and Reactome databases via STRING[28, 29] (**Figure 7c**). C8 cells were enriched for genes associated with homeostatic and constitutive cell functions, such as hemostasis, regulation of the actin cytoskeleton, and membrane trafficking, while being depleted for genes associated with infectious diseases and NOD-like receptor (NLR) signaling. C0 displayed positive enrichment for a small selection of pathways including cytokine signaling, responses in the innate immune system, necroptosis and FoxO signaling, while exhibiting downregulation of pathways such as apoptosis, protein processing in the endoplasmic reticulum, lysosomal function, and glycan degradation. In comparison, C5 displayed enrichment for a wide array of pathways; the top 20 positively enriched hits included a diversity of pathways related to infectious disease (e.g. measles, herpes simplex infection, influenza A) and pattern recognition (e.g. NLR-, TLR-, NF κ B-, RIG-I-like receptor (RLR)-signaling, cytosolic DNA sensing), while the top 20 negatively enriched pathways were associated with constitutive cell functions (e.g. ribosomal function, sphingolipid signaling, hemostasis, MAPK signaling), as well as insulin resistance, platelet activation, and hypoxia-inducible factor (HIF)-1 signalling. Of note, while

necroptosis was positively enriched and apoptosis negatively enriched in C0 cells, apoptosis was upregulated for C5 cells. Overall, scRNA-seq analysis identified two transcriptionally-related neutrophil subclusters in FM1-infected lungs, with CS-FM1 cells being relatively enriched for the more infected, highly inflammatory subset.

Neutrophil gene signatures from cigarette smoke-exposed, influenza-infected mice reflect an exacerbated form of typical disease with unique regulatory features

Lastly, we assessed transcriptional differences between CS-FM1 and RA-FM1 neutrophils directly. Relative to RA-FM1, CS-FM1 neutrophils displayed 191 genes that were significantly upregulated, and 118 that were downregulated (**Figure 8a**). Genes that were highly upregulated (Log_2 fold-change >1) included the interferon-stimulated genes (ISGs) *Ifit3*, *Ifit2*, and *Ifi207*, the antioxidant and metal-binding protein-encoding gene metallothionein-1 (*Mt1*), and serum amyloid A-3 (*Saa3*), among others. Highly downregulated genes included *Csf3r*, as well as others such as *Slc7a11*, *Lst1* and *Lyz2* (**Figure 8a**). Using these genes, we sought to determine whether transcriptional changes observed in neutrophils were unique to the smoking condition, or reflected exaggerated changes induced by influenza alone. To assess this, we restricted the neutrophil dataset to genes that were significantly up- or downregulated between CS-FM1/RA-FM1 (light green) and

assessed global expression trends in these genes following infection alone (RA-FM1/RA-PBS; gray; **Figure 8a**). Broadly, we observed that the transcriptional changes elicited in neutrophils by cigarette smoke were also induced by infection alone, as indicated by a significant increase in the mean expression of this gene set between RA-FM1/RA-PBS conditions. However, this represents the general trend; interestingly, we found 188 genes that exhibited a significant increase or decrease between CS-FM1/RA-FM1 but *not* between RA-FM1/RA-PBS (**File S1**). Three of these genes were regulated by >2 fold, including *Mt1*, *Saa3* and *Ifi207* (yellow; **Figure 8a/b**). However, even these genes demonstrate trends to increase with infection alone. In comparison, several genes were oppositely regulated by cigarette smoke: *Cxcr2*, *Socs3*, *Csf2rb*, *Pde4b*, *Sbno2*, and *Steap4* were all significantly upregulated by infection, but downregulated relative to infection-alone controls by concurrent smoke exposure (**Figure 8c**). Overall, these findings demonstrate that concurrent smoke exposure and influenza elicits an exaggerated influenza-typical neutrophil transcriptional signature with select unique regulatory features.

Discussion

Cigarette smoke exposure is a well-known risk factor for developing influenza-associated illness, transitioning to severe disease, and subsequent hospitalization/ICU admission[3–5]. At present, approximately one-seventh of the global population continues to smoke tobacco[8], exposing an additional one-third of all non-smokers to the harmful effects of second-hand smoke[30]. Consequently, it is critical to delineate the mechanisms by which cigarette smoke exacerbates influenza infection - understanding to what extent smoke-augmented influenza represents an exacerbated form of typical disease vs. a distinct disease sub-endotype may have important implications for the design and implementation of treatment strategies in this high-risk population.

In our model, smoke exposure augmented morbidity and mortality associated with influenza infection. In particular, a stark increase in hypothermia and hypoxemia was observed at endpoint in association with exacerbated systemic dehydration, pulmonary edema, and neutrophilia. Notably, while we did not observe an increase in replicating viral particles in the lungs of smoke-exposed mice, we did observe an accumulation of FM1 RNA transcripts in both whole lung tissue and single cells. This is in line with previous, but separate, observations; most mouse models featuring concurrent smoke/influenza demonstrate no change or a minor decrease in lung PFUs[10, 12–14] or viral protein[9] (with some exceptions at later timepoints e.g. 10dpi[31]), while studies in both humans and mice assessing *in vivo* replication by transcript expression have detected increases in viral load[11,

32]. Here we find that these observations are not mutually exclusive, in that virion accumulation and RNA load are uncoupled in the context of smoke exposure. Mechanistically, this may occur through the downregulation of ribosomal pathways (e.g. as we observe in C5 neutrophils), resulting in a limited translation, and hence accumulation of, viral transcription products. In addition, this phenomenon may provide valuable insights into mechanisms of exacerbated inflammatory responses we observed. vRNA can act as a potent pathogen-associated molecular pattern (PAMP) in host cells[33], and thus its accumulation may serve to drive excess inflammation independent of viral propagation. In support of this idea, we show that neutrophils with higher viral cRNA (C5) express more inflammatory genes than neutrophils with lower cRNA (C0). This disconnect between PFUs and RNA load may have important implications in terms of treatment strategies; direct-acting antivirals (DAAs) targeting vRNA synthesis, such as the PA endonuclease inhibitor baloxavir marboxil, may have a preferential benefit in smoking individuals compared to particle-directed therapies such as neuraminidase inhibitors.

Although excess neutrophilia has been frequently associated with severe influenza, the relative contribution of these cells to disease pathogenesis has not been fully elucidated. Neutrophils are thought to be important in normal viral clearance as their complete depletion promotes excess weight loss and mortality in some models[15, 16]. However, partial depletion appears to have a beneficial effect on survival during severe disease[19], presumably due to detrimental effects of neutrophils on the host tissue, suggesting that a balanced neutrophilia is optimal. It

is well known that cigarette smoke can exacerbate airspace neutrophilia following influenza infection[9, 13, 14], a finding that we replicate here. Interstitial neutrophilia has also been suggested to propagate focal inflammation following influenza [19]. However, to our knowledge it has not been conclusively determined to what extent the anatomical distribution of neutrophils plays a role in disease pathogenesis and morbidity. In this regard we observed that interstitial neutrophilia was a better positive predictor of morbidity than airspace neutrophilia in influenza-infected animals. These data do not preclude a pathogenic role for airspace neutrophils; rather, they suggest that a skew in the distribution of these cells away from the airspaces and toward the interstitium may contribute to negative outcome.

Using a novel dysregulation scoring approach, we identified several cytokines including IL-6, CSF3, and LIF which were exacerbated in CS-FM1 animals as they approached endpoint. Plasma CSF3 levels also correlated with hypothermia. CSF3 is a prototypical neutrophil chemoattractant[34] while IL-6 has been reported to negatively regulate neutrophil recruitment[35, 36]. LIF has been shown to directly modulate neutrophil phagocytic activity[37], and has been reported to promote IL-6/CSF3 expression in fibroblasts[38]. CSF3 and IL-6 have both been reported to be upregulated in pediatric influenza patients presenting with shock, acute lung injury, and extracorporeal membrane oxygenation requirements[39]. CSF3 is similarly upregulated in the BALF of patients with fatal acute respiratory distress syndrome (ARDS)[40], and serum IL-6 is overexpressed in cases of critically severe pandemic H1N1 infection[41]. Importantly though,

elevated expression is not inherently indicative of either negative or positive contribution to outcome. In mice, the genetic absence of either IL-6 or CSF3 has been implicated in exacerbating mortality in the context of influenza[42–44], suggesting a clear protective role for both. However, like neutrophils both a dearth and excess of cytokine may represent a pathological imbalance. In this regard we found that intranasal rCSF3 exacerbated influenza-associated morbidity and increased alveolar-capillary barrier permeability, phenocopying aspects of our CS-FM1 model. Several instances of hypoxemia, capillary leak syndrome and/or shock have been reported following systemic rCSF3 therapy in humans[45–47], supporting the idea that this cytokine can modulate alveolar-capillary barrier integrity and gas exchange when present in excess during influenza. In addition, several recent case studies have observed that CSF3 therapy for neutropenia during concurrent SARS-CoV-2 infection in humans was followed by rapid clinical deterioration and hypoxemia[48, 49]. In supporting these clinical observations, our findings demonstrate important limitations to rCSF3 administration during the course of viral infectious disease. Although we observed no increase in hypoxemia, this difference may be explained by the fact we delivered CSF3 locally rather than systemically, via which route functional efficiencies may be greater. In comparison to rCSF3, rIL-6 elicited no change in symptom score and modestly exacerbated weight loss, but provided a slight, near-significant ($p=0.057$) benefit to core temperature and reduced BALF albumin levels. Changes in weight may reflect the known role for IL-6 in promoting appetite suppression[50]. In summary, these data

clearly suggest that excess CSF3 can exacerbate morbidity and compromise vascular integrity during influenza infection, while IL-6 has a comparatively beneficial effect.

Because rCSF3 exacerbated morbidity/vascular leakage, we subsequently assessed the effect of CSF3R blockade on negative outcomes in our CS-FM1 mice. Although we observed no benefit to morbidity, this is in line with two previous reports showing no change in weight loss following anti-CSF3/CSF3R treatment of influenza-infected mice[51, 52]. Notably, however, anti-CSF3R was able to reduce BALF albumin levels compared to isotype. In tandem with rCSF3 supplementation and clinical observations[45–47], this provides clear evidence that CSF3-CSF3R signaling can regulate alveolar-capillary barrier function. Currently it is unclear whether this effects is neutrophil-dependent or -independent; although we do not detect substantial *Csf3r* transcript levels in stromal cells, CSF3 may act indirectly on these cells to modulate permeability. Although anti-CSF3R alone was insufficient to reduce morbidity in this model, its ability to increase alveolar-capillary barrier function may be of therapeutic potential. Further work testing anti-CSF3R alongside alternate experimental and/or existing therapies may be necessary to unveil a substantial therapeutic benefit.

We next used scRNAseq technology to assess whether cigarette smoke alters the distribution of cytokine expressing cells. Although IM/MLCs quantitatively represented the most dominant cell type expressing both *Csf3* and *Il6*, cigarette smoke exposure elicited a shift in *Csf3*⁺ cells towards neutrophils.

Neutrophils notably expressed *Csf3* at higher levels than IM/MLCs. Previous studies have reported monocytes/macrophages[53, 54], endothelial cells[55], fibroblasts[56] and myocytes[57] (among others) as CSF3-producing cell types. To our knowledge this is the first description of *Csf3* expression in neutrophils. This is of particular interest given that these cells are the prototypical CSF3R-expressing lineage, raising the possibility of a positive feedback loop within infected lungs. In support of this idea, similar loops featuring CXCL1/2 have been implicated in influenza-associated focal interstitial neutrophilia in the past[19]. Overall, these data suggest that expression of *Csf3*, a cytokine capable of exacerbating influenza-associated morbidity, is augmented within neutrophils under smoke-exposed conditions.

scRNA-seq analysis also provided valuable insights into neutrophil subpopulations. We identified two neutrophil subclusters within infected samples. By assessing genes unique to these clusters, we determined that the naïve-proximal (C0; low pseudotime) cluster was enriched for a limited number of pathways associated with cytokine signaling and necroptosis, while downregulating pathways associated with apoptosis and some constitutive cell functions. In contrast, the naïve-distal (C5; high pseudotime) cluster was enriched for FM1 cRNA, numerous inflammatory pathways spanning diverse pattern-recognition pathways / infectious diseases, and apoptosis among others, while downregulating a broader array of constitutive cell functions. This indicates that naïve-distal neutrophils were considerably more inflammatory than naïve-proximal cells. In addition, these

findings demonstrate a relative preference for apoptosis, the least inflammatory type of programmed cell death, in the infected, highly-activated neutrophils, whereas the less-infected population preferred necroptosis. This may reflect an autoregulatory mechanism aimed at maintaining a balanced release of danger-associated molecular patterns (DAMPs) with which to potentiate further inflammation.

Notably, unbiased algorithm-based trajectory analysis identified a transcriptional relationship defined by a gradient of expression of these unique genes between the clusters. If these cells were substantially distinct, developmentally or otherwise, one might expect more stark changes in gene expression at cluster interfaces and greater cluster separation. Thus, these data support the idea of an ontogenically-homogenous neutrophil population that demonstrates transcriptional subpopulations based on external influences. One such influence appears to be direct infection, although the majority of both clusters were *FMI*⁻ suggesting that other factors, such as anatomical distribution between the airspace and parenchyma, may play a greater role. Of note, a previous study also reported three different transcriptionally-related neutrophil subpopulations in the context of influenza, with the most infected / inflammatory being similarly enriched for PD-L1 (*Cd274*) expression[26]. Our work expands on this finding to demonstrate that, rather than eliciting unique neutrophil subpopulations, cigarette smoke skews the distribution of neutrophils in favour of this infected subtype.

In line with this idea, we lastly sought to directly answer whether transcriptional changes in neutrophils elicited by cigarette smoke reflected an exacerbated form of typical disease or a distinct disease sub-endotype. Ultimately, the majority of differential gene expression in CS-FM1 neutrophils represented exacerbations of changes elicited by influenza alone. However, some genes were oppositely regulated in CS-FM1 relative to RA-FM1 mice, such as *Cxcr2*, *Socs3*, *Csf2rb*, *Pde4b*, *Sbno2*, *Steap4*. Notable among these is *Socs3* which encodes a known negative regulator of CSF3 signaling, potentially explaining our observations of reduced death in BAL neutrophils[58]. In addition, some were uniquely up-/downregulated, such as *Mt1*, *Saa3* and *Ifi207*. Although metallothionein-1 genes are known to be upregulated by acute smoke exposure in humans[59], they are also induced in alternate models of influenza infection[60]. Similarly, serum amyloid A isoforms are induced by influenza early on[61] and *Saa3*-deficiency increases virus-induced mortality[62]. *Ifi207* is an ortholog of the human *IFI16* gene, which encodes a viral RNA-binding adaptor that augments RIG-I-mediated pattern recognition[63]. Consequently, upregulation of this gene in particular may contribute to an excessive inflammatory response to accumulating vRNA under smoke-exposed conditions.

In summary, our work provides valuable insights into cellular, molecular, and anatomical changes elicited by cigarette smoke exposure during influenza infection. A notable disconnect between viral particle synthesis and vRNA accumulation in smoke-augmented influenza may indicate a treatment preference

for endonuclease or other polymerase-targeted inhibitors (e.g. baloxavir) rather than neuraminidase inhibitors (e.g. oseltamivir) in this patient population. In focusing on neutrophils, which have been frequently associated with severe disease, we reveal that interstitial rather than airspace neutrophilia positively predicts morbidity. Furthermore, we define a capacity for CSF3, a potent neutrophilic cytokine, to exacerbate morbidity and alveolar-capillary barrier dysfunction during influenza infection, and identify neutrophils as a novel and expanded source of *Csf3* in smoke-augmented influenza. Finally, deep transcriptional analysis of neutrophils reveals distinct but related sub-identities elicited during infection and defines the response to cigarette smoke as largely reflecting an exacerbated version of typical disease with select unique regulatory features.

Materials & Methods

Animals. 6-10 week old female BALB/c mice were purchased from Charles River Laboratories (Montreal, QC, Canada), and housed in the McMaster Central Animal Facility. Mice were given *ad libitum* access to food and water, and subject to 12 hour light/dark cycling. All experiments were approved by the Animal Research Ethics Board at McMaster University.

Cigarette Smoke Exposure and Infections. Mice were exposed to room air, or cigarette smoke using a whole-body smoke exposure system (SIU48/SIU24;

Promech, Sweden) as reported previously[64]. After two weeks, animals were intranasally infected with 50 PFU of influenza A/Fort Monmouth/1/1947-mouse-adapted (MA; H1N1) in 35µl, or PBS vehicle. Smoke exposure resumed at 3dpi and continued until endpoint. Body weight and health status were monitored daily following viral infection. Health status was assessed based on appearance, provoked and unprovoked behaviour, hydration status, clinical signs, and breathing pattern. Mice with a weight loss >30% or reaching a health score of >9 on two consecutive readings four hours apart were euthanized. Refer to **File S1** for specific health score metrics.

Physiological Readouts. Core temperature was measured using a rectal wire-probe thermometer (VWR) inserted to a fixed depth of 2cm. Peripheral capillary oxygen saturation (SpO₂) was assessed in unanesthetized or lightly anesthetized mice (isoflurane + medical-grade air [21% O₂]) at endpoint using a MouseOx pulse oximeter (STARR Life Sciences).

Sample Collection. Anti-coagulated blood was collected from the retro-orbital sinus using heparinized capillary tubes. Plasma was separated by centrifugation at 13000rpm. Animals were euthanized under isoflurane anaesthesia by exsanguination. Lungs were removed and, after cannulation, bronchoalveolar lavage (BAL) was performed via two sequential instillations of 500µl of cold, sterile PBS. BAL recovery volume was measured; (e.g. **Figure S2d**). Cells were

then separated from BAL fluid (BALF) via centrifugation at 2500rpm. Right lungs were tied off and subdivided for RNA analysis (RNALater, Qiagen), protein analysis (rotor-stator homogenized in 1ml PBS), and flow cytometry. Left lungs were inflated with 10% buffered formalin for histological analysis. Protein homogenates were centrifuged at 13000rpm and supernatants collected.

Readouts of Alveolar-Capillary Barrier Function. Whole lungs were excised, and wet-to-dry lung weight ratio was determined by weighing lungs immediately following excision and after 24 hours of desiccation. BALF albumin was measured by ELISA (Abcam, ab108792). Hematocrit was assessed by centrifuging anti-coagulated blood. For quantification of peri-bronchovascular cuffs, formalin-fixed, paraffin-embedded tissue sections were stained with hematoxylin and eosin (H&E). Cuff formation was quantified using ImageJ and expressed as a percentage of total lung area.

PFU Assay. Plaque-forming units were quantified using Madin-Darby Canine Kidney (MDCK) cells. Refer to **Supplementary Methods** for more details.

Western blotting. Western blots were performed on lung homogenates using protocols described previously[64], with the following exceptions: i) an 8% resolving gel was used; ii) 40µg of protein was loaded per well, iii) target (VE-

cadherin) bands were normalized to control (actin) bands. Refer to **File S1** for antibody details.

RT-qPCR. To quantify RNA expression levels, RNALater-preserved tissues were thawed, washed in sterile PBS, and RNA was isolated using RNeasy kits (Qiagen). RNA was reverse transcribed into cDNA using Superscript II (Invitrogen), as per manufacturer's instructions. cDNA was then quantified by qPCR in a StepOnePlus real-time PCR system (Life Technologies Inc.) using either Taqman Gene Expression Mastermix (for *Csf3*, *Il6*, *Lif*; ThermoFisher Scientific) or GoTaq qPCR Mastermix (for *Gapdh*, *HA*; Promega). Gene expression was determined using the $\Delta\Delta CT$ method. Target gene expression was normalized to that of the housekeeping gene *Gapdh* and expressed as a fold change relative to the indicated control group. Refer to **File S1** for primers/probes.

Histological Ly6G⁺ Cell Quantification. Following formalin fixation for 48h, lungs were transferred to 70% ethanol, sectioned, and embedded in formalin. Tissue microarrays (TMAs) were generated from paraffin-embedded lung tissue ([65]section 3.7). Paraffin slides were stained with an anti-Ly6G antibody (Biolegend 127602, 1:1000) using an automated Leica Bond Rx (Leica Biosystems). TMAs were digitized and interstitial Ly6G⁺ cells were quantified using HALO software (v3.2.1851.229, Indica Labs; [65]section 3.8/3.8.1). Interstitial areas were determined with the assistance of a pathologist.

Flow Cytometry. Refer to **Supplementary Methods** for details. Specific stains used are provided in **File S1**.

Quantification of BALF cfDNA and Peroxidase Activity. cfDNA was quantified in 200µl of BALF using a DNeasy kit (Qiagen) as per the manufacturer's instructions. Peroxidase activity was quantified by incubating 10µl of BALF with 90µl of TMB containing H₂O₂ (Sigma) for 5min at 37°C. The reaction was stopped with 2N H₂SO₄. Data represent optical densities read at 450nm.

Cytokine Quantification and Dysregulation Scoring. Cytokines were quantified in lung homogenate using an MD31 mouse discovery assay (Eve Technologies, Calgary, AB), or in plasma by ELISA (R&D; DY414, DY406, DY449). For development and validation of dysregulation scores, refer to **Supplementary Methods**.

Cytokine Supplementation and Blockade Experiments. For supplementation experiments, BALB/c mice were infected with 50 PFU of FM1. Mice were then given intranasal doses of PBS, carrier-free recombinant mouse (r)CSF3 (R&D, 414-CS/CF, 7µg/35µl) or carrier-free recombinant mouse (r)IL-6 (R&D, 406-ML/CF, 7µg/35µl) at 4dpi (pm), 5dpi (am+pm) and 6dpi (am). Mice were assessed for physiological readouts and culled 3h after the last intranasal dose. For blockade experiments, mice were exposed to room air or cigarette smoke for two weeks and

infected at the end of the second week as in Figure 1. CS-FM1 animals were treated with anti-CSF3R (CSL Behring) or isotype control (400µg/200µl PBS vehicle) intraperitoneally at 2/4/6dpi, and culled at 7dpi.

Single-cell RNA Sequencing. Cells were prepared for scRNAseq at the Princess Margaret Genomics Centre (University of Toronto) using 10X Genomics 3' v3.1 chemistry, and transcripts were sequenced using a Novaseq 6000 (Illumina). Read mapping was performed using a custom reference comprised of mouse mm10 genome and influenza A/FM/1/47-MA cRNAs (PB2 (GenBank: CY087791.1), PB1 (CY087790.1), PA (CY087789.1), NEP/NS1 (CY087788.1), NP (CY087787.1), NA (CY087786.1), M1/M2 (CY087785.1), HA (CY087784.1). Cells were clustered after principal component analysis (PCA) and prior to via Uniform Manifold Approximation and Projection (UMAP[66]) using the Seurat package in R[67]. Clusters were classified into cell populations by using a list of markers obtained from literature sources (**Figure S4a**). Differential expression analyses were performed using FindMarkers (Seurat); adj.p-val.<0.05 were considered to be significant. Viral load of cells was estimated by summing the expression of all eight FM1 cRNAs on a per-cell basis to derive an '*FMI*' transcript readout. Cells with an *FMI* value >0 were considered to be infected; all other cells from infected samples were termed 'bystander' and cells from RA-PBS mice were termed 'naïve'. Pair-wise differential analysis was performed comparing neutrophil subclusters, yielding lists of genes uniquely expressed in each of these subclusters

as compared to the others. These gene lists were used for subsequent STRING[28, 29]-based pathway enrichment analysis using KEGG and Reactome databases. Pseudotime analysis was performed within the neutrophil population using Monocle3[27]. Refer to **Supplementary Methods** for further details.

Statistical Analysis. GraphPad Prism 9 (GraphPad Software, Inc.) was used for all statistical analyses except single-cell RNA sequencing (discussed above). Specific tests used are indicated in the relevant figure legends. Significance (*) was defined as $p < 0.05$.

References (not including Supplement)

1. World Health Organization. WHO Report on the Global Tobacco Epidemic, 2015. 2015.
2. Carter BD, Abnet CC, Feskanich D, Freedman ND, Hartge P, Lewis CE, Ockene JK, Prentice RL, Speizer FE, Thun MJ, Jacobs EJ. Smoking and Mortality - Beyond Established Causes. *N. Engl. J. Med.* 2015; 372: 631–640.
3. Lawrence H, Hunter A, Murray R, Lim WS, McKeever T. Cigarette smoking and the occurrence of influenza – Systematic review. *J. Infect.* 2019; 79: 401–406.
4. Kark JD, Lebiush M, Rannon L. Cigarette smoking as a risk factor for epidemic A(H1N1) influenza in young men. *N. Engl. J. Med.* 1982; 307: 1042–1046.
5. Han L, Ran J, Mak YW, Suen LKP, Lee PH, Peiris JSM, Yang L. Smoking and Influenza-associated Morbidity and Mortality: A Systematic Review and Meta-analysis. *Epidemiology* 2019; 30: 405–417.
6. Sethi S, Murphy TF. Infection in the pathogenesis and course of chronic obstructive pulmonary disease. *N. Engl. J. Med.* 2008; 359: 2355–2365.
7. Zarrabian B, Mirsaeidi M. A Trend Analysis of COPD Mortality in the United States by Race and Sex. *Ann. Am. Thorac. Soc.* American Thoracic Society; 2020.
8. Reitsma MB, Kendrick PJ, Ababneh E, Abbafati C, Abbasi-Kangevari M, Abdoli A, Abedi A, Abhilash ES, Abila DB, Aboyans V, Abu-Rmeileh NM, Adebayo OM, Advani SM, Aghaali M, Ahinkorah BO, Ahmad S, Ahmadi K, Ahmed H, Aji B, Akunna CJ, Al-Aly Z, Alanzi TM, Alhabib KF, Ali L, Alif SM, Alipour V, Aljunid SM, Alla F, Allebeck P, Alvis-Guzman N, et al. Spatial, temporal, and demographic patterns in prevalence of smoking tobacco use and attributable disease burden in 204 countries

- and territories, 1990–2019: a systematic analysis from the Global Burden of Disease Study 2019. *Lancet* 2021; 397: 2337–2360.
9. Kearley J, Silver JS, Sanden C, Liu Z, Berlin AA, White N, Mori M, Pham TH, Ward CK, Criner GJ, Marchetti N, Mustelin T, Erjefalt JS, Kolbeck R, Humbles AA. Cigarette smoke silences innate lymphoid cell function and facilitates an exacerbated type I interleukin-33-dependent response to infection. *Immunity* Elsevier Inc.; 2015; 42: 566–579.
 10. Kang MJ, Chun GL, Lee JY, Dela Cruz CS, Chen ZJ, Enelow R, Elias JA. Cigarette smoke selectively enhances viral PAMP- and virus-induced pulmonary innate immune and remodeling responses in mice. *J. Clin. Invest.* 2008; 118: 2771–2784.
 11. Lee SW, Sharma L, Kang YA, Kim SH, Chandrasekharan S, Losier A, Brady V, Bermejo S, Andrews N, Yoon CM, Liu W, Lee JY, Kang MJ, Cruz CSD. Impact of cigarette smoke exposure on the lung fibroblastic response after influenza pneumonia. *Am. J. Respir. Cell Mol. Biol.* 2018; 59: 770–781.
 12. Wang X, Wu W, Zhang W, Leland Booth J, Duggan ES, Tian L, More S, Zhao YD, Sawh RN, Liu L, Zou M-H, Metcalf JP. RIG-I overexpression decreases mortality of cigarette smoke exposed mice during influenza A virus infection. *Respir. Res.* 2017; 18: 166.
 13. Robbins CS, Bauer CMT, Vujcic N, Gaschler GJ, Lichty BD, Brown EG, Stampfli MR. Cigarette smoke impacts immune inflammatory responses to influenza in mice. *Am. J. Respir. Crit. Care Med.* 2006; 174: 1342–1351.
 14. Bauer CMT, Zavitz CCJ, Botelho FM, Lambert KN, Brown EG, Mossman KL, Taylor JD, Stämpfli MR. Treating viral exacerbations of chronic obstructive pulmonary disease: Insights from a mouse model of cigarette smoke and H1N1 influenza infection. *PLoS One* 2010; 5: e13251.

15. Tate MD, Deng Y-M, Jones JE, Anderson GP, Brooks AG, Reading PC. Neutrophils Ameliorate Lung Injury and the Development of Severe Disease during Influenza Infection. *J. Immunol.* 2009; 183: 7441–7450.
16. Tate MD, Ioannidis LJ, Croker B, Brown LE, Brooks AG. The Role of Neutrophils during Mild and Severe Influenza Virus Infections of Mice. *PLoS One* 2011; 6: 17618.
17. Ljungman P, de la Camara R, Perez-Bercoff L, Abecasis M, Campuzano JBN, Cannata-Ortiz MJ, Cordonnier C, Einsele H, Gonzalez-Vicent M, Espigado I, Halter J, Martino R, Mohty B, Sucak G, Ullmann AJ, Vázquez L, Ward KN, Engelhard D. Outcome of pandemic H1N1 infections in hematopoietic stem cell transplant recipients. *Haematologica* 2011; 96: 1231–1235.
18. Tang BM, Shojaei M, Teoh S, Meyers A, Ho J, Ball TB, Keynan Y, Pisipati A, Kumar A, Eisen DP, Lai K, Gillett M, Santram R, Geffers R, Schreiber J, Mozhui K, Huang S, Parnell GP, Nalos M, Holubova M, Chew T, Booth D, Kumar A, McLean A, Schughart K. Neutrophils-related host factors associated with severe disease and fatality in patients with influenza infection. *Nat. Commun.* 2019; 10: 1–13.
19. Brandes M, Klauschen F, Kuchen S, Germain RN. A systems analysis identifies a feedforward inflammatory circuit leading to lethal influenza infection. *Cell* 2013; 154: 197.
20. George ST, Lai J, Ma J, Stacey HD, Miller MS, Mullarkey CE. Neutrophils and influenza: A thin line between helpful and harmful. *Vaccines* 2021; 9.
21. Zhu L, Liu L, Zhang Y, Pu L, Liu J, Li X, Chen Z, Hao Y, Wang B, Han J, Li G, Liang S, Xiong H, Zheng H, Li A, Xu J, Zeng H. High Level of Neutrophil Extracellular Traps Correlates With Poor Prognosis of Severe Influenza A Infection. *J. Infect. Dis.* 2018; 428: 428–465.

22. Narasaraju T, Yang E, Samy RP, Ng HH, Poh WP, Liew A-A, Phoon MC, van Rooijen N, Chow VT. Excessive Neutrophils and Neutrophil Extracellular Traps Contribute to Acute Lung Injury of Influenza Pneumonitis. *Am. J. Pathol.* 2011; 179: 199–210.
23. Stacey HD, Golubeva D, Posca A, Ang JC, Atif Zahoor M, Kaushic C, Cairns E, E DM, Mullarkey CE, Miller MS. IgA Potentiates NETosis in Response to Viral Infection. *PNAS* 2021; 118.
24. Wong J, Saravolac E, Clement J, Nagata L. Development of a murine hypothermia model for study of respiratory tract influenza virus infection. *Lab Anim Sci.* 1997; 47: 143–147.
25. Boivin G, Faget J, Ancy PB, Gkasti A, Mussard J, Engblom C, Pfirschke C, Contat C, Pascual J, Vazquez J, Bendriss-Vermare N, Caux C, Vozenin MC, Pittet MJ, Gunzer M, Meylan E. Durable and controlled depletion of neutrophils in mice. *Nat. Commun.* 2020; 11: 1–9.
26. Zhang J, Liu J, Yuan Y, Huang F, Ma R, Luo B, Xi Z, Pan T, Liu B, Zhang Y, Zhang X, Luo Y, Wang J, Zhao M, Lu G, Deng K, Zhang H. Two waves of pro-inflammatory factors are released during the influenza A virus (IAV)-driven pulmonary immunopathogenesis. *PLOS Pathog.* 2020; 16: e1008334.
27. Trapnell C, Cacchiarelli D, Grimsby J, Pokharel P, Li S, Morse M, Lennon NJ, Livak KJ, Mikkelsen TS, Rinn JL. The dynamics and regulators of cell fate decisions are revealed by pseudotemporal ordering of single cells. *Nat. Biotechnol.* 2014; 32.
28. Snel B, Lehmann G, Bork P, Huynen MA. String: A web-server to retrieve and display the repeatedly occurring neighbourhood of a gene. *Nucleic Acids Res.* 2000; 28: 3442–3444.

29. Szklarczyk D, Gable AL, Lyon D, Junge A, Wyder S, Huerta-Cepas J, Simonovic M, Doncheva NT, Morris JH, Jensen LJ, Von Mering C. STRING v11: protein-protein association networks with increased coverage, supporting functional discovery in genome-wide experimental datasets. *Nucleic Acids Res.* 2018; 47: 607–613.
30. Öberg M, Jaakkola MS, Woodward A, Peruga A, Prüss-Ustün A. Worldwide burden of disease from exposure to second-hand smoke: a retrospective analysis of data from 192 countries. *Lancet* 2011; 377: 139–146.
31. Hong MJ, Gu BH, Madison MC, Landers C, Tung HY, Kim M, Yuan X, You R, Machado AA, Gilbert BE, Soroosh P, Elloso M, Song L, Chen M, Corry DB, Diehl G, Kheradmand F. Protective role of $\gamma\delta$ T cells in cigarette smoke and influenza infection. *Mucosal Immunol.* 2017; 11.
32. Noah TL, Zhou H, Monaco J, Horvath K, Herbst M, Jaspers I. Tobacco Smoke Exposure and Altered Nasal Responses to Live Attenuated Influenza Virus. *Environ. Health Perspect.* 2010; 119: 78–83.
33. Herold S, Becker C, Ridge KM, Budinger GRS. Influenza virus-induced lung injury: Pathogenesis and implications for treatment. *Eur. Respir. J.* 2015; 45: 1463–1478.
34. Semerad CL, Liu F, Gregory AD, Stumpf K, Link DC. G-CSF is an essential regulator of neutrophil trafficking from the bone marrow to the blood. *Immunity* 2002; 17: 413–423.
35. Xing Z, Gauldie J, Cox G, Baumann H, Jordana M, Lei XF, Achong MK. IL-6 is an antiinflammatory cytokine required for controlling local or systemic acute inflammatory responses. *J. Clin. Invest.* 1998; 101: 311–320.

36. Fielding CA, McLoughlin RM, McLeod L, Colmont CS, Najdovska M, Grail D, Ernst M, Jones SA, Topley N, Jenkins BJ. IL-6 Regulates Neutrophil Trafficking during Acute Inflammation via STAT3. *J. Immunol.* 2008; 181: 2189–2195.
37. Borish L, Rocklin RE. Effects of leukocyte inhibitory factor (LIF) on human neutrophil function. *Inflammation* 1987; 138.
38. Mizoguchi F, Huppertz C, Wei KS, Watts GFM, Brenner MB, Nguyen HN, Noss EH, Mizoguchi F, Huppertz C, Wei KS, Watts GFM. Autocrine Loop Involving IL-6 Family Member LIF , LIF Receptor , and STAT4 Drives Sustained Fibroblast Production of Inflammatory Mediators Article Autocrine Loop Involving IL-6 Family Member LIF , LIF Receptor , and STAT4 Drives Sustained Fibroblast. *Immunity* Elsevier Inc.; 2017; 46: 220–232.
39. Fiore-Gartland A, Panoskaltis-Mortari A, Agan AA, Mistry AJ, Thomas PG, Matthay MA, Hertz T, Randolph AG. Cytokine profiles of severe influenza virus-related complications in children. *Front. Immunol.* 2017; 8: 1–12.
40. Aggarwal A, Baker CS, Evans TW, Haslam PL. G-CSF and IL-8 but not GM-CSF correlate with severity of pulmonary neutrophilia in acute respiratory distress syndrome. *Eur. Respir. J.* 2000; 15: 895–901.
41. Paquette SG, Banner D, Zhao Z, Fang Y, Huang SSH. Interleukin-6 Is a Potential Biomarker for Severe Pandemic H1N1 Influenza A Infection. *PLoS One* 2012; 7: 38214.
42. Hermesh T, Moran TM, Jain D, López CB. Granulocyte colony-stimulating factor protects mice during respiratory virus infections. *PLoS One* 2012; 7.
43. Dienz O, Rud JG, Eaton SM, Lanthier PA, Burg E, Drew A, Bunn J, Suratt BT, Haynes L, Rincon M. Essential role of IL-6 in protection against H1N1 influenza virus by promoting neutrophil survival in the lung. *Mucosal Immunol.* 2012; 5: 258–266.

44. Yang ML, Wang CT, Yang SJ, Leu CH, Chen SH, Wu CL, Shiau AL. IL-6 ameliorates acute lung injury in influenza virus infection. *Sci. Rep.* 2017; 7.
45. de Azevedo AM, Goldberg Tabak D. Life-threatening capillary leak syndrome after G-CSF mobilization and collection of peripheral blood progenitor cells for allogeneic transplantation. *Bone Marrow Transplant.* 2001; 28: 311–312.
46. Yamamoto K, Doki N, Senoo Y, Najima Y, Kobayashi T, Kakihana K, Haraguchi K, Okuyama Y, Sakamaki H, Ohashi K. Case Report Severe Hypoxemia in a Healthy Donor for Allogeneic Hematopoietic Stem Cell Transplantation after Only the First Administration of Granulocyte-Colony Stimulating Factor. *Transfus Med Hemother* 2016; 43: 433–435.
47. Dagdemir A, Albayrak D, Dilber C, Totan M. G-CSF Related Capillary Leak Syndrome in a Child with Leukemia. *Leuk. Lymphoma* 2001; 42: 1445–1447.
48. Taha M, Sharma A, Soubani A. Clinical deterioration during neutropenia recovery after G-CSF therapy in patient with COVID-19. *Respir. Med. Case Reports* 2020; 31.
49. Nawar T, Morjaria S, Kaltsas A, Patel D, Perez-Johnston R, Daniyan AF, Mailankody S, Parameswaran R. Granulocyte-colony stimulating factor in COVID- 19: Is it stimulating more than just the bone marrow? *Am. J. Hematol.* 2020; 95: E208–E210.
50. Patsalos O, Dalton B, Himmerich H. Effects of IL-6 signaling pathway inhibition on weight and BMI: A systematic review and meta-analysis. *Int. J. Mol. Sci.* 2020; 21: 1–13.
51. Wang H, Aloe C, Wilson N, Bozinovski S. G-CSFR antagonism reduces neutrophilic inflammation during pneumococcal and influenza respiratory infections without compromising clearance. *Sci. Rep.* 2019; 9: 1–12.

52. Rutigliano JA, Sharma S, Morris MY, Oguin TH, McClaren JL, Doherty PC, Thomas PG. Highly Pathological Influenza A Virus Infection Is Associated with Augmented Expression of PD-1 by Functionally Compromised Virus-Specific CD8⁺ T Cells. *J. Virol.* 2014; 88: 1636–1651.
53. Oster W, Lindemann A, Mertelsmann R, Herrmann F. Production of macrophage-, granulocyte-, granulocyte-macrophage- and multi-colony-stimulating factor by peripheral blood cells. *Eur. J. Immunol.* 1989; 19: 543–548.
54. Yang TC, Chang PY, Kuo TL, Lu SC. Electronegative L5-LDL induces the production of G-CSF and GM-CSF in human macrophages through LOX-1 involving NF- κ B and ERK2 activation. *Atherosclerosis* 2017; 267: 1–9.
55. Zsebo KM, Yuschenkoff VN, Schiffer S, Chang D, McCall E, Dinarello CA, Brown MA, Altrock B, Bagby GC. Vascular endothelial cells and granulopoiesis: Interleukin-1 stimulates release of G-CSF and GM-CSF. *Blood* 1988; 71: 99–103.
56. Koeffler HP, Gasson J, Ranyard J, Souza L, Shepard M, Munker R. Recombinant human TNF(α) stimulates production of granulocyte colony-stimulating factor. *Blood* 1987; 70: 55–59.
57. Ordelheide AM, Gommer N, Böhm A, Hermann C, Thielker I, Machicao F, Fritsche A, Stefan N, Häring HU, Staiger H. Granulocyte colony-stimulating factor (G-CSF): A saturated fatty acid-induced myokine with insulin-desensitizing properties in humans. *Mol. Metab.* 2016; 5: 305–316.
58. Croker BA, Metcalf D, Robb L, Wei W, Mifsud S, DiRago L, Cluse LA, Sutherland KD, Hartley L, Williams E, Zhang JG, Hilton DJ, Nicola NA, Alexander WS, Roberts AW. SOCS3 Is a Critical Physiological Negative Regulator of G-CSF Signaling and Emergency Granulopoiesis. *Immunity* 2004; 20: 153–165.

59. Billatos E, Faiz A, Gesthalter Y, Leclerc A, Alekseyev YO, Xiao X, Liu G, Ten Hacken NHT, Heijink IH, Timens W, Brandsma CA, Postma DS, van den Berge M, Spira A, Lenburg ME. Impact of acute exposure to cigarette smoke on airway gene expression. *Physiol. Genomics* 2018; 50: 705–713.
60. Ghoshal K, Majumder S, Zhu Q, Hunzeker J, Datta J, Shah M, Sheridan JF, Jacob ST. Influenza Virus Infection Induces Metallothionein Gene Expression in the Mouse Liver and Lung by Overlapping but Distinct Molecular Mechanisms. *Mol. Cell. Biol.* American Society for Microbiology; 2001; 21: 8301–8317.
61. Vollmer AH, Gebre MS, Barnard DL. Serum amyloid A (SAA) is an early biomarker of influenza virus disease in BALB/c, C57BL/2, Swiss-Webster, and DBA.2 mice. *Antiviral Res.* 2016; 133: 196–207.
62. Ather JL, Dieng O, Boyson JE, Anathy V, Amiel E, Poynter ME. Serum Amyloid A3 is required for normal lung development and survival following influenza infection. 2018; .
63. Jiang Z, Wei F, Zhang Y, Wang T, Gao W, Yu S, Sun H, Pu J, Sun Y, Wang M, Tong Q, Gao C, Chang KC, Liu J. IFI16 directly senses viral RNA and enhances RIG-I transcription and activation to restrict influenza virus infection. *Nat. Microbiol.* 2021; .
64. McGrath JJC, Thayaparan D, Cass SP, Mapletoft JP, Zeng PYF, Koenig JFE, Fantauzzi MF, Bagri P, Ly B, Heo R, Schenck LP, Shen P, Miller MS, Stämpfli MR. Cigarette smoke exposure attenuates the induction of antigen-specific IgA in the murine upper respiratory tract. *Mucosal Immunol.* 2021. doi: 10.1038/s41385-021-00411-9.
65. Mekhael O, Naiel S, Vierhout M, Hayat AI, Revill SD, Abed S, Inman MD, Kolb MRJ, Ask K. Mouse Models of Lung Fibrosis. *Methods Mol. Biol.* 2021; 2299.

66. McInnes L, Healy J, Saul N, Großberger L. UMAP: Uniform Manifold Approximation and Projection. *J. Open Source Softw.* 2018; 3: 861.
67. Satija R, Farrell JA, Gennert D, Schier AF, Regev A. Spatial reconstruction of single-cell gene expression data. *Nat. Biotechnol.* 2015; 33: 495–502.

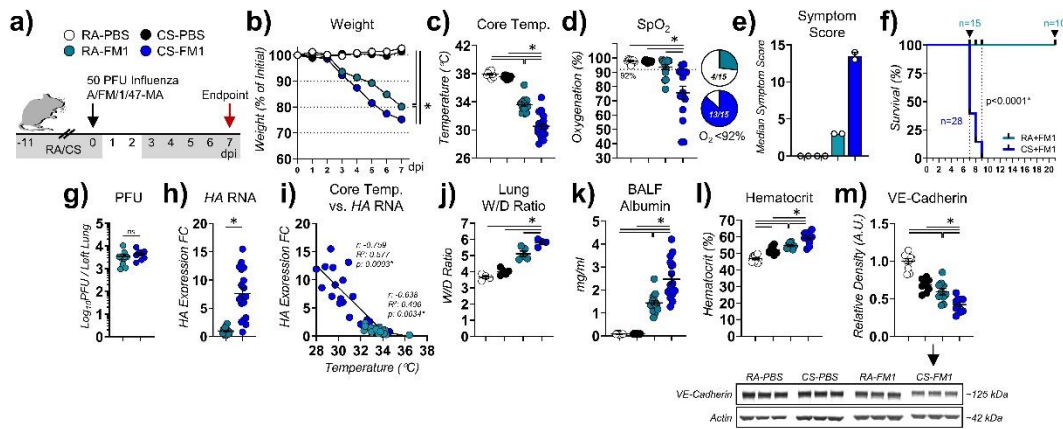


Figure 1. Cigarette smoke exposure exacerbates influenza-induced pulmonary edema and hypoxemia in association with PFU-independent vRNA accumulation. **a)** Experimental model. BALB/c mice were exposed to room air or cigarette smoke for two weeks and infected with 50 PFU of influenza A/FM/1/47-MA (H1N1; “FM1”) or PBS vehicle. Smoke exposure was resumed at 3dpi and continued until endpoint at 7dpi, at which time animals were culled. Data presented are from 7dpi unless otherwise indicated. **b)** Weight over time, normalized to starting weight. $n=13-25/\text{group}$ from three experiments. **c)** Core temperature was measured by rectal thermometry. $n=10-19/\text{group}$ from two experiments. **d)** SpO₂ was assessed by pulse oximetry. 92% represents a clinical threshold for systemic hypoxemia. $n=9-15/\text{group}$ from two experiments. **e)** Median symptom score per group (see Materials & Methods) from two experiments. **f)** Survival plot based on animals reaching a pre-determined weight-based/symptomatic endpoint score (refer to Materials & Methods). $n=25-28/\text{group}$ from three experiments. **g)** Plaque-forming units (PFUs) were assessed in lung homogenates. $n=8-9/\text{group}$. **h)** HA RNA was quantified in whole lung lysates by RT-qPCR. $n=18-19/\text{group}$ from two experiments. **i)** Core temperature was correlated against lung HA load. $n=18-19/\text{group}$ from two experiments. **j)** Lung wet-to-dry (W/D) ratio was determined by weighing lungs directly after excision and after 24h of desiccation. $n=4-5/\text{group}$. **k)** Mouse serum albumin was measured in the bronchoalveolar lavage fluid (BALF). $n=10-18/\text{group}$ from two experiments. **l)** Hematocrit as measured in anticoagulated blood. $n=8-10/\text{group}$ from two experiments. **m)** VE-cadherin as measured in lung homogenates by Western blot. $n=9-10/\text{group}$ from two experiments. **(b-d, j-m):** Two-way ANOVA with Tukey’s post-hoc test. **(f)** Logrank test. **(g, h)** Student’s unpaired t-test. **(i)** Pearson’s correlation. $p<0.05^*$. dpi: days post-infection.

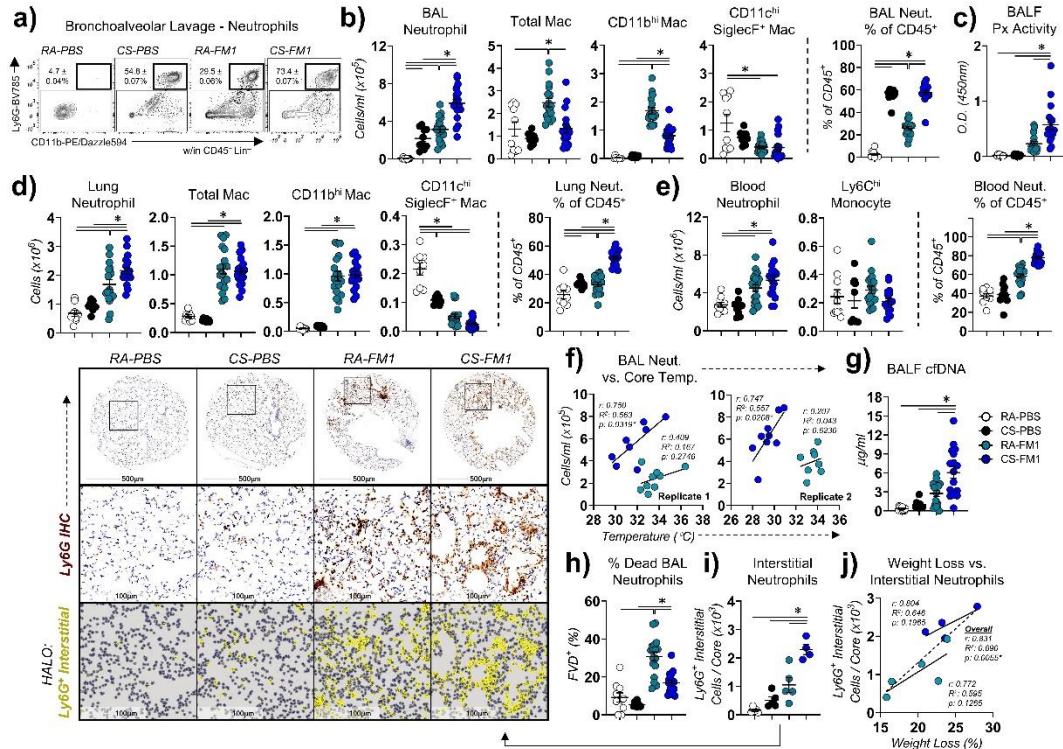


Figure 2. Accumulation of neutrophils in the pulmonary interstitium correlates with disease severity in cigarette smoke-augmented influenza. a) Flow cytometry plot demonstrating neutrophils in the BAL. Frequencies represent mean ± SD. **(b,d,e)** Cell populations (as indicated) were quantified in the **b)** BAL, **d)** whole lung, and **e)** blood by flow cytometry. **b)** n=10-17/group, **d)** n=9-18/group, **e)** n=10-19/group, each from two experiments. **c)** Peroxidase activity was measured in BALF by direct incubation with TMB. n=10-17/group from two experiments. **f)** BAL neutrophils were correlated against core temperature. Two independent experiments are shown (n=8-9/group each). **g)** Cell-free (cf)DNA was extracted and quantified in the BALF. n=10-17/group from two experiments. **h)** The proportion of dead (FVD⁺) neutrophils was quantified as a proportion of total neutrophils by flow cytometry. n=10-17/group from two experiments. **i)** Neutrophils were identified by Ly6G staining of tissue microarrays. Interstitial areas were defined with the help of a pathologist, and Ly6G⁺ events were quantified in each core using HALO software. Representative staining and HALO overlay images are presented at left. n=4-5/group. **j)** Interstitial neutrophilia was correlated against weight loss. n=4-5/group. **(b-e, g-i):** Two-way ANOVA with Tukey’s post-hoc test. **(f, j)** Pearson’s correlation. p<0.05*. ACN: absolute cell number.

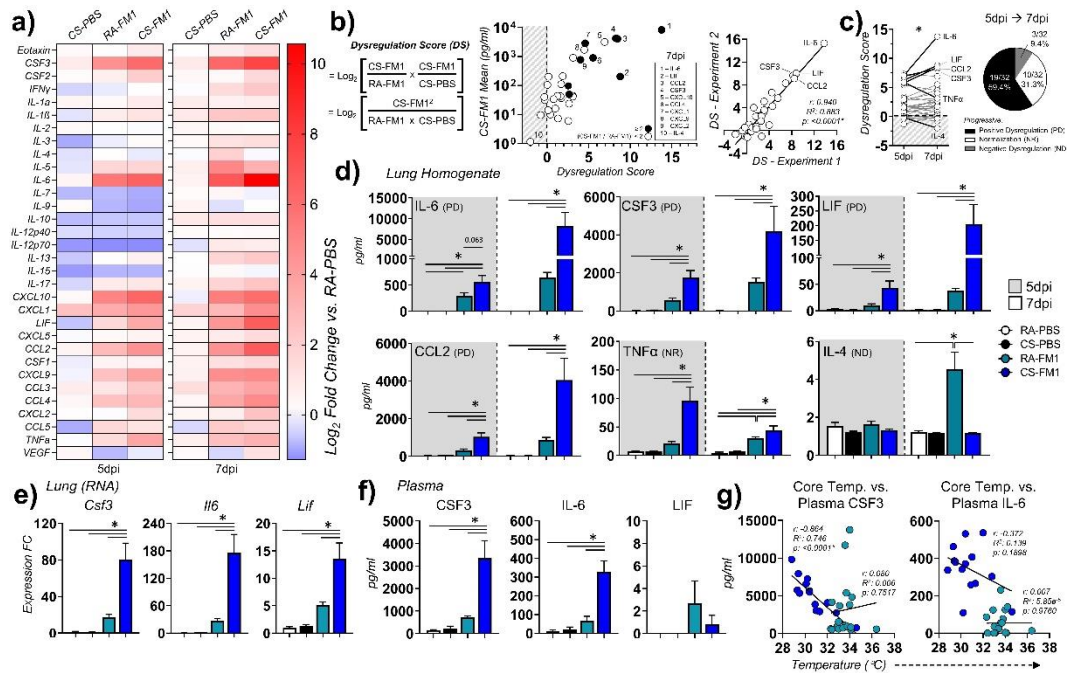


Figure 3. Progressive positive dysregulation of CSF3 and IL-6 in the lungs and systemic circulation characterizes cigarette smoke-augmented influenza. **a)** Multiplex analysis of cytokines in lung homogenates at 5dpi and 7dpi. Values represent Log_2 fold changes vs. the RA-PBS group for each timepoint. $n=4-5$ group, one representative experiment is shown. **b)** Dysregulation scores were derived for each cytokine using the equation at left. Scores were plotted against mean pg/ml values for each group. Cytokines were further stratified based on CS-FM1/RA-FM1 fold change ≥ 2 (black dots) or < 2 (white). One representative experiment (7dpi; $n=4-5$ /group) is displayed in the middle panel. The right hand panel displays a correlation between dysregulation scores for this and a second replicate experiment ($n=5-10$ /group). **c)** Dysregulation scores were compared between 5dpi and 7dpi (left panel), and cytokines were binned according to the relative change in dysregulation during this timeframe (right panel). **d)** Specific lung homogenate cytokines from **(a)** are displayed. $n=4-5$ /group, one experiment of two is shown. **e)** Cytokines were quantified in whole lung tissue by RT-qPCR. $n=5-10$ /group, one experiment of two is shown. **f)** Cytokines were quantified in plasma by ELISA. $n=5-9$ /group, one experiment of two is shown. **g)** Plasma CSF3 and IL-6 were correlated against core temperature. $n=14-18$ /group from two experiments. **(c)** Student's unpaired t-test. **(d-f)**: Two-way ANOVA with Tukey's post-hoc test. **(b, g)** Pearson's correlation. $p < 0.05$ *. PD: positive dysregulation, NR: normalization, ND: negative dysregulation.

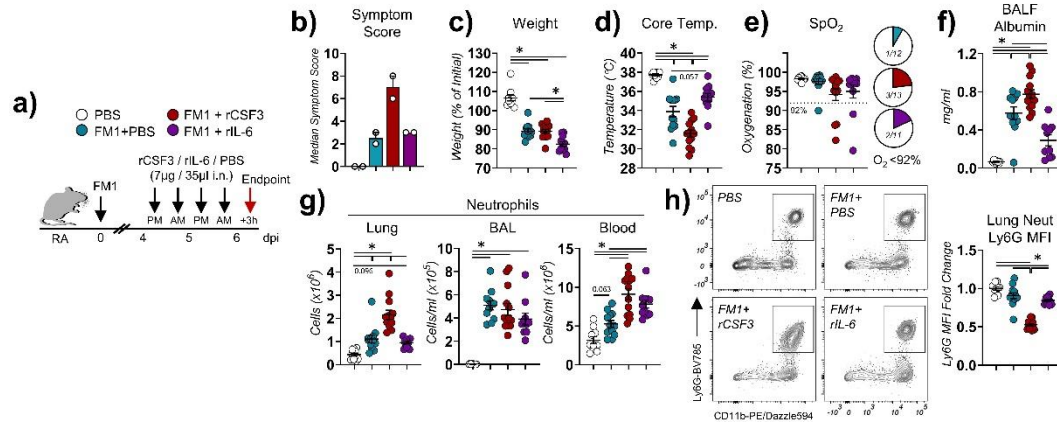


Figure 4. CSF3 supplementation exacerbates morbidity and alveolar-capillary barrier dysfunction during influenza infection. **a)** Experimental model. BALB/c mice were infected with 50 PFU of FM1 or PBS vehicle. At the indicated timepoints, recombinant (r)CSF3, rIL-6 (7µg/35µl) or PBS vehicle was delivered intranasally under anaesthesia. Three hours after the last dose on 6dpi, animals were culled. **b)** Median symptom score per group (see Materials & Methods) from two experiments. **c)** Weight over time, normalized to starting weight. **d)** Core temperature was measured by rectal thermometry. **e)** SpO₂ was assessed by pulse oximetry. 92% represents a clinical threshold for systemic hypoxemia. **f)** Mouse serum albumin was measured in the bronchoalveolar lavage fluid (BALF). n=10-13/group from two experiments **g)** Absolute number of neutrophils were quantified in the lung, BAL and blood using flow cytometry. **h)** Ly6G median fluorescence intensities (MFI) values were quantified for lung neutrophils. Representative flow cytometry plots are shown at left. n=9-13 mice per group from two experiments. One-way ANOVA with Tukey's post-hoc test. p<0.05*.

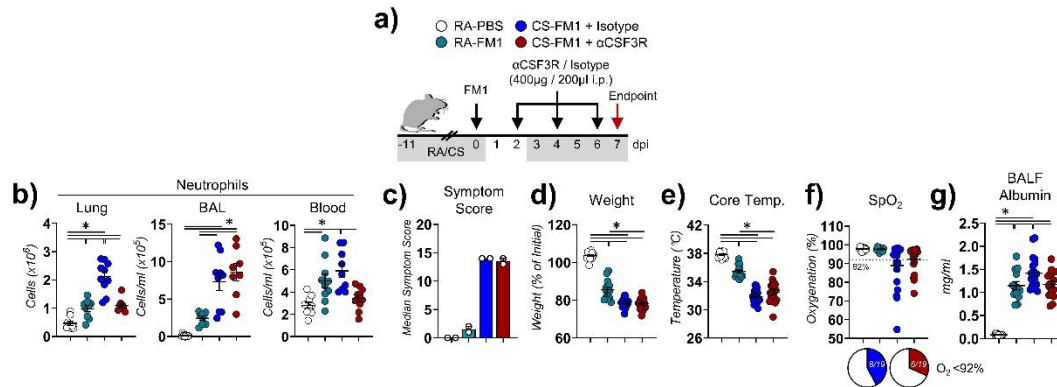


Figure 5. Systemic CSF3R inhibition improves alveolar-capillary barrier function during smoke-augmented influenza. **a)** Experimental model. BALB/c mice were exposed to room air or cigarette smoke and infected with 50 PFU of FM1 as described in **Figure 1a**. At 2/4/6dpi, anti-CSF3R (α CSF3R) antibody or isotype control (400 μ g/200 μ l PBS vehicle) was delivered intraperitoneally to CS-FM1 mice. Animals were culled at 7dpi. **b)** Absolute number of neutrophils were quantified in the lung, BAL and blood using flow cytometry. n=8-10/group from two experiments. **c)** Median symptom score per group (see Materials & Methods) from two experiments. **d)** Weight over time, normalized to starting weight. n=14-20/group from three experiments. **e)** Core temperature was measured by rectal thermometry. n=14-20/group from three experiments **f)** SpO₂ was assessed by pulse oximetry. 92% represents a clinical threshold for systemic hypoxemia. n=10-19/group from three experiments **g)** Mouse serum albumin was measured in the bronchoalveolar lavage fluid (BALF). n=13-19/group from three experiments. One-way ANOVA with Tukey's post-hoc test. p<0.05*.

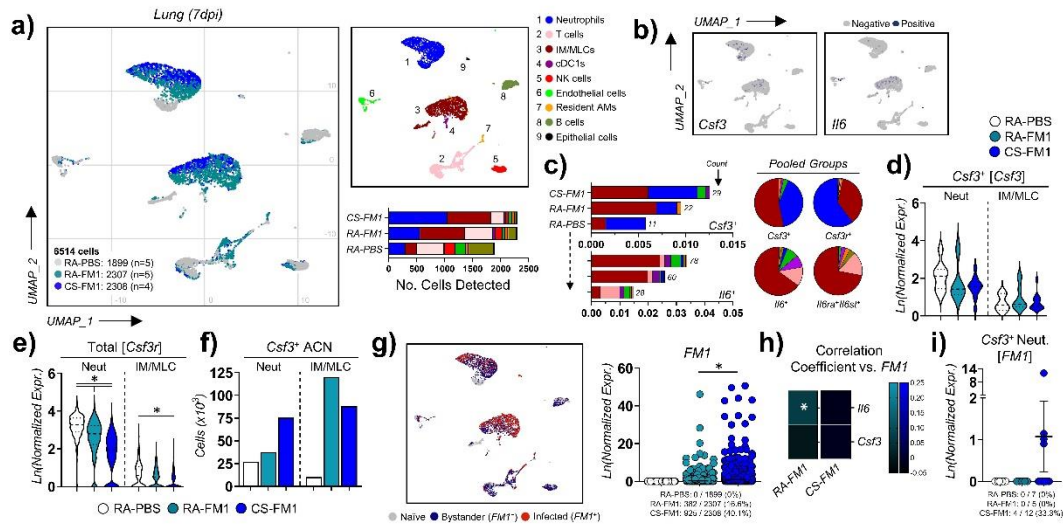


Figure 6. Cigarette smoke skews the distribution of *Csf3*-expressing cells towards neutrophils. Single cell suspensions prepared from the lungs of RA-PBS (n=5 pooled, 1899 cells), RA-FM1 (n=5 pooled, 2307 cells) and CS-FM1 mice (n=4 pooled, 2308 cells) were analyzed by single cell RNA sequencing at 7dpi for both mouse and FM1-MA cRNA transcripts. **a)** UMAP plots of all cells coloured by sample (left) or cell identity (top right), and number of cells of each cell type detected per group (bottom right). **b)** Overlay plots for *Csf3* and *Il6*. **c)** Frequencies of cytokine-expressing cells broken down by cell type. ‘Cytokine’ pie charts reflect summed values from group breakdowns at left. ‘Counts’ represent the absolute number of positive cells detected. **d)** Expression of *Csf3* within *Csf3*⁺ neutrophils and macrophages. **e)** *Csf3r* expression within total neutrophils and IM/MLCs (interstitial macrophages/monocyte-lineage cells). **f)** Approximated absolute number of *Csf3*⁺ neutrophils and IM/MLCs. **g)** UMAP overlay demonstrating the distribution of infected (*FMI*⁺), bystander (*FMI*⁻) cells from influenza-infected groups and naïve cells (RA-PBS; left); Expression of *FMI* cRNA transcripts between groups and quantification of *FMI*⁺ cells (right). **h)** *FMI* expression values were correlated against the specified cytokine genes. **i)** Expression of *FMI* cRNA transcripts in *Csf3*⁺ neutrophils per group. **(d, e)** FindMarkers, Seurat package (R) **(h)** Pearson’s correlation. p<0.05*. ACN: absolute cell number.

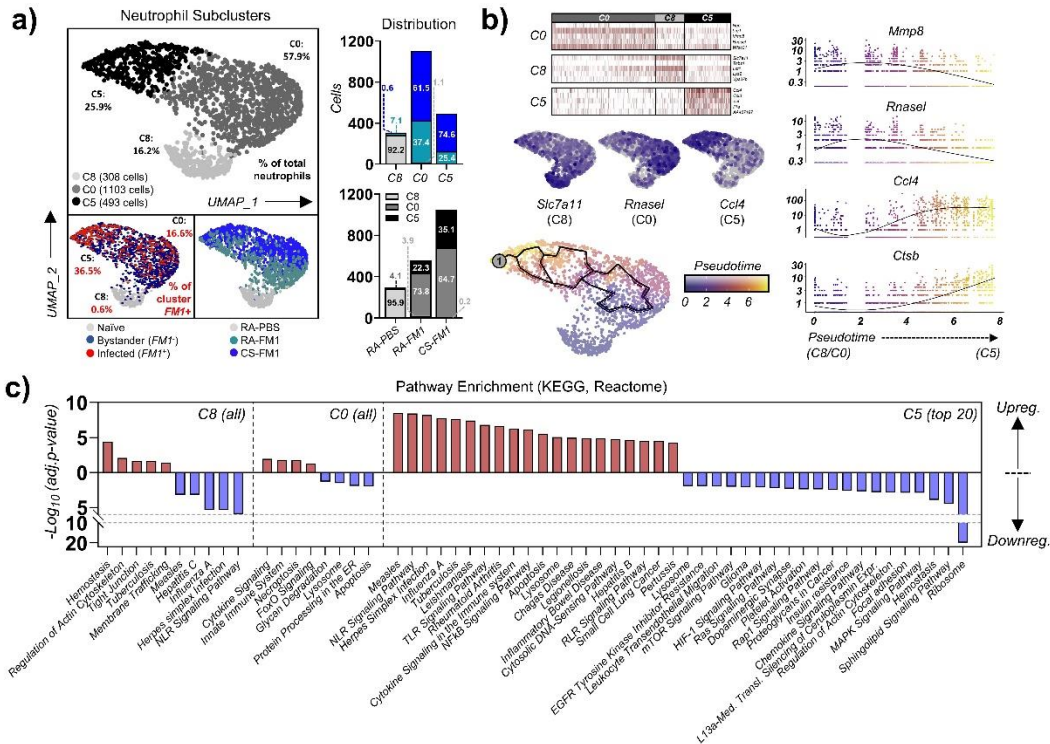


Figure 7. Subcluster analysis indicates that cigarette smoke-exposed lungs are enriched for infected, highly inflammatory neutrophils. Lung cells were assessed by scRNAseq as described in Figure 6. **a)** UMAP plots showing the distribution of transcriptional subclusters (top), infected cells (bottom left) and sample types (bottom right) within neutrophils. The distribution of samples across subclusters (and vice versa) are quantified in the bar charts at right. **b)** Unique positively-regulated genes were identified for each cluster by pairwise differential expression analysis; the top 5 are presented in heat maps (top left). UMAP overlays are included for one gene from each subcluster. Unbiased Monocle pseudotime trajectory analysis was conducted within all neutrophils (bottom left). The ① symbol represents an algorithmically-defined unique cell state. Expression plots (right) represent four genes that were uniquely expressed within the two infected subclusters. **c)** Genes unique to each subcluster were assessed for positive and negative pathway enrichment using KEGG and Reactome databases (via STRING). All significantly enriched pathways are shown for C8/C0, while only the top 20 (up- and downregulated, of 135 total) pathways are shown for C5.

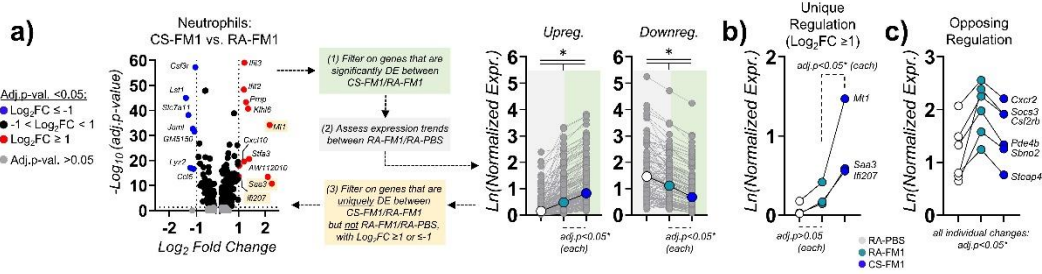


Figure 8. Neutrophil gene signatures from smoke-exposed, influenza-infected mice reflect an exacerbated form of typical disease with unique regulatory features. Lung cells were assessed by scRNAseq as described in Figure 6. **a)** Left: Volcano plot demonstrating differentially-expressed genes (DEGs) between CS-FM1 and RA-FM1 neutrophils. Top, Right: Significant DEGs were broken down into those that were up- and down-regulated and plotted (light green). Mean expression trends were assessed between RA-FM1 and RA-PBS for these genes (grey). Significance bars at top represent one-way ANOVA with Tukey’s post-hoc test comparing population means. Large dots represent median values for each group. Bottom: Genes were filtered to assess those that were uniquely differentially expressed between CS-FM1/RA-FM1 by >2 -fold, but not differentially expressed between RA-FM1/RA-PBS (yellow). The mean expression values for these genes are presented in **(b)**. **c)** Genes in A were screened for those that displayed opposing regulation between CS-FM1/RA-FM1 and RA-FM1/RA-PBS. Shown are the genes that were significantly upregulated by infection alone but downregulated by concurrent smoke exposure. No genes displayed the reciprocal pattern (significantly downregulated by influenza but upregulated by concurrent smoke). $\text{adj. } p < 0.05^*$.

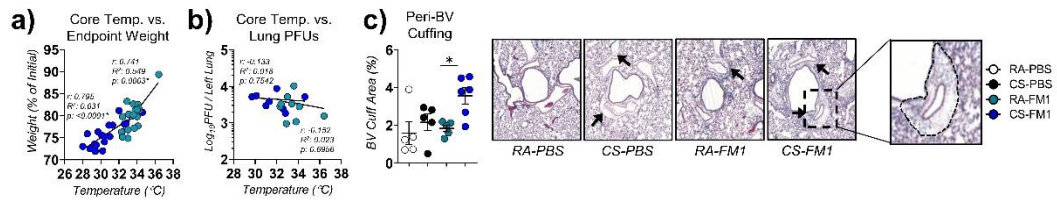


Figure S1. Extended data for Figure 1. Core temperature was correlated against **a)** endpoint weight (n=18-19/group from two experiments) and **b)** lung PFUs (n=8-9/group) at 7dpi. **c)** Area of peri-bronchovascular (BV) cuffing was quantified in lung histology sections. n=5/group. **(a-b)** Pearson’s correlation. **(c)** Two-way ANOVA with Tukey’s post-hoc test. $p < 0.05^*$.

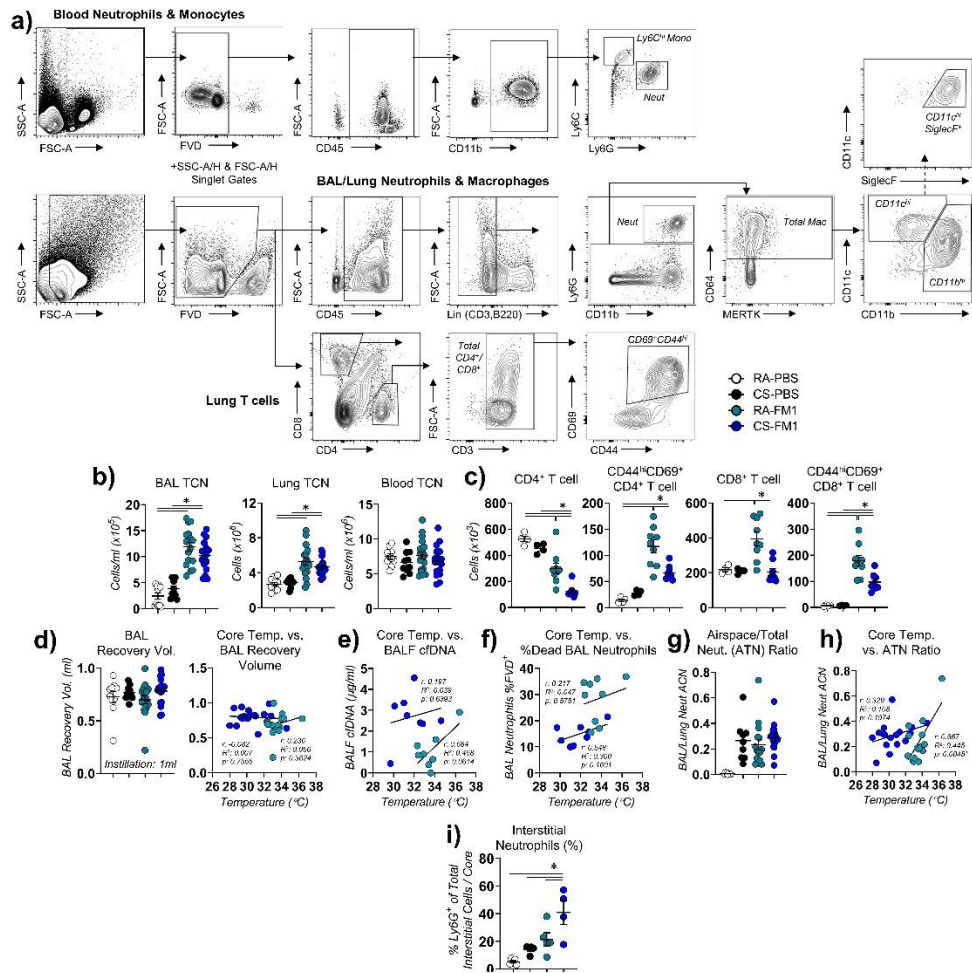


Figure S2. Extended data for Figure 2. Animals were treated as in Figure 1A, and culled at 7dpi. **a)** Gating strategy for immune cell populations in the blood, lungs and bronchoalveolar lavage (BAL). **b)** Total cell number (TCN) for BAL, lungs and blood. BAL: n=10-17/group, lung: n=9-18/group, blood: n=10-19/group, each from two experiments. **c)** Absolute number of T cell subsets in the lung. n=4-9/group. **d)** BAL recovery volume per mouse and correlation with core temperature. n=10-19/group from two experiments. **e)** BALF cell-free (cf)DNA levels or **f)** the proportion of neutrophils that were dead (FVD+) in the BAL. n=8-9/group, one representative experiment of two is shown. **g)** Airspace-to-total (ATN) ratios were derived of absolute cell numbers for each mouse. n=16-17/group from two experiments. **h)** Core temperature was correlated against ATN ratio. n=16-17/group from two experiments. **i)** Neutrophils were identified by Ly6G staining of tissue microarrays. Interstitial areas were defined with the help of a pathologist, and Ly6G⁺ events were quantified in each core using HALO software. The proportion of interstitial neutrophils was derived relative to total cells per core. n=4-5/group. FVD: fixable viability dye. **(b-d, g, i)** Two-way ANOVA with Tukey's post-hoc test. **(e-f, h)** Pearson's correlation. $p < 0.05^*$.

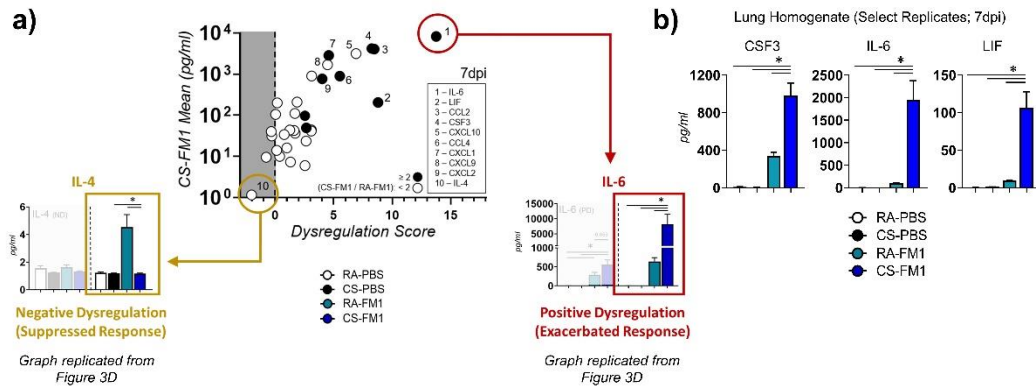


Figure S3. Extended data for Figure 3. **a)** Validation of dysregulation scoring. After deriving the equation in Figure 3B, dysregulation scores were calculated for each cytokine at each timepoint. As a means of validation, we assessed the expression profiles of cytokines with a negative and highly positive dysregulation score. Those cytokines with a positive score (e.g. IL-6, red) displayed an exaggerated expression in CS-FM1 mice relative to all other controls, while those with a negative score (e.g. IL-4, yellow) displayed were upregulated following infection but suppressed with concurrent smoke exposure, as intended. **b)** Replicate lung homogenate cytokine data for select cytokines of interest. n=5-10/group. Two-way ANOVA with Tukey's post-hoc test. p<0.05*.

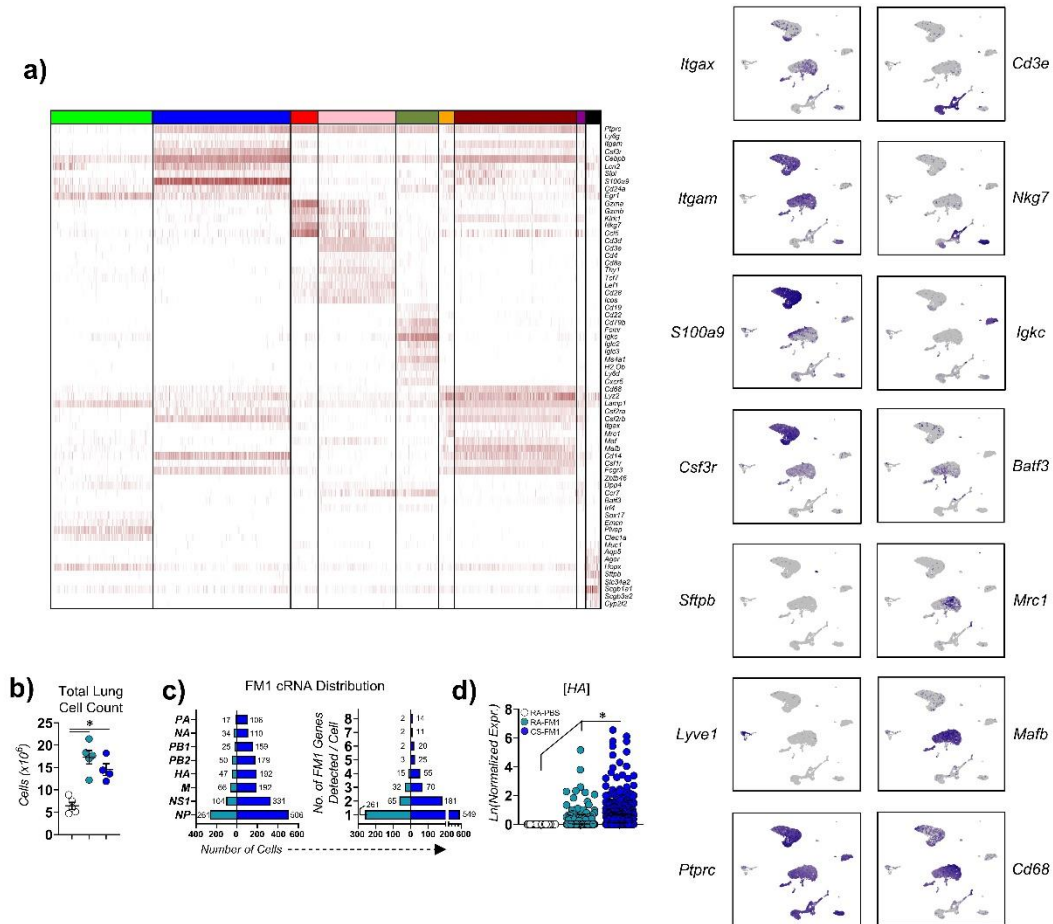


Figure S4. Extended data for Figure 6. Lung cells were assessed by scRNAseq as described in Figure 6. **a)** Heatmap displaying key genes used for identifying cell populations, and overlays displaying the expression of select genes. **b)** Total cell number of lung single cell suspensions used in this study. **c)** Count of cells (left) expressing each individual cRNA segment or (right) co-expressing multiple cRNAs. **d)** Quantification of HA cRNA expression in all cells per group. One-way ANOVA with Tukey’s post-hoc test. $p < 0.05^*$.

Supplementary Results:

**References for supplementary material are provided separately below.

ATN Ratio (Figure 2/S2):

We considered whether a differential accumulation of neutrophils in the interstitium relative to the airspaces correlated with negative outcome. To do so, we derived an airspace-to-total lung neutrophil (ATN) ratio. Smoke-exposed and influenza-infected mice independently had an elevated ATN ratio over room air, uninfected controls, while no difference was observed between infected groups (**Figure S2g**). However, we found a strong, significant positive correlation between ATN ratio and core temperature (**Figure S2h**) in RA-FM1 mice and a similar but non-significant trend in CS-FM1 mice, suggesting that those mice with a lower airspace relative to total neutrophils had a greater morbidity.

FM1 cRNA Detection (Figure 4/S4):

Each FM1 cRNA segment was expressed at a different frequency in our dataset: *NP* and *NS* were detected in the most cells, followed by *M*, *HA*, *PB2*, *PB1*, *NA* and *PA* segments (**Figure S4e**). The extent to which individual cells expressed multiple FM1 genes concurrently also varied, with the majority of *FM1*⁺ cells exhibiting co-expression of only 1 (17.6%) or 2 (5.3%) different segments (**Figure S4e**). Detection of all eight segments occurred in only 0.3% of cells in

infected samples, although this value was again elevated in smoke-exposed, influenza-infected mice relative to infected controls by a factor of seven-fold.

Supplementary Methods:

PFU Assays

Madin-Darby Canine Kidney (MDCK) cells were seeded into 6-well plates in complete (c)DMEM (10% FBS, 2mM L-glutamine, 0.1mg/ml penicillin and streptomycin) and incubated (37°C, 5% CO₂) until confluent. Lung homogenates were serial diluted in 2x plaque media (2x MEM, 0.25% sodium bicarbonate, 4mM L-glutamine, 0.2mg/ml penicillin and streptomycin, 20mM HEPES, 0.42% BSA) diluted 1:1 with distilled water and supplemented with TPCK-trypsin to a final concentration of 1µg/ml. After washing with PBS, sample dilutions (500µl, 1:2 to 1:2e⁵) were added to the cells and incubated for 1 hour with occasional gentle agitation. After removing the samples, cells were washed twice with PBS and overlaid with a 2ml of a 1:1 mixture of agar (OXOID, Thermo Fisher) and 2x plaque media supplemented with 0.01% DEAE-Dextran and 1µg/ml TPCK-trypsin. After 48-72 hours, overlays were removed, cells were fixed with 4% PFA and subsequently stained with 1% crystal violet in PBS. Counts from the most reliable dilution were used to determine plaque forming units (PFUs) per sample.

Dysregulation Scoring

Dysregulation scores (DS) for lung homogenate cytokines were derived by multiplying the expression fold-change between infected groups (CS-FM1/RA-FM1) by the fold-change induced following infection in the smoke-exposed groups (CS-FM1/CS-PBS), and \log_2 -transforming the resulting value. The DS for each cytokine was then plotted against the respective mean pg/ml value for CS-FM1 mice. Cytokines entered into this equation were further stratified based on whether or not they possessed a CS-FM1/RA-FM1 fold change ≥ 2 in order to ensure that scores were not elevated as a result of changes over baseline alone. Attempts to validate this approach (**Figure S3a**) demonstrate that cytokines with a positive DS showed an exaggerated expression profile in CS-FM1 mice (e.g. IL-6, 7dpi), while those with a negative DS exhibit a suppressed expression profile (e.g. IL-4, 7dpi), as intended. For binning (**Figure 3c**), positive dysregulation was defined as instances when the absolute value of DS increased to a greater positive value between 5dpi/7dpi, normalization as instances when the absolute value approached zero, and negative dysregulation as instances when the value decreased to a greater negative value.

Flow Cytometry

To generate single cell suspensions, lungs were finely minced, agitated for 1h at 37C in 10ml of RPMI containing 150U/ml collagenase I, and pressed through 40 μ m mesh filters. Red blood cells were lysed in the resulting single cell suspensions

using ACK lysis buffer (0.15M NH₄Cl, 10mM KHCO₃, 0.1nM Na₂EDTA in water), and resuspended in PBS. Cells were counted using a haemocytometer. For flow cytometry, cells were transferred to a 96-well plate. Cells were stained for viability using LIVE/DEAD Fixable Yellow Dead Cell Stain (Molecular Probes; 1:400 in PBS), and blocked with anti-CD16/32 (Biolegend; 1:100 in FACS buffer (0.5% BSA, 2mM EDTA in PBS)). Subsequently, cells were stained with fluorophore-conjugated antibodies targeting specific antigens (**File S1**) diluted in FACS buffer. Fluorescence-minus-one controls were used to determine thresholds for gating strategies. Data was collected using a BD LSRFortessa (BD Biosciences), and data analysis performed using FlowJo software (V10; TreeStar, Inc.). Absolute cell number (ACN) quantification was performed by multiplying the frequency of the given population with regards to live singlet events (for lung and blood cells) or live CD45⁺ events (for BAL cells) by the total haemocytometer cell count for that sample.

Single-cell RNA Sequencing (Expanded)

At 7dpi, whole lungs were processed into single cell suspensions as described above. Samples were pooled per group. scRNAseq was performed at the Princess Margaret Genomics Centre (University of Toronto, Toronto, ON). Pooled cells were counted manually using a haemocytometer and loaded for 3' v3.1 chemistry according to standard 10X Genomics protocol. Viabilities ranged from 74-80% following processing. Cells were sequenced using a Novaseq 6000 platform. Raw

sequencing data (BCL format) were processed to FASTQ and demultiplexed using bcl2fastq (Illumina). FASTQ files were processed using 10X Genomics Cell Ranger pipeline version 3.1.0. Read mapping was performed using a custom reference genome comprised of mouse mm10 and influenza A/FM/1/47-MA cRNAs (PB2 (GenBank: CY087791.1), PB1 (CY087790.1), PA (CY087789.1), NEP/NS1 (CY087788.1), NP (CY087787.1), NA (CY087786.1), M1/M2 (CY087785.1), HA (CY087784.1). Because cRNAs are produced during active infection and are not contained within viral particles, positive expression of these transcripts identifies infected cells rather than co-encapsulated viral particles. Cells with unique counts over 6,000 or less than 200 were filtered out. Next, cells with mitochondrial counts < 6, 7 and 9% were selected for CS-FM1, RA-FM1 and RA-PBS, respectively to best approximate viabilities acquired by haemocytometry. After filtering, a total of 6514 cells were retained for further analysis. Raw counts were log-normalized and used for PCA, which was followed by unsupervised clustering analysis and Uniform Manifold Approximation and Projection (UMAP[1]) for dimensionality reduction and visualization (Seurat package in R[2]). Cell clusters were classified into cell populations by using a list of markers obtained from literature sources (**Figure S4a**). Differential expression analyses were carried for neutrophil and IM/MLC populations using FindMarkers function in the Seurat package; adjusted p-values < 0.05 were considered to be significant. Viral load of cells was estimated by summing the expression of all eight FM1 cRNAs on a per-cell basis to derive an ‘*FMI*’ transcript readout. This value was

used to classify cells from infected samples (CS-FM1 and RA-FM1) into “bystander cells” ($FMI = 0$) and “infected cells” (score > 0). Cells from RA-PBS sample were referred to as “naïve cells”.

Unsupervised clustering performed prior to the UMAP revealed three subclusters in the neutrophil population (C8, C0 and C5). Pair-wise differential analysis was performed comparing these subclusters, yielding lists of genes uniquely expressed in each of these subclusters as compared to the others. These gene lists were used for subsequent STRING[3, 4]-based pathway enrichment analysis using KEGG and Reactome databases. Pseudotime analysis was performed within the neutrophil population using Monocle3[5].

References for Supplementary Material

1. McInnes L, Healy J, Saul N, Großberger L. UMAP: Uniform Manifold Approximation and Projection. *J. Open Source Softw.* 2018; 3: 861.
2. Satija R, Farrell JA, Gennert D, Schier AF, Regev A. Spatial reconstruction of single-cell gene expression data. *Nat. Biotechnol.* 2015; 33: 495–502.
3. Snel B, Lehmann G, Bork P, Huynen MA. String: A web-server to retrieve and display the repeatedly occurring neighbourhood of a gene. *Nucleic Acids Res.* 2000; 28: 3442–3444.
4. Szklarczyk D, Gable AL, Lyon D, Junge A, Wyder S, Huerta-Cepas J, Simonovic M, Doncheva NT, Morris JH, Jensen LJ, Von Mering C. STRING v11: protein-protein association networks with increased coverage, supporting functional discovery in genome-wide experimental datasets. *Nucleic Acids Res.* 2018; 47: 607–613.
5. Trapnell C, Cacchiarelli D, Grimsby J, Pokharel P, Li S, Morse M, Lennon NJ, Livak KJ, Mikkelsen TS, Rinn JL. The dynamics and regulators of cell fate decisions are revealed by pseudotemporal ordering of single cells. *Nat. Biotechnol.* 2014; 32.

****Note: File S1 will be provided as an adjunct .xlsx file.**

CHAPTER 5 – DISCUSSION

The central focus of this thesis was to gain a better understanding of the relationship between cigarette smoke and antimicrobial host defense in the respiratory tract. Two of the studies completed herein (Chapters 2 and 4) directly address this relationship in different contexts (IgA induction in the upper airways, responses to influenza in the lower airways). The last is a methodological study that aimed to optimize methods with which to study antibodies in human mucoid respiratory samples (Chapter 3), with future applications to smoking-related disease.

5.1 – Summary of Results and General Discussion

**Discussion provided in this section is intended to supplement existing discussion presented in the manuscripts above (Chapter 2-4).*

5.1.1 – Cigarette Smoke & IgA Induction in the Upper Airways

Work conducted early in my graduate studies focused on investigating the relationship between smoke exposure and antibody responses in the upper airways (Chapter 2). Smokers have been demonstrated to exhibit less LPS-specific IgA in their nasal secretions²⁰². However, prior to this thesis it was specifically unknown to what extent smoke exposure could affect IgA induction in the upper airways. This is an important knowledge gap given the increased interest within the immunological community regarding the development of IgA-oriented intranasal vaccines (e.g. NCT04751682, NCT04798001, NCT04816019 for SARS-CoV-2).

To address this concern, we developed a mouse model of concurrent cigarette smoke exposure and intranasal immunization with a model antigen/adjuvant. Using this model, we demonstrated that tobacco smoke suppresses the induction of antigen-specific IgA in the upper respiratory tract, reproductive tract and systemic circulation without compromising systemic IgG or IgM induction. This latter finding notably supports previous reports in which smokers were observed to induce similar HAI titres in the blood compared to non-smokers following LAIV vaccination¹⁸⁶, as well as work from our group showing no difference in influenza-specific IgG induction following pulmonary infection of cigarette smoke-exposed with influenza¹⁷⁶. To our knowledge, however, our finding of attenuated antigen-specific IgA induction in the upper airways following intranasal immunization is novel. Excitingly, a recent clinical study similarly showed a reduced induction of nasal influenza-specific IgA following LAIV vaccination in humans²⁰³, corroborating our findings in mice.

In addition to antibody quantity, we also assessed metrics of nasal IgA antigen-binding avidity and *Igha* mutational load. In this regard, IgA produced in the nose of smoke-exposed mice demonstrated reduced avidity compared to room air controls, although this deficit was only observed during the acute post-immunization period, recovering by 14-28dbp. This is one of the first reports of antibody avidity in the context of smoke exposure; one prior study demonstrated that human smokers more frequently produce low-avidity HPV-specific IgG compared to non-smokers¹⁹⁰, but none have assessed IgA to date to our knowledge.

Surprisingly, despite our observations of reduced avidity we noted higher mutational burden in nasal *Igha* transcripts of smoke-exposed mice, both at baseline and following immunization. In terms of NALT germinal centres, basal activity was increased by cigarette smoke exposure alone, while immunization, which elicited an increase in activity in room air mice, actually diminished activity in smoke-exposed mice. In seeking to explain the discrepancy between mutational load and avidity at the same timepoint (3dbp), we suggest in Chapter 2 (Discussion) that excess mutations, potentially caused through the effects of early elevated basal germinal centre activity, interfere with affinity-based selection of OVA-specific clones. This may thereby reduce the avidity of polyclonal IgA produced after immunization. However, the means by which avidity equalizes over time are not known. This may occur through a delay, rather than a suppression, of germinal centre activation and affinity maturation in smoke-exposed mice. Finally, also unclear are the mechanisms by which smoke augments basal germinal centre activity in the NALT. Although not completely analogous, cigarette smoke is capable of promoting lymphoid neogenesis (i.e. induction of tertiary lymphoid tissues; TLTs) in the lungs, a feature commonly observed in COPD²⁰⁴. These TLTs can develop germinal centres in some instances²⁰⁵. NALT germinal centre activation may thus reflect a similar process in an existing secondary lymphoid tissue, by means of the activation of B cell clones specific for smoke-derived antigens, or an ability of smoke-derived chemicals to stimulate germinal centre cycling against endogenous antigens or neo-antigens. In this regard, cigarette

smoke itself contains bacterial LPS²⁰⁶, a potent B cell mitogen²⁰⁷, which may drive this process.

Mechanistically, deficits in IgA induction were associated with a reduced accumulation of antigen-specific IgA ASCs in the nasal mucosa, nasal-draining lymphoid tissues (e.g. the NALT, cervical lymph nodes, and spleen), and blood, but not bone marrow. We also observed that smoke exposure attenuated the upregulation of VCAM-1 and pIgR, two molecules critical to IgA ASC homing and transepithelial transcytosis respectively¹²⁹, in the nasal mucosa. Notably, this suggests that in addition to IgA-specific processes, cigarette smoke affects molecular functions of stromal cells associated with mucosal immunity more broadly. pIgR, for instance, is known to transcytose any J chain-containing immunoglobulins, including both polymeric IgA and IgM¹²⁹, although we did not observe IgM induction in the NALF even under room air immunized conditions. VCAM-1 has even broader function, in that it can facilitate endothelial adhesion for a variety of cell types beyond ASCs including neutrophils, lymphocytes and eosinophils²⁰⁸. These deficits in VCAM-1 upregulation may thus have implications for the recruitment of immune effector cells to the nasal mucosa under infectious conditions, although this remains to be determined.

The effects of cigarette smoke appear to be multifactorial, causing evident deficits in both hematopoietic (ASC induction, which may relate to function of dendritic cells, Tfh cells and/or B cells) and stromal (epithelial pIgR, endothelial VCAM-1) compartments with apparent effect on nasal IgA. Within the stromal

compartment, one potential mechanism of inhibition might be an autoregulatory refractory inhibition of NF κ B signaling. Cigarette smoke contains bioactive LPS²⁰⁶, which could activate TLR-4-dependent NF κ B signaling in nasal epithelial and endothelial cells. NF κ B activation is known to trigger autoregulatory pathways to self-limit inflammation²⁰⁹⁻²¹¹. This self-limiting process may explain why subsequent exposure to our chosen adjuvants LPS and polyI:C, which can act in part through NF κ B signaling^{210,212}, fails to upregulate molecules such as pIgR and VCAM-1. This hypothesis, however, does not necessarily capture why IgA-specific deficits occur given that changes to NF κ B signaling in critical hematopoietic cells such as dendritic cells would likely affect all isotypes. Instead, a specific lack of IgA relative to IgG and IgM may relate to, for instance, an impaired activation of TGF- β -secreting Tfh cells which are known to promote IgA class switch recombination in secondary lymphoid tissues¹⁵⁰. Multiple avenues of investigation remain open to assess mechanisms by which smoke exposure inhibits IgA induction in the URT.

Overall, this study provides compelling evidence that cigarette smoke affects IgA induction in the upper airways, and defines potential mechanisms underpinning this deficit. These findings may have implications for the design and implementation of IgA-oriented intranasal vaccination strategies in our highly smoke-exposed global population, as discussed below (section 5.2.1).

5.1.2 – PBS- vs. DTT-based Sputum Processing for Antibody Detection

The second study presented here (Chapter 3) was a methodological investigation aimed at optimizing antibody recovery from human sputum. Prior to this thesis, no study had systematically compared PBS²¹³- and DTT²¹⁴-based sputum processing methods for their effects on antibody recovery. In pursuing this study we found that, although these methods were largely comparable in terms of total IgM and IgG recovery, DTT increased IgA yield both from neat samples and following immunoprecipitation, while IgE recovery was reduced. IgG, IgA and IgM were stable over several freeze-thaw cycles independent of the processing buffer used. Previous reports have indicated that all major isotypes are susceptible to denaturation by DTT to some degree through the chemical's ability to interfere with disulfide bonds²¹⁵⁻²¹⁸. However, it was unclear previously whether these reductive effects would also manifest in the context of the specific concentrations and incubation periods used in clinical sputum protocols²¹⁴. In this regard, IgE appears to be more susceptible to the reductive effects of DTT than the other isotypes under the utilized conditions. In terms of increased IgA recovery, the isotype is known to directly interact with mucin proteins²¹⁹, and thus DTT-mediated mucolysis may explain the increased yield. Dithioerythritol (DTE), the optimal isomer of DTT, has been shown previously to increase IgA yields from sputum²²⁰; however, DTT is more commonly used in clinical sputum processing than DTE, and the effects of DTT were unknown in this regard. Thus, an analysis of IgA

recovery using DTT-based clinical protocols was still warranted within our broader assessments of yield and stability for all major isotypes.

Finally, in addition to total IgA, DTT enhanced the detection of a known disease-associated autoantibody (anti-EPX IgG)²²¹ in immunoprecipitated sputum samples. This antibody specificity has been observed to be enriched in the sputum of eosinophilic, prednisone-dependent asthma patients with recurrent lung infections in the past²²¹. Consequently, this finding may have implications for the sensitive assessment of single antibody and autoantibody specificities in sputum for use in biomarker discovery. Overall, our work shows that the choice between PBS- and DTT-based sputum processing should be made based on the isotype of interest, thereby informing protocol choice in future studies of smoking-related diseases. If IgA/IgM/IgG are of primary consideration, DTT provides benefit to yield without reducing stability during freeze-thaw cycles. If IgE is of primary interest, DTT should be avoided. Ultimately, the best approach may be to split samples and process one half with each of DTT and PBS, so as to maximize analytical value.

5.1.3 – Cigarette Smoke and Pulmonary Influenza Infection

The third study of this thesis (Chapter 4) focused on investigating the mechanisms by which cigarette smoke exacerbates the severity of influenza-associated disease. Smokers are well known to be at increased risk of acquiring influenza⁴¹, developing severe disease⁴³, and undergoing hospital/ICU admission⁴²,

although the mechanisms underpinning these predispositions are not well understood.

Following infection of mice with H1N1 influenza (A/FM/1/47-MA), we found that concurrent smoke exposure augmented weight loss, hypoxemia, hypothermia, morbidity, and mortality relative to infection-only controls. While excess weight loss and mortality have been reported previously^{173,175}, to our knowledge ours is the first study to assess oxygen saturation and core temperature under these conditions. These findings were notably associated with augmented pulmonary edema, elevated hematocrit, and a reduced pulmonary expression of the endothelial adherens junction molecule VE-cadherin²²² in smoke-exposed infected mice. Overall, these data suggest that smoke exposure exacerbates alveolar-capillary barrier dysfunction elicited by influenza. Notably, although smoking alone is known to increase pulmonary edema and hypoxia in humans²²³, previous studies using mouse models of concurrent smoke/infection at similar timepoints have found a reduced or similar amount of protein leakage into the BALF of smoke-exposed, infected mice relative to infection-only controls^{175,224}. However, these findings were made using sub-lethal infectious doses, in the context of which leakage kinetics may be different. In terms of viral burden, we observed an accumulation of viral RNA in the lungs of smoke-exposed, infected mice independent of replication-competent viral particles. These data appear to unify prevailing observations in the field, as discussed in detail in Chapter 4.

In assessing inflammatory cell infiltrates in the lungs, we noted excess pulmonary neutrophilia both in the airspaces and interstitium. However, in correlating neutrophilia in each compartment with available metrics of morbidity, we found that interstitial and airspace neutrophilia positively and negatively predicted morbidity, respectively. This is despite the fact that neutrophils were elevated overall in the BAL of highly morbid smoke-exposed, infected mice, which had initially led us to hypothesize that BAL neutrophilia would negative correlate with core temperature (i.e. animals with more severe disease would have more BAL neutrophils). This indicates that a skewed distribution of neutrophils between interstitial and airspace niches is associated with negative outcome, and raises an interesting question as to what molecular factors or conditions regulate this distribution. One such factor may be the extent of pathogen infection within the submucosa, such as within endothelial cells. Elevated endothelial infection may result in chemotactic gradients skewed in favour of neutrophil retention in the parenchyma, thus reducing neutrophils migration into the alveoli. In support of this idea, we observe more infection of endothelial cells in smoke-exposed, infected mice than infection-only controls using scRNA-seq. Further experiments aimed at correlating the extent of endothelial cell infection with relative interstitial vs. airspace neutrophilia may therefore be warranted.

Using a novel dysregulation scoring system, we identified IL-6 and CSF3 as being highly exacerbated in the lungs and blood of smoke-exposed influenza-infected mice, with plasma CSF3 levels strongly correlating with hypothermia.

Mechanistically, intranasal CSF3 supplementation during influenza increased hypothermia, morbidity, and BALF albumin levels, while anti-CSF3R blockade reduced albumin levels without modulating morbidity. Ultimately, these data suggest that CSF3 signaling can play a pathogenic role in influenza, especially in the context of several clinical reports indicating an increase in hypoxemia and/or capillary leakage following systemic CSF3 treatment in humans^{225–227}, including during SARS-CoV-2 infection^{228,229}. However, they also suggest that these roles are redundantly mediated by other cytokines or mediators in the context of influenza. This work is discussed in more detail in Chapter 4 (Discussion) and below (section 5.2.2).

Next, we pursued scRNA-seq to assess whether smoke exposure skews the distribution of cytokine-producing cells during influenza. Excitingly, this analysis revealed neutrophils as a novel and prominent expressor of *Csf3* in the lungs. Furthermore, it defined a skew in the distribution of *Csf3*⁺ cells towards neutrophils (without a bias in terms of infection status) and away from monocyte/macrophage-lineage cells in the context of smoke exposure and influenza infection. This is of great interest given that neutrophils are the canonical CSF3R-expressing cell type²³⁰, thus suggesting the existence of a recruitment positive feedback loop between *in situ* pulmonary neutrophils and additional neutrophil recruitment. Similar loops featuring CXCR1/2-binding cytokines have previously been implicated in focal interstitial neutrophilia during influenza in mice⁸⁹. Notably, it should be considered that our analysis was restricted to a late stage of infection;

earlier on, it is likely that resident interstitial macrophages (or other cell types) are the initial producers of CSF3 given their known inflammatory predisposition²³¹, with recruited neutrophils subsequently propagating this process.

After assessing cytokine distribution, we specifically pursued a deep transcriptional analysis of neutrophils given their increased presence in our model and known association with severe disease. Three neutrophil subclusters were algorithmically identified; one (C8) was derived almost entirely of naive cells, while the other two (C0/C5) were comprised of neutrophils from infected samples. The most naive-distal infected-sample subcluster (C5) contained neutrophils that were enriched for pro-inflammatory genes and influenza cRNA transcripts relative to the naive-proximal infected-sample subcluster (C0). However, an unbiased trajectory analysis defined a gradient of gene expression change between these infected clusters, suggesting that although at their respective termini they represent relatively different transcriptional states, these cells are likely ontogenically related. Neutrophils from smoke-exposed, infected mice were enriched in C5 relative to C0 populations compared to room air-exposed infected controls. Notably, two other studies have assessed the lung cell environment during influenza infection using scRNA-seq^{232,233}, although our study is the first to consider the effects of cigarette smoke. One of these studies similarly quantified viral infection in lung cells by sequencing influenza cRNAs, and although they found that that neutrophils could support direct infection, they did not include a neutrophil subcluster analysis²³². The second study did perform a subcluster analysis and, similar to our work, found

three clusters of granulocytes with differing degrees of activation, with the most activated cells possessing the highest levels of *HA* and *Cd274* (PD-L1) expression²³³. Although the distribution of neutrophil subclusters differed slightly in the latter paper compared to our analysis, with highly-activated cells clearly separating from lowly-activated cells, overall our findings complement those in the existing literature and inform on differences caused by cigarette smoke.

Finally, we sought to assess to what extent changes elicited within neutrophils represented an exacerbated form of typical disease (quantitative change) vs. a distinct disease subendotype (qualitative changes). By comparing gene changes elicited by cigarette smoke during infection to those elicited by infection alone, we determined that the gene signature within neutrophils largely represented an exacerbated form of typical influenza with select unique regulatory features. Specifically, six genes (*Cxcr3*, *Socs3*, *Csf2rb*, *Pde4b*, *Sbno2*, *Steap4*) displayed significant opposing regulation in that they were upregulated by influenza and downregulated by concurrent smoke exposure. These represent an apparent mix of pro-inflammatory and inhibitory genes. *Cxcr3* and *Csf2rb* encode cytokine receptors (or subunits thereof)^{234,235}, and *Pde4b*, a phosphodiesterase that facilitates neutrophil recruitment during inflammatory lung conditions²³⁶. In contrast, *Sbno2* may play a role in inhibiting NFκB signaling²³⁷, and *Steap4* a role in mitigating neutrophil migration²³⁸. Most interestingly, SOCS3 has specifically been implicated in negatively regulating CSF3 signaling, neutrophilia, and neutrophil

survival²³⁹ - with this in mind, reduced *Socs3* levels in the context of smoke exposure may explain the reduced neutrophil death observed in our model.

Overall, this study provides insight into the mechanisms by which cigarette smoke exacerbates influenza. In doing so, it identifies CSF3-CSF3R signaling as a potential druggable target, and unveils a potential preference for specific DAAs targeting viral polymerase function in smoke-exposed individuals, as discussed in the next section (5.2.2).

5.2 – Clinical & Therapeutic Implications

Cigarette smoking represents an enormous health care burden. Each year, exposure to tobacco smoke causes unnecessary direct health care costs of more than \$500 billion CAD worldwide¹⁰, total economic costs (including lost productivity) exceeding \$1.8 trillion¹⁰, and mortality amounting to 6-8 million individuals^{5,9}. Smoking cessation strategies, whether governmental (e.g. taxation, packaging and marketing limitations) or personal (e.g. nicotine supplementation, psychological intervention, etc.) are a critical means with which to reduce the burden of smoking-related disease. However, the addictive and refractory nature of cigarette smoking represents a significant impediment to these strategies, as evidenced by the continued use of tobacco by more than one-seventh of the world's population to date^{5,9}. Notably, the harmful effects of smoking are not restricted to smokers themselves; one-third of the world's population is estimated to be regularly exposed to second-hand smoke, with demonstrable contribution to mortality in non-smoking

individuals⁶. Moreover, smoke exposure is the primary cause of COPD, a progressive and poorly-reversible airway disease¹⁵ which results in substantial morbidity, mortality, and economic costs^{68,240}. In total, although abstractly preventable, the continued burden instigated by tobacco exposure is enormous both in terms of morbidity/mortality and economic cost.

Given the limited efficacy of smoking cessation strategies, it is necessary to consider how cigarette smoke modulates disease predisposition and progression, as well the efficacy of preventative strategies. In Chapter 2, we discovered that cigarette smoke exposure attenuates the induction of IgA antibodies, which are considered to be an important component of existing and novel intranasal vaccination strategies^{105,110,120,121,241}, following intranasal immunization of mice. This finding has important implications for the efficacious design of intranasal vaccines against both respiratory and reproductive pathogens intended for use in smokers and smoke-exposed individuals. In Chapter 3, we conducted a methodological study aimed at optimizing antibody detection in human respiratory samples, finding that DTT-based processing provided significant benefit to IgA yield in sputum while reducing IgE recovery. Although this study did not consider smoking status, the methodological inferences made from it have direct application to the optimal investigation of antibodies in future investigations of human smoking-related disease, and in intranasal vaccination studies. These implications were discussed previously during the course of section 5.1.2, and are therefore not reiterated herein. Finally, in Chapter 4 we investigated the relationship between

smoke exposure and viral infection in the lower respiratory tract, finding that CSF3 signaling and excess viral RNA accumulation represent potential therapeutic targets in smoke-augmented influenza. Clinical implications for Chapters 2 and 4 are expanded in further detail below.

5.2.1 – Cigarette Smoke & IgA: Implications for Vaccination

Many existing vaccination strategies targeting respiratory pathogens, such as influenza, are intramuscularly administered and relatively efficient at inducing antigen-specific IgG antibodies⁷⁸. By virtue of their secretion into the systemic circulation and exudation into the lungs, these IgG can protect the fragile lower respiratory tract^{103,104} from inflammatory sequelae which can compromise gas exchange. This isotype is thus of great utility in promoting protective immunity, thus reducing morbidity/mortality⁷⁸. In terms of influenza, although IgG is efficient at protecting the lower airways, its efficacy is seemingly limited in the upper airways^{101,103,104}, a site which is heavily involved in air filtration and thereby frequently exposed to airborne pathogens. At this site, IgA, rather than IgG, is much more effective at precluding viral entry¹⁰³. This means that, although individuals that receive intramuscular immunizations acquire (under optimal conditions) *protective* immunity, they do not typically acquire *sterilizing* immunity¹¹⁰. In other words, although vaccinated individuals may be protected from acquiring symptomatic or severe disease as a result of infection, they are still susceptible to the initial stages of infection, particularly in the upper airways. In this way,

vaccinees may still serve as vectors for viral transmission. This is a potential impediment to vaccination strategies aimed at rapidly reducing case loads and mortality rates, such as those required during the spread of pandemic viruses¹¹⁰. Even while protection is optimal, a lack of sterilizing immunity can theoretically permit enhanced viral access to unvaccinated portions of the population and slow the development of herd immunity.

To remedy this issue, intranasal vaccination has been proposed as a viable method with which to enhance sterilizing immunity against viral pathogens. This is in part by virtue of the ability of mucosal infection/vaccination to elicit neutralizing secretory IgA responses in the upper airways alongside IgG/T cell responses^{102,105,110,140}. Currently, LAIV is the only intranasal vaccine approved for human use in Canada²⁴². However, efforts to develop alternate intranasal, IgA-producing vaccines against influenza virus, SARS-CoV-2 and other respiratory pathogens are underway^{105,163–167}. In addition, given the known connection between the upper airway and reproductive tracts via the common mucosal immune system there is also some interest in developing intranasal IgA-oriented vaccines for protection against urogenital pathogens such as *Chlamydia trachomatis* and herpes simplex virus (HSV)-2^{243,244}. Thus, although the majority of existing and novel vaccine candidates prioritize systemic immunity, there is a growing interest and value in developing secretory IgA-oriented intranasal vaccines which can both preclude pathogen acquisition and protect against infectious disease.

With this growing interest in intranasal vaccines, a question arises as to whether these vaccines will demonstrate full efficacy in individuals that have chronic respiratory diseases and/or are frequently exposed to respiratory irritants. These subsets of the population can be substantial; cigarette smokers, for instance, currently comprise approximately one-seventh of the world's populace⁵. Tobacco smoke is well known to affect many aspects of respiratory immunity²⁴⁵, including IgA in some cases as discussed above (section 5.1.1). However, prior to this thesis, it was unclear to what extent cigarette smoke exposure could affect local IgA induction following exposure to intranasal antigen. Understanding whether such a deficit exists is critical for future intranasal vaccine design and implementation strategies. In terms of design, a reduced induction may warrant investigation into alternate adjuvants or adjunct vaccine components which could promote increased efficacy in smokers (refer to section 5.3.1). In addition, clinical trials for intranasal vaccines would have to take smoking status into consideration in order to ensure a) that immunogenicity analyses are not confounded by this variable, and b) that the given vaccine candidate was effective in this substantial subgroup of the population. Ultimately, defining whether smoke exposure affects IgA induction has the potential to increase the efficiency of intranasal vaccine development.

This thesis focused on addressing the above question – to what extent does cigarette smoke modulate IgA in the upper airways following intranasal immunization. Our findings of attenuated IgA induction suggest that smokers indeed may specifically demonstrate reduced IgA-mediated efficacy following

intranasal vaccination against respiratory or urogenital pathogens. In support of this idea, a recent publication found that smokers and e-cigarette users did not induce vaccine-specific IgA in nasal lavage fluid to the same magnitude as non-smokers following intranasal LAIV administration²⁰³. Thus, our data and this clinical comparison provide compelling evidence that the IgA axis is compromised in the upper airways of smokers. This may warrant the following recommendations for future intranasal vaccine development efforts:

Smoking status should be considered in the clinical testing of intranasal vaccines.

1. Phase I clinical trials focusing on intranasal IgA-oriented vaccines should, given their typically limited cohort size, exclude smokers in order to ensure that immunogenicity analyses are not confounded by this variable. In addition, it may be pertinent to include an additional cohort consisting of smokers to assess immunogenicity in this subpopulation prior to the onset of next phase clinical trials.
2. Phase 2-4 clinical trials focusing on intranasal IgA-oriented vaccines should include subgroup analyses of individuals that smoke and/or that are regularly exposed to second-hand smoke in order to assess immunogenicity and efficacy in this subpopulation.

Some phase I clinical trials for IgA-oriented intranasal vaccines (e.g. NCT01354379 for influenza, NCT04148118 for anthrax) already exclude smokers

and individuals with a smoking history in line with our recommendations, while others (e.g. NCT04751682, NCT04798001, NCT04816019 for SARS-CoV-2) do not. Our study highlights the importance of this factor. Ultimately, by pursuing these recommendations, the efficiency of clinical trials may be increased. This is a critical consideration given that such trials for vaccines against epidemic infectious diseases often cost hundreds of millions of dollars²⁴⁶; with every variable that is unaccounted for comes an increased risk of data misinterpretation and wasted cost/effort.

5.2.2 – Cigarette Smoke & Influenza: Therapeutic Implications

To date, treatments for severe influenza are limited; direct-acting antivirals (DAAs) comprise the only approved therapies²⁴⁷. This class of drugs directly targets viral proteins, including subclasses such as M2 ion channel inhibitors (i.e. adamantanes), neuraminidase inhibitors (e.g. oseltamivir), and polymerase inhibitors (e.g. PA endonuclease inhibitors which block cap-snatching, such as baloxavir marboxil)^{247,248}. However, these drugs are thought to have a relatively narrow window of therapeutic benefit; currently, it is theorized that viral replication is a greater determinant of outcome early during the infectious disease process, whereas the magnitude and/or composition of the ensuing immune responses dictates outcome after sufficient viral replication has occurred^{248,249}. This is also hypothesized to be the case in the context of COVID-19²⁵⁰. In other words, during early infection the most efficient therapeutic strategy is likely to reduce viral

replication to prevent excess downstream inflammation, while intervention during late infection should aim to limit inflammation directly. Thus, while DAAs are initiated early, and can be effective in limiting disease progression²⁴⁸, few other medical options, including host-acting drugs, are available to complement this approach during the inflammation-dominant phase of disease^{247,249}. Corticosteroids, which may be hypothesized to be beneficial in such a context based on their broad anti-inflammatory activity, appear to clearly increase mortality in patients with severe influenza^{71,251,252}. In terms of SARS-CoV-2 infection, some reports have demonstrated improved outcome following steroid use, but others studies contradict these findings^{253–257}. Although a wide diversity of host-acting therapeutics are currently in preclinical development or clinical trials²⁴⁹, aside from DAAs care for influenza patients is largely restricted to antibiotic/antifungal treatment for secondary infections and supportive care²⁵⁸. The latter comes in the form of intravenous fluids, prone positioning to promote gas exchange, and various levels of oxygen therapy (nasal cannulation, invasive mechanical ventilation, extracorporeal membrane oxygenation (ECMO)) as needed depending on the level of hypoxemia²⁵⁸.

Further complicating the drug discovery process is the fact that it is currently not well known to what extent influenza-related disease is pathogenetically homogenous or diverse. On one hand, influenza is caused by the variants of the influenza virus, so it may be assumed that infection with a given strain would produce a similar immune response, with similar druggable targets, in

diverse individuals. However, not all infected individuals experience similar disease progression. While some efficiently combat the virus and have minimal to no symptoms, others progress to severe disease and require substantial medical intervention. This suggests that additional variables regulate disease progression. In this regard, numerous diverse risk factors can increase the risk of developing influenza, including cigarette smoke exposure, young and old age, obesity, pregnancy, and genetics, among many others^{41,69,73}. Given that these conditions are diverse in nature, it may be instead hypothesized that the pathogenetic process differs between these patient subgroups. Ultimately, the strongest hypothesis is likely that the truth lies somewhere in between; various risk factors may predispose individuals to severe influenza through differing mechanisms, and although many aspects of disease pathogenesis are similar thereafter, patient subgroups may display unique immunopathological elements in severe disease. If this were to be the case, treatment strategies may differ slightly between such subgroups. Thus, it is critical to investigate the mechanistic processes underlying different subendotypes of influenza disease – understanding, for instance, to what extent pathogenetic elements of smoke-augmented influenza resemble that of influenza in non-smokers may reveal unique druggable targets in this population. This concept provided part of the rationale for pursuing our study in Chapter 4.

Following concurrent smoke exposure and H1N1 infection in mice we found that smoke-exposed, infected mice displayed an elevated *HA* RNA load, but no difference in replicating viral particles, compared to room air, infected controls.

Viral RNA is a known pathogen-associated molecular pattern that can trigger inflammatory responses via interaction with pattern-recognition receptors such as RIG-I/MDA-5⁷⁹, providing potential mechanistic insight into the excess inflammation observed in these animals. Our findings are notably in line with previous observations that smoke exposure attenuates the upregulation of IRF-7 mediated antiviral signaling in stromal cells following viral infection²⁵⁹, given the known role of downstream ISGs in vRNA detection, degradation and translation inhibition²⁶⁰. These observations may also have clinical ramifications as well. If smoke exposure promotes an excess vRNA burden without augmenting the number of replicating viral particles, and this vRNA is potentiating inflammation, there may be a rationale to preferentially administer DAAs that target vRNA synthesis in smoking individuals. Specifically, PA endonuclease inhibitors (e.g. baloxavir) that block vRNA ‘cap-snatching’ may be more helpful in precluding/reducing inflammation than particle-directed therapies such as neuraminidase inhibitors (NAIs; e.g. oseltamivir), which block virion release. Ultimately, my work suggests that clinical studies comparing these treatment regimens in smokers and smoke-exposed individuals may be warranted.

Along with excess vRNA load, we found that smoke-exposed infected animals displayed a prominent exacerbation of several cytokines, including IL-6 and CSF3, in the lungs and bloodstream relative to room air controls. Supplementing IL-6 and CSF3 over the background of influenza infection produced different results; IL-6 modestly improved core temperature and BALF albumin

leakage without modulating symptom score, while CSF3 increased BALF albumin, aggravated hypothermia and increased symptom scores. These findings are notably in line with clinical reports of hypoxemia and rapid clinical deterioration following recombinant CSF3 therapy in humans²²⁵⁻²²⁷, including in the context of active SARS-CoV-2 infection^{228,229}, as well as previously described anti-inflammatory roles for IL-6²⁶¹. Although treatment with an anti-CSF3R antibody did not modify overall morbidity, weight loss, hypothermia or hypoxemia relative to isotype controls, it was effective at reducing neutrophils in the lungs and blood and did reduce BALF albumin levels. As they pertain to overall morbidity, these findings are in line with observations made using similar treatment strategies in models of mild influenza infection previously^{262,263}. However, they also suggests that there may be some therapeutic benefit of anti-CSF3R in preventing or ameliorating pulmonary edema in the context of smoke-augmented influenza. Moving forward, it may be pertinent to test anti-CSF3R in combination with DAAs (e.g. oseltamivir and/or baloxavir marboxil) or other prospective host-acting treatments. It is likely that such multivalent therapeutic approaches will be necessary to treat influenza given the complex inflammatory nature of this viral infectious disease.

Importantly, in addition to identifying a novel potential druggable target (CSF3-CSF3R signaling), these data provide valuable insight into our understanding of the role of exacerbated cytokine responses in severe viral disease. To date it is well known that various severe infections are associated with ‘cytokine storms’, wherein a number of cytokines are secreted in excess²⁶⁴. Less clear is the

specific contribution of these cytokines to outcome. At these exaggerated levels, are individual cytokines contributing to, or limiting, disease pathogenesis? For instance, in our model both IL-6 and CSF3 were observed to be highly positively dysregulated in smoke-exposed, infected mice. Genetically modified mice lacking either the *Il6* or *Csf3* genes exhibit increased mortality following influenza infection²⁶⁵⁻²⁶⁷, suggesting these cytokines are necessary for viral clearance and promote survival. However, while necessary in appropriate amounts it may also be true that, when present in excess, these cytokines can contribute to collateral tissue damage and negative outcome. Thus genetic models are insufficient to address the question of the role of these cytokines in severe disease, in that complete elimination of a cytokine may be just as detrimental to host health as overexpression. In contrast, supplementation over the background of influenza infection permits an isolated excess of the given cytokine, while antibody-mediated blockade allows for a more regulated inhibition of the intended target. In utilizing these approaches, we found that while the CSF3 axis contributed to negative outcome, excess IL-6 did not. Thus, these data suggest that cytokines can have markedly different effects on outcome despite being similarly positively dysregulated in severe disease. In terms of clinical practice, they also provide clear, experimentally-controlled evidence that rCSF3 therapy for neutropenia during viral infectious diseases^{228,229} carries substantial risk.

5.3 – Limitations & Future Directions

The studies contained within this thesis provide novel insights within their respective subfields. However, each has its limitations, and could be expanded upon. Below is a discussion of such limitations and potential future directions for each project.

5.3.1 – Cigarette Smoke & IgA Induction in the Upper Airways

In Chapter 2, we demonstrated that cigarette smoke exposure attenuated the induction of antigen-specific IgA in the upper airways and systemic circulation following intranasal immunization with a model antigen/adjuvant combination. A mixture of LPS, a prototypical TLR-4 agonist, and OVA, a chicken egg-white derived protein, was used as our intranasal immunization agent for several technical reasons. OVA is a well characterized antigen, and as such multiple reagents are available with which to characterize OVA-specific immunity. These include OVA itself, which is purchasable at low cost and high volume, as well as the fluorescent OVA-AF647 conjugates which can be used to detect antigen-specific ASCs. In addition, OVA-MHC tetramers and OT-II mice (which only generate T cells with T cell receptors specific for OVA peptide) are available for analyzing OVA-specific CD4⁺ T cell responses, although this study did not ultimately pursue a T cell arm of investigation. Intranasal administration of LPS/OVA permitted us to effectively investigate the impact of cigarette smoke on antigen-specific antibody responses to

intranasal immunization, and derive findings that supported and extended clinical observations (e.g.^{202,203}). Overall, this approach yielded significant benefits. However, this model system does not permit us to easily assess whether there is a functional impairment that occurs as a result of impaired IgA responses, a finding which is lacking in the clinical sphere as well. Nasal secretory IgA has been suggested to be an important component of intranasal influenza vaccine efficacy^{105,120,121}, suggesting that deficits in IgA induction elicited by smoke exposure could detrimentally impact components of vaccine efficacy that rely on this isotype.

Moving forward, it will be necessary to assess the functional capacity of IgA induced in the context of smoke exposure. To this end, the best approach would likely be to alter the immunization agent to contain a pathogen-specific antigen, such as influenza HA. This could take the form of an adjuvanted subunit vaccine, using the same schedule as we have developed with or without modifying the adjuvant. Alternatively, a live attenuated influenza strain could be administered. First, although we do observe this phenomenon consistently across different antigens (OVA and LPS) and adjuvants (LPS and polyI:C), it would be necessary to assess whether deficits in IgA induction caused by cigarette smoke were conserved in this new model. If deficits were maintained, we would then test the functional implications. One approach would be to nasally infect mice with the cognate strain of influenza 7 and 14 days after vaccination, and assess viral load at pre-determined timepoints (e.g. 1-4 days) post-infection. However, cigarette smoke

is known to alter the innate antiviral capacity of airway epithelial cells to promote excess viral replication^{181,184}, which may confound such experimental designs by permitting excess replication of those virions that do bypass IgA defenses. As an alternative, nasal lavage may be collected from smoke- and room air-exposed vaccinated animals at 7 or 14 days post-vaccination. This lavage could then be tested for its ability to reduce viral infectivity via microneutralization assay. Although IgA is the dominant isotype in mucosal spaces, IgA isolation may be necessary rather than using neat samples to avoid confounding effects of mucosal IgG and other soluble mediators in the lavage. This and similar study designs could inform whether the observed deficits in IgA translated to impairments in antiviral function.

Mechanistically, we defined three aspects of the IgA induction axis which may be impaired in the context of cigarette smoke exposure: ASC induction in nasal-draining lymphoid tissues, nasal ASC homing and transepithelial IgA transport. In the case of ASC induction, evidence was direct in that fewer OVA-specific IgA ASCs were detected in the NALT, CLNs, spleen and blood of smoke-exposed mice following immunization. In comparison, proposed deficits in ASC homing and transepithelial transport were based off of an attenuated upregulation of molecules that have been identified as non-redundant or critical in these processes. For instance, VCAM-1 is known to be important for the binding of ASCs to endothelial surfaces in the nasal submucosa, while pIgR is known to have an essential and non-redundant role in shuttling IgA across mucosal surfaces^{129,157}.

However, in the current study we did not demonstrate whether deficits in the upregulation of these molecules was associated with a functional inefficiency of the respective processes. Adoptive transfer models would be able to address both scenarios. In terms of homing, one could FACS sort OVA-IgA ASCs from the blood of immunized room air mice, label them with a fluorescent dye, and intravenously inject them into smoke- or room air-exposed immunized recipients. Quantification of labelled OVA-IgA ASCs in the nasal mucosa after 4-6 hours should indicate the relative ability of these cells to migrate into the submucosa. Similarly, intravenous adoptive transfer of secretory IgA of a known specificity into smoke- and room air-exposed immunized recipients and subsequent quantification in the nasal lavage at a given time interval could be used to monitor the efficiency of transepithelial transport. Both of these protocols, however, are have technical/logistical limitations. OVA-IgA ASCs are not abundant in the blood, necessitating the use of an excessive number of donor mice, while mouse J-chain containing secretory IgA clones of known specificity do not appear to be commercially available and would take considerable effort to produce in sufficient quantities for adoptive transfer. However, each protocol is plausible and would sufficiently address their respective objectives.

Notably, the fact that deficits in the IgA induction cascade elicited by cigarette smoke are multifactorial is informative in and of itself. This suggests that smoke exposure affects multiple cell types simultaneously, and thus that the cellular processes affected by smoke are diverse, conserved, or both. Experiments aimed at

unveiling the pathway(s) that are negatively affected by cigarette smoke are warranted. Deriving pharmaceutical interventions to restore specific affected pathways represents one approach to addressing the issue of diminished IgA responses. Alternatively, compounds with known benefit in ameliorating other smoke-associated sequelae could be screened for similar benefits to IgA induction in the absence of such knowledge. For instance, antioxidants such as glutathione have been shown to reduce the inhibitory effects of smoke on innate antiviral immunity¹⁸⁰, while prophylactic molecular activation of nuclear erythroid 2 p45 related factor-2 (NRF2)-mediated antioxidant signaling can prevent emphysema and cardiovascular sequelae following smoke exposure in mice²⁶⁸. Given the seemingly broad detrimental relationship between oxidative stress and host health, it is plausible that antioxidants may have similar benefit in the restoration of impaired IgA induction. Using either method (targeted or screening-based drug derivation), derived products may manifest themselves as adjunct intranasal vaccine components, incorporated alongside antigen and adjuvant to enhance IgA responses in smokers. In addition, there is yet another approach; screening diverse adjuvants and adjuvant doses to see if there are some that display preferential efficacy in the context of smoke, and prioritizing these adjuvants/conditions for use in vaccines. This may be the most appropriate pursuit, in that selection of an optimal adjuvant/dose may circumvent regulatory hurdles associated with adding adjunct components to existing or candidate vaccines.

5.3.2 – PBS- vs. DTT-based Sputum Processing for Antibody Detection

In Chapter 3, we demonstrated that DTT-based processing increased IgA recovery from human sputum samples. The sample processing approach taken was both a strength and a weakness of this study. Following collection, sputum plugs were split equally, with separate portions from the same sample being then processed concurrently with either PBS or DTT. Although sufficient to address our objective, theoretically this approach does not optimally minimize intrasample variability (i.e. variability between PBS and DTT subsamples within one sample) given that different sections of a given sputum plug may contain different levels of antibodies. As an alternate approach, the entire sputum plug could be processed with PBS and then split for additional DTT or PBS processing²¹³. In this case, the entire antibody fraction of the sputum would be more precisely split into the PBS and DTT arms. However, in our study we observed that PBS processing sometimes resulted in an incomplete mucolysis of the final sample. In such samples, sputum plug processing and subsampling would remain imprecise. Crucially, any intact mucous plugs may also sequester antibody and therefore decrease the absolute amount of antibody detectable in sputum. Further efforts to optimize homogenization in PBS-disbursed samples are likely warranted. Ultimately, even considering such minor limitations both protocols are of relatively high fidelity, with our approach allowing us to identify a relative preference in the ability of DTT to increase IgA (and to an extent IgG) yields while simultaneously reducing IgE recovery.

Moving forward it would be pertinent to validate whether our findings are applicable to other mucoid human samples such as saliva, NAL, BAL, and CVL. Although IgA is plentiful at mucosal surfaces, the study of IgA-oriented intranasal vaccines targeting the respiratory or genital tracts would necessitate the analysis of *antigen-specific* IgA at these sites. Not infrequently, the study of antigen-specific responses is impeded by the relatively paucity of specific antibody clones. Maximizing antibody recovery would thus be an important consideration in protocol design. However, although beneficial in sputum, a highly mucoid sample, DTT may not be necessary in some other sample types which are somewhat less mucoid (e.g. NAL, BAL). Given that DTT may have as-of-yet undetermined effects on other soluble components of these samples (e.g., as was newly discovered here for IgE), avoiding unnecessary DTT treatment may be important; thus, specific studies of each sample type are warranted.

After testing this protocol in upper airway-associated samples, we would be in an optimal position to move forward with a clinical extension of our murine intranasal immunization study. A recent investigation showed that smokers and e-cigarette users demonstrated a reduced induction of influenza-specific IgA in nasal lavage following LAIV vaccination compared to non-smokers, corroborating the main finding of our study²⁰³. However, it is still currently unknown whether these deficits extend into the circulation or to distal mucosal sites (e.g. the reproductive tract), as we observe in mice. Given the known role of circulating IgA in promoting effector functions such as NETosis¹²⁵, and the increased interest in intranasal

vaccination against both respiratory and urogenital pathogens, such a study is warranted. This could similarly take the form of intranasal LAIV vaccination in smokers and non-smokers, with NAL, sputum/BAL, reproductive tract lavage and serum being serially collected in order to quantify the induction of IgA antibodies and circulating ASCs over time. In addition, similar to future directions proposed in mice (refer to section above) it would also be pertinent to assess whether nasal IgA elicited in smokers have functional implications to viral neutralization by using microneutralization assays.

5.3.3 – Cigarette Smoke & Pulmonary Influenza Infection

In Chapter 4, we observed that cigarette smoke increased the severity of influenza-associated disease despite animals being given the same initial dose of influenza. Our approach is scientifically sound – only one variable (cigarette smoke exposure) changes between our infected groups, and we have both room air- and smoke-exposed, uninfected controls for comparison. However, an additional comparison that may have provided value would have been a group of room air-exposed mice given a higher, lethal dose of influenza. In these animals one would expect that symptoms of infection would be greater than those room air mice given the typical non-lethal dose (50 PFU). Thus, while mice receiving the non-lethal dose would be appropriate comparators for viral load, mice receiving the lethal dose would be more similar in terms of morbidity. It may be that changes observed in

the context of cigarette smoke are more reflective of severe disease rather than a unique inflammatory state elicited by cigarette smoke itself. This idea is supported by our analysis of neutrophil gene signatures, which demonstrate that most transcriptional changes elicited in these cells by cigarette smoke are exacerbated versions of changes caused by influenza alone, with the exception of select genes. Whether this applies beyond neutrophils to the entire disease phenotype could be ascertained by comparing readouts such as neutrophils levels, cytokine expression, transcription and cellular cytokine distribution between all three infectious conditions: room air with low influenza dose and low morbidity, cigarette smoke with low dose and high morbidity, and room air with high dose and high morbidity. While the approach we took is the standard of the field, and although the comparison would be across two modified variables (smoke/low dose vs. room air/high dose, this additional control group may have enhanced our ability to interpret our findings, and should be included in future experiments of this nature.

Within our existing comparisons, data demonstrated that smoke-exposed mice had elevated viral *HA* RNA burden, but no difference in replicating viral particles (PFUs), compared to room air-exposed infected controls. As discussed previously (refer to section 5.2.2) this may have implications for the use of specific DAA classes in smoking or smoke-exposed individuals, with those targeting viral RNA synthesis (e.g. PA endonuclease inhibitors) having a preference over those targeting virion release (e.g. neuraminidase inhibitors). However, this is predicated on the idea that the observed viral RNA accumulation is playing a pathogenic role

in driving cigarette smoke-augmented influenza. Although this seems likely given that viral RNA is a known pathogen-associated molecular pattern and can trigger inflammation⁷⁹, these excess transcripts may accumulate purely as a consequence of immunological changes elicited by smoke exposure rather than being a causative factor in the exacerbated disease pathogenesis. In assessing this question, it would be necessary to specifically block viral RNA transcription without interfering with host transcription or other viral processes. Consequently, the best way to address this limitation conceptually is also an optimal next step in terms of clinical implications – to directly test PA endonuclease or other polymerase inhibitors in our model of cigarette smoke-augmented influenza, and compare them to neuraminidase inhibitors to assess whether there is any preferential benefit for one over the other.

Through our dysregulation scoring approach, we identified CSF3 as being highly dysregulated in cigarette smoke-exposed, infected mice. Using supplementation experiments, we found that recombinant CSF3 given intranasally during influenza infection could exacerbate symptoms, hypothermia and BALF albumin levels over the background of PBS vehicle. We chose to deliver our cytokines to the lungs directly given that this is the site of infection and likely the site of cells orchestrating the ensuing inflammatory cascades. The dose of both CSF3 and IL-6 was chosen to be maximal based on technical limitations – rIL-6 was supplied pre-dissolved at a given concentration (approximating 0.2mg/ml) and 35µl was the maximum volume appropriate for mouse intranasals, thus permitting

a dose of 7 μ g per administration. CSF3 dosing was kept consistent for comparison. Ultimately, though, this protocol does not fully emulate the *in vivo* scenario. During infection, cytokine would be produced in a (relatively) continuous manner with fluctuations depending on dynamic factors such as cell recruitment and transcription/translation rates. In contrast, we sporadically delivered boli of cytokine intranasally, a route which is convenient and relatively non-invasive compared to other methods (e.g. intratracheal), but somewhat less efficient at pulmonary delivery²⁶⁹. Consequently, we do not know how effectively this administration protocol recapitulates the effects of cytokine longitudinally secreted *in vivo*. In this regard, changes in hypothermia and morbidity may have been artifacts of sporadic high-dose cytokine spikes, given that anti-CSF3R therapy could not ameliorate these attributes in smoke-augmented influenza. It is equally possible, however, that this discrepancy is attributable to immunological differences in the respective models. It may be that supplementation with CSF3 is sufficient to induce these phenotypes over the background of influenza alone, but blockade of CSF3R signaling in smoke-augmented influenza is insufficient because of overlapping and redundant effects of other cytokines. With all of this in mind, systemic therapeutic CSF3 supplementation has been reported to induce endothelial barrier function and hypoxemia in humans^{225–227}, including when administered during the course of SARS-CoV-2 infection^{228,229}, suggesting that our data pertaining to CSF3 has clinical relevance. Ultimately, these findings warrant further research into the utility of anti-CSF3R therapy in viral infectious disease,

potentially in the context of multivalent therapeutic approaches alongside DAAs or alternate host-acting therapies. If, for instance, additional cytokines which regulated pulmonary edema or morbidity are identified, concurrent blockade of this signaling pathway alongside CSF3R inhibition could have an additive effect to preclude negative outcomes.

Single cell RNA sequencing data provided valuable insights into the expression of specific cytokines on a single cell level. This allowed us to assign cytokine expression and infection characteristics to specific cell types, such as neutrophils. However, although it is an efficient and high-resolution approach to assess these variables, our approach had some drawbacks. Firstly, in terms of cellular composition, it is clear that stromal cells were underrepresented in our dataset. The majority of live cells were hematopoietic (expressing *Ptprc*, CD45), while endothelial and epithelial cells comprised an unexpectedly small fraction of the overall dataset. This issue has been observed by other groups performing similar analyses²³³, and is notably in line with typical lung digests as analyzed by flow cytometry in which over 90% of live cells are typically CD45⁺. This suggests that our lung digestion protocol, which features collagenase I digestion, 40µm filtration and ACK red blood cell lysis, elicits significant stromal cell death or removal. This did benefit our approach by providing a high analytical resolution within lung immune cells, allowing us to make valuable inferences about *Csf3* and *Il6* expression in neutrophils and macrophages. Conversely though, we did not capture enough stromal cells, specifically epithelium, to make definite conclusions about

the contributions of these cells. This notably has implications for addressing one of the key questions underpinning our study – whether smoke-augmented influenza is an exacerbated form of typical disease, or a distinct transcriptional subendotype. Ultimately, we were able to effectively address this question within neutrophils, but deficits in stromal cells preclude a similar analysis of total cells. Moving forward, it will be pertinent to optimize tissue digestion protocols to ensure sufficient stromal cell survival for both flow cytometric and single cell analyses.

Using single cell sequencing, we found that *Csf3* expression was modulated in the context of cigarette smoke, with smoke-exposed mice demonstrating a shift in the distribution of *Csf3*⁺ cells towards neutrophils and away from macrophage/monocyte lineage cells. This description of *Csf3* expression in neutrophils is, to our knowledge, the first. Previous studies have demonstrated CSF3 expression in other cell types such as macrophages and fibroblasts, among others^{270–274}, but not in neutrophils. This is exciting and of great interest given that neutrophils are the classical CSF3R-expressing cell subset²³⁰. However, one drawback is that our approach is limited to analysis of RNA transcript expression – whether neutrophils are a significant contributor to CSF3 protein secretion has yet to be determined. While there is a shift in the relative distribution of *Csf3* expression towards neutrophils, macrophages may still be the dominant source of CSF3 protein. However, it is notable that *Csf3*⁺ neutrophils demonstrated higher transcript levels than *Csf3*⁺ monocyte-macrophage lineage cells, which could be indicative of enhanced cytokine production. Alternatively, it could be a consequence of less *Csf3*

translation within neutrophils. Moving forward, it will be necessary to assess CSF3 protein expression and secretion from neutrophils, monocyte, and macrophage subsets. This could be performed by FACS sorting individual populations from infected lungs. Once isolated, intracellular protein expression could be analyzed by cell lysis and Western blot, while secretion could be analyzed by culturing cells in media and assessing supernatants by ELISA. Having now identified candidate cells and cytokines of interest through single cell RNA sequencing, pursuing protein-based analyses forms a logical next step to extend and validate these findings.

An additional consideration is that, although mouse models can provide valuable insights into pathogenic processes by virtue of the ability to better control variables, they do not fully recapitulate all aspects of human disease. A good example to illustrate this difference is the change in temperature each species undergoes. In humans, a classical feature of influenza-associated illness is fever, while mice conversely become hypothermic, losing up to 8°C of core temperature depending on infection severity in our experiments. However, hypothermia induced by influenza infection in mice has been validated as a correlate of morbidity²⁷⁵, justifying its use as such in our study. This is an example of a known and clear difference between mice and humans; more challenging for study interpretation are unknown differences. For instance, although IL-6 has been reported to be highly upregulated in pandemic influenza²⁷⁶, and CSF3 in diverse ARDS²⁷⁷, to our knowledge there is no data comparing influenza-afflicted smokers and non-smokers with which to corroborate our CSF3 findings. This warrants the pursuit of future

clinical studies into cytokine expression profiles in influenza patients with and without prior exposure to cigarette smoke. One approach might be to enroll smokers and non-smoking patients upon admission to hospital/ICU, assessing CSF3 at this time and with subsequent disease progression. However, such studies may be biased somewhat by the fact that, upon admission, severity will likely be normalized between smokers and non-smokers to an extent, given that a sufficient symptomatic response to infection usually prompts admission. Thus, if smoke exposure elicits an exacerbated immune response and an increased risk of severe disease but does not elicit a distinct disease subendotype in terms of CSF3 expression, no difference in CSF3 levels may be detectable between hospitalized smokers and non-smokers. In this regard, studies relying on admission-based enrolment would be restricted to understanding differences in biological metrics when severity is normalized.

An alternate and perhaps optimal study might be to perform a pulmonary influenza challenge in a cohort of young, healthy smokers and non-smokers without additional influenza-related risk factors. Such influenza challenge models have recently been used to assess the efficacy of experimental monoclonal antibody therapies and intranasal vaccines, and are effectively terminated with the administration of approved DAAs to promote infection resolution^{105,278,279}. Similar challenge studies using rhinovirus have recently been performed in human smokers and COPD patients²⁸⁰, demonstrating the feasibility of such an approach in our population of interest. Importantly, experimental challenge models such as this

allow for control of the viral dose and duration of exposure. Collection of serum and sputum pre-infection and at multiple timepoints post-infection would be used to monitor neutrophil and CSF3 levels. Analysis of temperature and symptoms may permit a correlation between neutrophilia/CSF3 induction and morbidity. Ultimately though, although preceded and optimally informative, such experiments may encounter hurdles in terms of ethical approval.

5.4 – Concluding Remarks

This dissertation summarizes the work conducted during my PhD to investigate the relationship between cigarette smoke and antimicrobial host defense in the respiratory tract. In the first study (Chapter 2), we assessed the effect of cigarette smoke on antibody responses to intranasal immunization in mice. We found that smoke exposure attenuated the induction of IgA responses at both local (nasal) and distal (vaginal) mucosae, as well as in the systemic circulation, and defined potential mechanisms through which this inhibition may occur. These findings may have considerable implications for the appropriate design, testing and implementation of IgA-oriented intranasal vaccination strategies targeting both respiratory and urogenital pathogens for use in smoke-exposed individuals.

The second study (Chapter 3) does not address the relationship between smoking and infectious disease directly, but rather aimed to optimize methodologies used to assess antibody responses in mucoid human samples. By

comparing standardized clinical PBS- and DTT-based processing protocols, we found that DTT-mediated mucolysis enhanced the recovery of IgA, and to an extent IgG, from sputum samples. IgE recovery, in contrast, was reduced by DTT. Pending validation in additional sample types, these data suggest that DTT may be used to enhance IgA yield in future studies assessing mucosal IgA responses in smoking-related disease and/or in the context of intranasal vaccination.

Finally, the third study (Chapter 4) focused on investigating the mechanisms by which cigarette smoke exacerbates influenza infection in the lower respiratory tract. In this regard, smoke-exposed infected mice exhibited elevated viral RNA burden, but not replicating viral particles, compared to room air controls. Although excess neutrophilia was also detected in both the airways and interstitium of these animals, interstitial neutrophilia was a better positive predictor of morbidity. In terms of soluble mediators, cigarette smoke exposure caused a disproportionate upregulation of CSF3 and IL-6 in the lungs, and through supplementation/blockade experiments we defined a pathogenic role for CSF3 in promoting morbidity and compromising alveolar-capillary barrier function during influenza infection. Single cell RNA sequencing revealed a shift in the distribution of *Csf3*-expressing cells towards neutrophils, while defining the overall transcriptional response in these cells as an exacerbated form of typical disease with unique regulatory features. These data may have therapeutic implications for the preferential use of specific DAA subclasses in smoke-exposed infected individuals, provide rationale for further exploration into the use of CSF3R blockade in ameliorating influenza, and

provide clear limitations to CSF3 therapy for neutropenia during viral infectious disease.

In summary, the work presented here provides novel insights into the relationship between cigarette smoke and antimicrobial immunity in the respiratory tract, opens new avenues of therapeutic pursuit, and advances methodologies with which to assess aspects of this relationship in human respiratory samples.

CHAPTER 6 – REFERENCES (CHAPTERS 1 AND 5 ONLY)

1. Tushingham, S., Snyder, C. M., Brownstein, K. J., Damitio, W. J. & Gang, D. R. Biomolecular archaeology reveals ancient origins of indigenous tobacco smoking in North American Plateau. *PNAS* **115**, 11742–11747 (2018).
2. Cross, G. S. & Proctor, R. N. *Packaged Pleasures: How Technology and Marketing Revolutionized Desire*. (University of Chicago Press, 2014).
3. Stephens, T. *A Critical Review of Canadian Survey Data on Tobacco Use, Attitudes and Knowledge*. (Health and Welfare Canada, 1988).
4. Proctor, R. N. The history of the discovery of the cigarette lung cancer link: Evidentiary traditions, corporate denial, global toll. *Tob. Control* **21**, 87–91 (2012).
5. Reitsma, M. B. *et al.* Spatial, temporal, and demographic patterns in prevalence of smoking tobacco use and attributable disease burden in 204 countries and territories, 1990–2019: a systematic analysis from the Global Burden of Disease Study 2019. *Lancet* **397**, 2337–2360 (2021).
6. Öberg, M., Jaakkola, M. S., Woodward, A., Peruga, A. & Prüss-Ustün, A. Worldwide burden of disease from exposure to second-hand smoke: a retrospective analysis of data from 192 countries. *Lancet* **377**, 139–146 (2011).
7. Ng, M. *et al.* Smoking prevalence and cigarette consumption in 187 countries, 1980–2012. *JAMA* **311**, 183–92 (2014).
8. World Health Organization. *WHO Report on the Global Tobacco Epidemic, 2015*. (2015).
9. GBD 2015 Tobacco Collaborators. Smoking prevalence and attributable disease burden in 195 countries and territories, 1990–2015: A systematic analysis from the global burden of disease study 2015. *Lancet* **389**, 1885–1906 (2017).
10. Goodchild, M., Nargis, N. & D’Espaignet, E. T. Global economic cost of smoking-attributable diseases. *Tob. Control* **27**, 58–64 (2018).
11. Flor, L. S., Reitsma, M. B., Gupta, V., Ng, M. & Gakidou, E. The effects of tobacco control policies on global smoking prevalence. *Nat. Med.* **27**, 239–243 (2021).
12. Mitchell, R. S., Vincent, T. N. & Filley, G. F. Cigarette Smoking, Chronic Bronchitis, and Emphysema. *JAMA* **188**, 12–16 (1964).
13. Forey, B. A., Thornton, A. J. & Lee, P. N. Systematic review with meta-

- analysis of the epidemiological evidence relating smoking to COPD, chronic bronchitis and emphysema. *BMC Pulm. Med.* **11**, (2011).
14. Polosa, R. *et al.* Cigarette smoking is associated with a greater risk of incident asthma in allergic rhinitis. *J. Allergy Clin. Immunol.* **121**, 1428–1434 (2008).
 15. Barnes, P. J. *et al.* Chronic obstructive pulmonary disease. *Nat. Rev. Dis. Prim.* **1**, 1–21 (2015).
 16. Schiess, R. *et al.* Tobacco smoke: A risk factor for pulmonary arterial hypertension? A case-control study. *Chest* **138**, 1086–1092 (2010).
 17. Baumgartner, K. B., Samet, J. M., Stidley, C. A., Colby, T. V & Waldron, J. A. Cigarette smoking: A risk factor for idiopathic pulmonary fibrosis. *Am. J. Respir. Crit. Care Med.* **51**, 242–248 (1997).
 18. Howard, G. *et al.* Cigarette smoking and progression of atherosclerosis: The atherosclerosis risk in communities (ARIC) study. *JAMA* **279**, 119–124 (1998).
 19. Kamimura, D. *et al.* Cigarette Smoking and Incident Heart Failure: Insights from the Jackson heart study. *Circulation* **137**, 2572–2582 (2018).
 20. Wilmink, T. B. M., Quick, C. R. G. & Day, N. E. The association between cigarette smoking and abdominal aortic aneurysms. *J. Vasc. Surg.* **30**, 1099–1105 (1999).
 21. Mons, U. *et al.* Impact of smoking and smoking cessation on cardiovascular events and mortality among older adults: Meta-analysis of Individual participant data from prospective cohort studies of the CHANCES consortium. *Br. Med. J.* **350**, (2015).
 22. O’Keeffe, L. M. *et al.* Smoking as a risk factor for lung cancer in women and men: A systematic review and meta-analysis. *BMJ Open* **8**, 1–12 (2018).
 23. Jacob, L., Freyn, M., Kalder, M., Dinas, K. & Kostev, K. Impact of tobacco smoking on the risk of developing 25 different cancers in the UK: A retrospective study of 422,010 patients followed for up to 30 years. *Oncotarget* **9**, 17420–17429 (2018).
 24. Franceschi, S. *et al.* Smoking and Drinking in Relation to Cancers of the Oral Cavity, Pharynx, Larynx, and Esophagus in Northern Italy. *Cancer Res.* **50**, (1990).
 25. Hannan, L. M., Jacobs, E. J. & Thun, M. J. The association between cigarette smoking and risk of colorectal cancer in a large prospective cohort from the United States. *Cancer Epidemiol. Biomarkers Prev.* **18**, 3362–

- 3367 (2009).
26. Leonardi-Bee, J., Britton, J. & Venn, A. Secondhand smoke and adverse fetal outcomes in nonsmoking pregnant women: A meta-analysis. *Pediatrics* **127**, 734–741 (2011).
 27. Leonardi-Bee, J., Smyth, A., Britton, J. & Coleman, T. Environmental tobacco smoke and fetal health: Systematic review and meta-analysis. *Arch. Dis. Child. Fetal Neonatal Ed.* **93**, (2008).
 28. Flenady, V. *et al.* Major risk factors for stillbirth in high-income countries: a systematic review and meta-analysis. *Lancet* **377**, 1331–1340 (2007).
 29. Boldo, E. *et al.* Health impact assessment of environment tobacco smoke in European children: Sudden Infant Death Syndrome and asthma episodes. *Public Health Rep.* **125**, 478–487 (1386).
 30. Mitchell, E. A. *et al.* Smoking and the Sudden Infant Death Syndrome. *Pediatrics* **91**, 893–896 (1993).
 31. Ekblad, M., Gissler, M., Lehtonen, L. & Korkeila, J. Prenatal smoking exposure and the risk of psychiatric morbidity into young adulthood. *Arch. Gen. Psychiatry* **67**, 841–849 (2010).
 32. Arcavi, L. & Benowitz, N. L. Cigarette Smoking and Infection. *Arch. Intern. Med.* **164**, 2206–2216 (2004).
 33. Huttunen, R., Heikkinen, T. & Syrjänen, J. Smoking and the outcome of infection. *J. Intern. Med.* **269**, 258–269 (2011).
 34. Cohen, S., Tyrrell, D. A. J., Russell, M. H., Jarvis, M. J. & Smith, A. P. Smoking, Alcohol Consumption, and Susceptibility to the Common Cold. *Am. J. Public Health* **83**, 1277–1283 (1993).
 35. Nuorti, J. P. *et al.* Cigarette smoking and invasive pneumococcal disease. *N. Engl. J. Med.* **342**, 681–689 (2000).
 36. Almirall, J., González, C. A., Balanzó, X. & Bolívar, I. Proportion of community-acquired pneumonia cases attributable to tobacco smoking. *Chest* **116**, 375–9 (1999).
 37. Almirall, J., Blanquer, J. & Bello, S. Community-acquired pneumonia among smokers. *Arch. Bronconeumol.* **50**, 250–254 (2014).
 38. Bello, S. *et al.* Tobacco Smoking Increases the Risk for Death From Pneumococcal Pneumonia. *Chest* **146**, 1029–1037 (2014).
 39. Lee, C. C., Middaugh, N. A., Howie, S. R. C. & Ezzati, M. Association of secondhand smoke exposure with pediatric invasive bacterial disease and bacterial carriage: A systematic review and meta-analysis. *PLoS Med.* **7**, 1–

- 14 (2010).
40. Bagaitkar, J., Demuth, D. R. & Scott, D. Tobacco use increases susceptibility to bacterial infection. *Tob. Induc. Dis.* **4**, 12 (2008).
 41. Lawrence, H., Hunter, A., Murray, R., Lim, W. S. & McKeever, T. Cigarette smoking and the occurrence of influenza – Systematic review. *J. Infect.* **79**, 401–406 (2019).
 42. Han, L. *et al.* Smoking and Influenza-associated Morbidity and Mortality: A Systematic Review and Meta-analysis. *Epidemiology* **30**, 405–417 (2019).
 43. Kark, J. D., Lebiush, M. & Rannon, L. Cigarette smoking as a risk factor for epidemic A(H1N1) influenza in young men. *N. Engl. J. Med.* **307**, 1042–6 (1982).
 44. Lowe, K. E., Zein, J., Hatipoğlu, U. & Attaway, A. Association of Smoking and Cumulative Pack-Year Exposure with COVID-19 Outcomes in the Cleveland Clinic COVID-19 Registry. *JAMA Intern. Med.* **181**, 709–711 (2021).
 45. Reddy, R. K. *et al.* The effect of smoking on COVID-19 severity: A systematic review and meta-analysis. *J. Med. Virol.* **93**, 1045–1056 (2021).
 46. Hou, H. *et al.* Smoking Is Independently Associated With an Increased Risk for COVID-19 Mortality: A Systematic Review and Meta-analysis Based on Adjusted Effect Estimates. *Nicotine Tob. Res.* (2021) doi:10.1093/ntr/ntab112.
 47. Patanavanich, R. & Glantz, S. A. Smoking is associated with COVID-19 progression: A meta-analysis. *Nicotine Tob. Res.* **22**, 1653–1656 (2020).
 48. Farsalinos, K. *et al.* Smoking prevalence among hospitalized COVID-19 patients and its association with disease severity and mortality: an expanded re-analysis of a recent publication. *Harm Reduct. J.* **18**, (2021).
 49. Zhou, F. *et al.* Clinical course and risk factors for mortality of adult inpatients with COVID-19 in Wuhan, China: a retrospective cohort study. *Lancet* **395**, 1054–1062 (2020).
 50. Usman, M. S. *et al.* Is there a smoker’s paradox in COVID-19? *BMJ Evidence-Based Med.* **0**, (2020).
 51. Shen, P. *et al.* Cigarette smoke attenuates the nasal host response to *Streptococcus pneumoniae* and predisposes to invasive pneumococcal disease in mice. *Infect. Immun.* **84**, 1536–1547 (2016).
 52. Iles, K., Poplawski, N. K. & Couper, R. T. Passive exposure to tobacco

- smoke and bacterial meningitis in children. *J. Paediatr. Child Health* **37**, 388–91 (2001).
53. Wu, J. *et al.* Cigarette smoking and the oral microbiome in a large study of American adults. *ISME J.* **10**, 2435–2446 (2016).
 54. Zhang, Y., He, J., He, B., Huang, R. & Li, M. Effect of tobacco on periodontal disease and oral cancer. *Tob. Induc. Dis.* **17**, 1–15 (2019).
 55. Rogers, M. a M. *et al.* Higher rates of *Clostridium difficile* infection among smokers. *PLoS One* **7**, e42091 (2012).
 56. Barker, A. K., Van Galen, A., Sethi, A. K., Shirley, D. & Safdar, N. Tobacco use as a screener for *Clostridium difficile* infection outcomes. *J. Hosp. Infect.* **98**, 36–39 (2018).
 57. Haas, J. P., Evans, A. M., Preston, K. E. & Larson, E. L. Risk factors for surgical site infection after cardiac surgery: The role of endogenous flora. *Hear. Lung* **34**, 108–114 (2005).
 58. Luksamijarulkul, P., Parikumsil, N., Poomsuwan, V. & Konkeaw, W. Nosocomial surgical site infection among Photharam Hospital patients with surgery: incidence, risk factors and development of risk screening form - PubMed. *J Med Assoc Thai* **89**, 81–89 (2006).
 59. Cheadle, W. G. Risk Factors for Surgical Site Infection. *Surg. Infect. (Larchmt)*. **7**, (2006).
 60. Bafadhel, M. *et al.* Acute exacerbations of chronic obstructive pulmonary disease: Identification of biologic clusters and their biomarkers. *Am. J. Respir. Crit. Care Med.* **184**, 662–671 (2011).
 61. Burge, S. & Wedzicha, J. A. COPD exacerbations: Definitions and classifications. *Eur. Respir. Journal, Suppl.* **21**, (2003).
 62. Dransfield, M. T. *et al.* Acute exacerbations and lung function loss in smokers with and without chronic obstructive pulmonary disease. *Am. J. Respir. Crit. Care Med.* **195**, 324–330 (2017).
 63. Kerkhof, M. *et al.* Association between COPD exacerbations and lung function decline during maintenance therapy. *Thorax* **75**, 744–753 (2020).
 64. Hoogendoorn, M., Hoogenveen, R. T., Rutten-van Mólken, M. P., Vestbo, J. & Feenstra, T. L. Case fatality of COPD exacerbations: A meta-analysis and statistical modelling approach. *Eur. Respir. J.* **37**, 508–515 (2011).
 65. Sethi, S. & Murphy, T. F. Infection in the pathogenesis and course of chronic obstructive pulmonary disease. *N. Engl. J. Med.* **359**, 2355–2365 (2008).

66. Johnston, N. W. *et al.* Colds as predictors of the onset and severity of COPD exacerbations. *Int. J. COPD* **12**, 839–848 (2017).
67. Zarrabian, B. & Mirsaedi, M. A Trend Analysis of COPD Mortality in the United States by Race and Sex. *Ann. Am. Thorac. Soc.* (2020) doi:10.1513/annalsats.202007-822oc.
68. Vos, T. *et al.* Global burden of 369 diseases and injuries in 204 countries and territories, 1990-2019: a systematic analysis for the Global Burden of Disease Study 2019. *Lancet* **394**, 1204–1222 (2020).
69. Krammer, F. *et al.* Influenza. *Nat. Rev. Dis. Prim.* **4**, 460-465.e2 (2018).
70. Gu, X., Zhou, F., Wang, Y., Fan, G. & Cao, B. Respiratory viral sepsis: Epidemiology, pathophysiology, diagnosis and treatment. *Eur. Respir. Rev.* **29**, 1–12 (2020).
71. Brun-Buisson, C., Richard, J. C. M., Mercat, A., Thiébaud, A. C. M. & Brochard, L. Early corticosteroids in severe influenza A/H1N1 pneumonia and acute respiratory distress syndrome. *Am. J. Respir. Crit. Care Med.* **183**, 1200–1206 (2011).
72. Paget, J. *et al.* Global mortality associated with seasonal influenza epidemics: New burden estimates and predictors from the GLaMOR Project. *J. Glob. Health* **9**, 1–12 (2019).
73. Paules, C. & Subbarao, K. Influenza. *Lancet* **390**, 697–708 (2017).
74. Lee, S. W. *et al.* Impact of cigarette smoke exposure on the lung fibroblastic response after influenza pneumonia. *Am. J. Respir. Cell Mol. Biol.* **59**, 770–781 (2018).
75. Rothberg, M. B., Haessler, S. D. & Brown, R. B. Complications of Viral Influenza. *Am. J. Med.* **121**, 258–264 (2008).
76. Dou, D., Revol, R., Östbye, H., Wang, H. & Daniels, R. Influenza A virus cell entry, replication, virion assembly and movement. *Front. Immunol.* **9**, 1–17 (2018).
77. Matsuoka, Y. *et al.* A comprehensive map of the influenza A virus replication cycle. *BMC Syst. Biol.* **7**, 97 (2013).
78. Krammer, F. The human antibody response to influenza A virus infection and vaccination. *Nat. Rev. Immunol.* **19**, 383–397 (2019).
79. Herold, S., Becker, C., Ridge, K. M. & Budinger, G. R. S. Influenza virus-induced lung injury: Pathogenesis and implications for treatment. *Eur. Respir. J.* **45**, 1463–1478 (2015).
80. Iwasaki, A. & Pillai, P. S. Innate immunity to influenza virus infection.

- Nat. Rev. Immunol.* **14**, 315–328 (2014).
81. Klinkhammer, J. *et al.* IFN- λ prevents influenza virus spread from the upper airways to the lungs and limits virus transmission. *Elife* **7**, 1–18 (2018).
 82. Ivashkiv, L. B. & Donlin, L. T. Regulation of type I interferon responses. *Nat. Rev. Immunol.* **14**, 36–49 (2013).
 83. Galani, I. E. *et al.* Interferon- λ Mediates Non-redundant Front-Line Antiviral Protection against Influenza Virus Infection without Compromising Host Fitness. *Immunity* **46**, 875-890.e6 (2017).
 84. Braciale, T. J., Sun, J. & Kim, T. S. Regulating the adaptive immune response to respiratory virus infection. *Nat. Rev. Immunol.* **12**, 295–305 (2012).
 85. Marshall, H. D. *et al.* The transforming growth factor beta signaling pathway is critical for the formation of CD4 T follicular helper cells and isotype-switched antibody responses in the lung mucosa. *Elife* **4**, 1–16 (2015).
 86. La Gruta, N. L. & Turner, S. J. T cell mediated immunity to influenza: Mechanisms of viral control. *Trends Immunol.* **35**, 396–402 (2014).
 87. Tate, M. D. *et al.* Neutrophils Ameliorate Lung Injury and the Development of Severe Disease during Influenza Infection. *J. Immunol.* **183**, 7441–7450 (2009).
 88. Tate, M. D., Ioannidis, L. J., Croker, B., Brown, L. E. & Brooks, A. G. The Role of Neutrophils during Mild and Severe Influenza Virus Infections of Mice. *PLoS One* **6**, 17618 (2011).
 89. Brandes, M., Klauschen, F., Kuchen, S. & Germain, R. N. A systems analysis identifies a feedforward inflammatory circuit leading to lethal influenza infection. *Cell* **154**, 197 (2013).
 90. Allen, L.-A. H., Anes, E., Jonsson, C. B. & Camp, J. V. A Role for Neutrophils in Viral Respiratory Disease. *Front. Immunol.* **8**, 1–17 (2017).
 91. Reilly, E. C., Lambert-Emo, K. & Topham, D. J. The effects of acute neutrophil depletion on resolution of acute influenza infection, establishment of tissue resident memory (TRM), and heterosubtypic immunity. *PLoS One* **11**, 1–20 (2016).
 92. Tak, T. *et al.* Neutrophil-mediated Suppression of Influenza-induced Pathology Requires CD11b/CD18 (MAC-1). *Am. J. Respir. Cell Mol. Biol.* **58**, 492–499 (2018).

93. Ljungman, P. *et al.* Outcome of pandemic H1N1 infections in hematopoietic stem cell transplant recipients. *Haematologica* **96**, 1231–1235 (2011).
94. Tang, B. M. *et al.* Neutrophils-related host factors associated with severe disease and fatality in patients with influenza infection. *Nat. Commun.* **10**, 1–13 (2019).
95. Schönrich, G. & Raftery, M. J. Neutrophil extracellular traps go viral. *Front. Immunol.* **7**, 1–7 (2016).
96. Zhu, L. *et al.* High Level of Neutrophil Extracellular Traps Correlates With Poor Prognosis of Severe Influenza A Infection. *J. Infect. Dis.* **217**, 428–465 (2018).
97. Narasaraju, T. *et al.* Excessive Neutrophils and Neutrophil Extracellular Traps Contribute to Acute Lung Injury of Influenza Pneumonitis. *Am. J. Pathol.* **179**, 199–210 (2011).
98. Yipp, B. G. & Kubes, P. NETosis: how vital is it? *Blood* **122**, 2784–94 (2013).
99. Czaikoski, P. G. *et al.* Neutrophil extracellular traps induce organ damage during experimental and clinical sepsis. *PLoS One* **11**, 1–19 (2016).
100. Sugamata, R. *et al.* Contribution of neutrophil-derived myeloperoxidase in the early phase of fulminant acute respiratory distress syndrome induced by influenza virus infection. *Microbiol. Immunol.* **56**, 171–182 (2012).
101. Tamura, S. *et al.* Functional role of respiratory tract haemagglutinin-specific IgA antibodies in protection against influenza. *Vaccine* **8**, 479–485 (1990).
102. Suzuki, T. *et al.* Relationship of the quaternary structure of human secretory IgA to neutralization of influenza virus. *PNAS* **112**, 7809–14 (2015).
103. Renegar, K. B., Small, P. A., Boykins, L. G. & Wright, P. F. Role of IgA versus IgG in the control of influenza viral infection in the murine respiratory tract. *J. Immunol.* **173**, 1978–1986 (2004).
104. Ramphal, R., Cogliano, R. C., Shands, J. W. & Small, P. A. Serum antibody prevents lethal murine influenza pneumonitis but not tracheitis. *Infect. Immun.* **25**, 992–997 (1979).
105. Lambkin-Williams, R. *et al.* An intranasal Proteosome-adjuvanted trivalent influenza vaccine is safe, immunogenic & efficacious in the human viral influenza challenge model. Serum IgG & mucosal IgA are important correlates of protection against illness associated with infection. *PLoS One*

- 11**, 1–20 (2016).
106. Wang, W. *et al.* Human antibody 3E1 targets the HA stem region of H1N1 and H5N6 influenza A viruses. *Nat. Commun.* **7**, 1–12 (2016).
107. Gilchuk, I. M. *et al.* Influenza H7N9 Virus Neuraminidase-Specific Human Monoclonal Antibodies Inhibit Viral Egress and Protect from Lethal Influenza Infection in Mice. *Cell Host Microbe* **26**, 715-728.e8 (2019).
108. Schroeder, H. W. J. & Cavacini, L. Structure and Function of Immunoglobulins. *J. Allergy Clin. Immunol.* **125**, S41–S52 (2010).
109. Mostafa, H. H. *et al.* SARS-CoV-2 Infections in mRNA Vaccinated Individuals are Biased for Viruses Encoding Spike E484K 1 and Associated with Reduced Infectious Virus Loads that Correlate with Respiratory Antiviral IgG levels. *bioRxiv (Preprint)*
doi:10.1101/2021.07.05.21259105.
110. Krammer, F. SARS-CoV-2 vaccines in development. *Nature* **586**, 516–527 (2020).
111. Woof, J. M. & Russell, M. W. Structure and function relationships in IgA. *Mucosal Immunol.* **4**, 590–597 (2011).
112. Janoff, E. N. *et al.* Pneumococcal IgA1 protease subverts specific protection by human IgA1. *Mucosal Immunol.* **7**, 249–56 (2014).
113. Cerutti, A. The regulation of IgA class switching. *Nat. Rev. Immunol.* **8**, 421–434 (2008).
114. Terauchi, Y. *et al.* IgA polymerization contributes to efficient virus neutralization on human upper respiratory mucosa after intranasal inactivated influenza vaccine administration. *Hum. Vaccines Immunother.* **14**, 1351–1361 (2018).
115. Saito, S. *et al.* IgA tetramerization improves target breadth but not peak potency of functionality of anti-influenza virus broadly neutralizing antibody. *PLOS Pathog.* **15**, 1–23 (2019).
116. Wang, Z. *et al.* Enhanced SARS-CoV-2 neutralization by dimeric IgA. *Sci. Transl. Med.* **13**, 1–11 (2021).
117. Johansen, F., Braathen, R. & Brandtzaeg, P. Role of J chain in secretory immunoglobulin formation. *Scand. J. Immunol.* **52**, 240–248 (2000).
118. Woof, J. M. & Mestecky, J. Mucosal Immunoglobulins. *Immunol. Rev.* **206**, 64–82 (2005).
119. Okuya, K. *et al.* A potential role of non-neutralizing IgA antibodies in cross-protective immunity against influenza A viruses of multiple

- hemagglutinin subtypes. *J. Virol.* **92**, e00408-20 (2020).
120. Belshe, R. B. *et al.* Correlates of immune protection induced by live, attenuated, cold-adapted, trivalent, intranasal influenza virus vaccine. *J. Infect. Dis.* **181**, 1133–1137 (2000).
 121. Ambrose, C. S., Wu, X., Jones, T. & Mallory, R. M. The role of nasal IgA in children vaccinated with live attenuated influenza vaccine. *Vaccine* **30**, 6794–6801 (2012).
 122. Moor, K. *et al.* High-avidity IgA protects the intestine by enchainning growing bacteria. *Nature* **544**, 498–502 (2017).
 123. Stokes, C. R., Soothill, J. F. & Turner, M. W. Immune Exclusion is a function of IgA. *Nature* **255**, 745–746 (1975).
 124. Corthésy, B. Multi-faceted functions of secretory IgA at mucosal surfaces. *Front. Immunol.* **4**, 1–11 (2013).
 125. Stacey, H. D. *et al.* IgA Potentiates NETosis in Response to Viral Infection. *PNAS* **118**, 1–9 (2021).
 126. Oortwijn, B. D. *et al.* Monomeric and polymeric IgA show a similar association with the myeloid FcαRI/CD89. *Mol. Immunol.* **44**, 966–973 (2007).
 127. He, W. *et al.* Broadly neutralizing anti-influenza virus antibodies: enhancement of neutralizing potency in polyclonal mixtures and IgA backbones. *J. Virol.* **89**, 3610–8 (2015).
 128. van Riet, E., Ainai, A., Suzuki, T. & Hasegawa, H. Mucosal IgA responses in influenza virus infections; thoughts for vaccine design. *Vaccine* **30**, 5893–5900 (2012).
 129. Macpherson, A. J., McCoy, K. D., Johansen, F.-E. & Brandtzaeg, P. The immune geography of IgA induction and function. *Mucosal Immunol.* **1**, 11–22 (2008).
 130. Brandtzaeg, P. Potential of nasopharynx-associated lymphoid tissue for vaccine responses in the airways. *Am. J. Respir. Crit. Care Med.* **183**, 1595–1604 (2011).
 131. Pabst, O. New concepts in the generation and functions of IgA. *Nat. Rev. Immunol.* **12**, 821–832 (2012).
 132. Kurosaki, T., Kometani, K. & Ise, W. Memory B cells. *Nat. Rev. Immunol.* **15**, 149–59 (2015).
 133. Victora, G. D. & Wilson, P. C. Germinal Center Selection and the Antibody Response to Influenza. *Cell* **163**, 545–548 (2015).

134. Lingwood, D. *et al.* Structural and genetic basis for development of broadly neutralizing influenza antibodies. *Nature* **489**, 566–570 (2012).
135. Pappas, L. *et al.* Rapid development of broadly influenza neutralizing antibodies through redundant mutations. *Nature* **516**, 418–422 (2014).
136. Anttila, M., Eskola, J., Ahman, H. & Käyhty, H. Avidity of IgG for *Streptococcus pneumoniae* type 6B and 23F polysaccharides in infants primed with pneumococcal conjugates and boosted with polysaccharide or conjugate vaccines. *J. Infect. Dis.* **177**, 1614–21 (1998).
137. Lucas, A. H. & Granoff, D. M. Functional differences in idiotypically defined IgG1 anti-polysaccharide antibodies elicited by vaccination with *Haemophilus influenzae* type B polysaccharide-protein conjugates. *J. Immunol.* **154**, 4195–4202 (1995).
138. Schlesinger, Y. & Granoff, D. M. Avidity and bactericidal activity of antibody elicited by different *Haemophilus influenzae* type b conjugate vaccines. *JAMA* **267**, 1489–94 (1992).
139. Tamura, S. I. *et al.* Antibody-forming cells in the nasal-associated lymphoid tissue during primary influenza virus infection. *J. Gen. Virol.* **79**, 291–299 (1998).
140. Neutra, M. R. & Kozlowski, P. A. Mucosal vaccines: the promise and the challenge. *Nat Rev Immunol* **6**, 148–158 (2006).
141. Wiley, J. A. *et al.* Upper Respiratory Tract Resistance to Influenza Infection Is Not Prevented by the Absence of Either Nasal-Associated Lymphoid Tissue or Cervical Lymph Nodes. *J. Immunol.* **175**, 3186–3196 (2005).
142. Rescigno, M., Martino, M., Sutherland, C. L., Gold, M. R. & Ricciardi-Castagnoli, P. Dendritic Cell Survival and Maturation Are Regulated by Different Signaling Pathways. *J. Exp. Med.* **188**, 2175–2180 (1998).
143. Granucci, F. *et al.* Early events in dendritic cell maturation induced by LPS. *Microbes Infect.* **1**, 1079–1084 (1999).
144. Förster, R., Davalos-Missslitz, A. C. & Rot, A. CCR7 and its ligands: balancing immunity and tolerance. *Nat. Rev. Immunol.* **8**, 362–71 (2008).
145. Song, J.-H. *et al.* CCR7-CCL19/CCL21-Regulated Dendritic Cells Are Responsible for Effectiveness of Sublingual Vaccination. *J. Immunol.* **182**, 6851–6860 (2009).
146. Ballesteros-Tato, A. & Randall, T. D. Priming of T follicular helper cells by dendritic cells. *Immunol. Cell Biol.* **92**, 22–7 (2014).

147. León, B. *et al.* Regulation of T(H)2 development by CXCR5+ dendritic cells and lymphotoxin-expressing B cells. *Nat. Immunol.* **13**, 681–90 (2012).
148. Kerfoot, S. M. *et al.* Germinal Center B Cell and T Follicular Helper Cell Development Initiates in the Interfollicular Zone. *Immunity* **34**, 947–960 (2011).
149. Choi, Y. S. *et al.* ICOS Receptor Instructs T Follicular Helper Cell versus Effector Cell Differentiation via Induction of the Transcriptional Repressor Bcl6. *Immunity* **34**, 932–946 (2011).
150. Dullaers, M. *et al.* A T Cell-Dependent Mechanism for the Induction of Human Mucosal Homing Immunoglobulin A-Secreting Plasmablasts. *Immunity* **30**, 120–129 (2009).
151. Shimoda, M. *et al.* Isotype-specific selection of high affinity memory B cells in nasal-associated lymphoid tissue. *J. Exp. Med.* **194**, 1597–607 (2001).
152. Lazarus, N. H. *et al.* A Common Mucosal Chemokine (Mucosae-Associated Epithelial Chemokine/CCL28) Selectively Attracts IgA Plasmablasts. *J. Immunol.* **170**, 3799–3805 (2003).
153. Kunkel, E. J. *et al.* CCR10 expression is a common feature of circulating and mucosal epithelial tissue IgA Ab-secreting cells. *J. Clin. Invest.* **111**, 1001–1010 (2003).
154. Kunkel, E. J. & Butcher, E. C. Plasma-cell homing. *Nat Rev Immunol* **3**, 822–829 (2003).
155. Ohori, J. *et al.* TNF- α upregulates VCAM-1 and NF- κ B in fibroblasts from nasal polyps. *Auris Nasus Larynx* **34**, 177–183 (2007).
156. Zarnegar, B. *et al.* Influenza infection in mice induces accumulation of lung mast cells through the recruitment and maturation of mast cell progenitors. *Front. Immunol.* **8**, 310 (2017).
157. Johansen, F. E. *et al.* Absence of epithelial immunoglobulin a transport, with increased mucosal leakiness, in polymeric immunoglobulin receptor/secretory component-deficient mice. *J. Exp. Med.* **190**, 915–921 (1999).
158. Johansen, F.-E., Braathen, R. & Brandtzaeg, P. The J Chain Is Essential for Polymeric Ig Receptor-Mediated Epithelial Transport of IgA. *J. Immunol.* **167**, 5185–5192 (2001).
159. Su, F., Patel, G. B., Hu, S. & Chen, W. Induction of mucosal immunity through systemic immunization: Phantom or reality? *Hum. Vaccines*

- Immunother.* **12**, 1070–1079 (2016).
160. Holmgren, J. & Czerkinsky, C. Mucosal immunity and vaccines. *Nat. Med.* **11**, S45-53 (2005).
161. PHAC. Canadian Immunization Guide: Chapter on Influenza and Statement on Seasonal Influenza Vaccine for 2020-2021. <https://www.canada.ca/en/public-health/services/publications/vaccines-immunization/canadian-immunization-guide-statement-seasonal-influenza-vaccine-2020-2021.html> (2016).
162. Chan, W., Zhou, H., Kemble, G. & Jin, H. The cold adapted and temperature sensitive influenza A/Ann Arbor/6/60 virus, the master donor virus for live attenuated influenza vaccines, has multiple defects in replication at the restrictive temperature. *Virology* **380**, 304–311 (2008).
163. Amorij, J. P., Hinrichs, W. L. J., Frijlink, H. W., Wilschut, J. C. & Huckriede, A. Needle-free influenza vaccination. *Lancet Infect. Dis.* **10**, 699–711 (2010).
164. Fukuyama, Y. *et al.* Nanogel-based pneumococcal surface protein A nasal vaccine induces microRNA-associated Th17 cell responses with neutralizing antibodies against *Streptococcus pneumoniae* in macaques. *Mucosal Immunol.* **8**, 1–10 (2015).
165. Calzas, C. & Chevalier, C. Innovative mucosal vaccine formulations against influenza A virus infections. *Front. Immunol.* **10**, 1–21 (2019).
166. Hassan, A. O. *et al.* A Single-Dose Intranasal ChAd Vaccine Protects Upper and Lower Respiratory Tracts against SARS-CoV-2. (2020) doi:10.1016/j.cell.2020.08.026.
167. Mudgal, R., Nehul, S. & Tomar, S. Prospects for mucosal vaccine: shutting the door on SARS-CoV-2. *Hum. Vaccines Immunother.* **16**, 2921–2931 (2020).
168. Esther, C. R. *et al.* Mucus accumulation in the lungs precedes structural changes and infection in children with cystic fibrosis. *Sci. Transl. Med.* **11**, 1–11 (2019).
169. Willner, D., Daly, J., Whiley, D., Grimwood, K. & Wainwright, C. E. Comparison of DNA Extraction Methods for Microbial Community Profiling with an Application to Pediatric Bronchoalveolar Lavage Samples. *PLoS One* **7**, 1–12 (2012).
170. Efthimiadis, A., Pizzichini, M. M. M., Pizzichini, E., Dolovich, J. & Hargreave, F. E. Induced sputum cell and fluid-phase indices of inflammation: comparison of treatment with dithiothreitol vs phosphate-buffered saline. *Eur Respir J* **10**, 1336–1340 (1997).

171. Takatsu, K., Ishizaka, T. & Ishizaka, K. Biologic significance of disulfide bonds in human IgE molecules. *J. Immunol.* **114**, 1838–18345 (1975).
172. Lu, L. L., Suscovich, T. J., Fortune, S. M. & Alter, G. Beyond binding: Antibody effector functions in infectious diseases. *Nat. Rev. Immunol.* **18**, 46–61 (2018).
173. Kearley, J. *et al.* Cigarette smoke silences innate lymphoid cell function and facilitates an exacerbated type I interleukin-33-dependent response to infection. *Immunity* **42**, 566–579 (2015).
174. Kang, M. J. *et al.* Cigarette smoke selectively enhances viral PAMP- and virus-induced pulmonary innate immune and remodeling responses in mice. *J. Clin. Invest.* **118**, 2771–2784 (2008).
175. Wang, X. *et al.* RIG-I overexpression decreases mortality of cigarette smoke exposed mice during influenza A virus infection. *Respir. Res.* **18**, 166 (2017).
176. Robbins, C. S. *et al.* Cigarette smoke impacts immune inflammatory responses to influenza in mice. *Am. J. Respir. Crit. Care Med.* **174**, 1342–1351 (2006).
177. Bauer, C. M. T. *et al.* Treating viral exacerbations of chronic obstructive pulmonary disease: Insights from a mouse model of cigarette smoke and H1N1 influenza infection. *PLoS One* **5**, 1–11 (2010).
178. Botelho, F. M. *et al.* IL-1 α /IL-1R1 expression in chronic obstructive pulmonary disease and mechanistic relevance to smoke-induced neutrophilia in mice. *PLoS One* **6**, 1–13 (2011).
179. Hong, M. J. *et al.* Protective role of $\gamma\delta$ T cells in cigarette smoke and influenza infection. *Mucosal Immunol.* **11**, 894–908 (2017).
180. Bauer, C. *et al.* Cigarette smoke suppresses Type I Interferon-Mediated Antiviral Immunity in Lung Fibroblast and Epithelial Cells. *J. Interf. Cytokine Res.* **28**, 167–179 (2008).
181. Jaspers, I. *et al.* Reduced Expression of IRF7 in Nasal Epithelial Cells from Smokers after Infection with Influenza. *Am. J. Respir. Cell Mol. Biol.* **43**, 368–375 (2010).
182. Eddleston, J., Lee, R. U., Doerner, A. M., Herschbach, J. & Zuraw, B. L. Cigarette smoke decreases innate responses of epithelial cells to rhinovirus infection. *Am. J. Respir. Cell Mol. Biol.* **44**, 118–126 (2010).
183. Kovalhuk, L. C. S., Telles, E. Q., Lima, M. N. & Rosario Filho, N. A. Nasal lavage cytology and mucosal histopathological alterations in patients with rhinitis. *Braz. J. Otorhinolaryngol.* **86**, 434–442 (2020).

184. Noah, T. L. *et al.* Tobacco Smoke Exposure and Altered Nasal Responses to Live Attenuated Influenza Virus. *Environ. Health Perspect.* **119**, 78–83 (2010).
185. Tavares, L. P. *et al.* CXCR1/2 antagonism is protective during influenza and post-influenza pneumococcal infection. *Front. Immunol.* **8**, 1–14 (2017).
186. MacKenzie, J. S., MacKenzie, I. H. & Holt, P. G. The effect of cigarette smoking on susceptibility to epidemic influenza and on serological responses to live attenuated and killed subunit influenza vaccines. *J Hyg* **77**, 409–417 (1976).
187. Cruijff, M. *et al.* The effect of smoking on influenza, influenza vaccination efficacy and on the antibody response to influenza vaccination. *Vaccine* **17**, 426–432 (1999).
188. Woolpert, T. *et al.* Health-related behaviors and effectiveness of trivalent inactivated versus live attenuated influenza vaccine in preventing influenza-like illness among young adults. *PLoS One* **9**, 1–9 (2014).
189. Nicholson, K. G., Kent, J. & Hammersley, V. Influenza A among community-dwelling elderly persons in Leicestershire during winter 1993-4; cigarette smoking as a risk factor and the efficacy of influenza vaccination. *Epidemiol. Infect.* **123**, 103–8 (1999).
190. Namujju, P. B. *et al.* Impact of smoking on the quantity and quality of antibodies induced by human papillomavirus type 16 and 18 AS04-adjuvanted virus-like-particle vaccine - A pilot study. *BMC Res. Notes* **7**, 2–7 (2014).
191. Winter, A. P., Follett, E. A. C., McIntyre, J., Stewart, J. & Symington, I. S. Influence of smoking on immunological responses to hepatitis B vaccine. *Vaccine* **12**, 771–772 (1994).
192. Robbins, C. S. *et al.* Cigarette Smoke Decreases Pulmonary Dendritic Cells and Impacts Antiviral Immune Responsiveness. *Am. J. Respir. Cell Mol. Biol.* **30**, 202–211 (2004).
193. Wang, J., Li, Q., Xie, J. & Xu, Y. Cigarette smoke inhibits BAFF expression and mucosal immunoglobulin A responses in the lung during influenza virus infection. *Respir. Res.* **16**, 1–12 (2015).
194. Cass, S. P. *et al.* Current smoking status is associated with reduced sputum immunoglobulin M and G expression in chronic obstructive pulmonary disease. *Eur. Respir. J.* **57**, 1902338 (2020).
195. Barton, J. R., Riad, M. A., Gaze, M. N., Maran, A. G. D. & Ferguson, A. Mucosal immunodeficiency in smokers, and in patients with epithelial head

- and neck tumours. *Gut* **31**, 378–382 (1990).
196. Giuca, M. R., Pasini, M., Tecco, S., Giuca, G. & Marzo, G. Levels of salivary immunoglobulins and periodontal evaluation in smoking patients. *BMC Immunol.* **15**, 1–5 (2014).
 197. Bennet, K. R. & Reade, P. C. Salivary immunoglobulin A levels in normal subjects, tobacco smokers, and patients with minor aphthous ulceration. *Oral Surgery, Oral Med. Oral Pathol. Oral Radiol.* **53**, 461–465 (1982).
 198. Agarwal, A., Rao, S. ., Sowmya, S. ., Augustine, D. & Patil, S. Estimation of Salivary Immunoglobulin A and Serum Immunoglobulin A in Smokers and Nonsmokers : A Comparative Study. *J. Int. Oral Heal.* **8**, 1008–1011 (2016).
 199. Norhagen Engström, G. & Engström, P. E. Effects of tobacco smoking on salivary immunoglobulin levels in immunodeficiency. *Eur. J. Oral Sci.* **106**, 986–91 (1998).
 200. Mandel, M. A., Dvorak, K. & Decosse, J. J. Salivary Immunoglobulins In Patients with Oropharyngeal and Bronchopulmonary Carcinoma. *Cancer* **31**, 1408–1413 (1973).
 201. Miller, R. D., Gleich, G. J., Offord, K. P. & Dunnette, S. L. Immunoglobulin concentrations in serum and nasal secretions in chronic obstructive pulmonary disease. A matched-pair study. *Am Rev Respir Dis* **119**, 229–238 (1979).
 202. Rylander, R., Wold, A. & Haglind, P. Nasal antibodies against gram-negative bacteria in cotton-mill workers. *Int. Arch. Allergy Appl. Immunol.* **69**, 330–4 (1982).
 203. Rebuli, M. E. *et al.* Electronic-cigarette use alters nasal mucosal immune response to live-attenuated influenza virus: A clinical trial. *Am. J. Respir. Cell Mol. Biol.* **64**, 126–137 (2021).
 204. Roos, A. B. *et al.* IL-17A Is Elevated in End-Stage Chronic Obstructive Pulmonary Disease and Contributes to Cigarette Smoke-induced Lymphoid Neogenesis. *Am. J. Respir. Crit. Care Med.* **191**, 1232–1241 (2015).
 205. Yadava, K., Bollyky, P. & Lawson, M. A. The formation and function of tertiary lymphoid follicles in chronic pulmonary inflammation. *Immunology* **149**, 262–269 (2016).
 206. Hasday, J. D., Bascom, R., Costa, J. J., Fitzgerald, T. & Dubin, W. Bacterial endotoxin is an active component of cigarette smoke. *Chest* **115**, 829–835 (1999).

207. Xu, H. *et al.* The modulatory effects of lipopolysaccharide-stimulated B cells on differential T-cell polarization. *Immunology* **125**, 218–228 (2008).
208. Kong, D. H., Kim, Y. K., Kim, M. R., Jang, J. H. & Lee, S. Emerging roles of vascular cell adhesion molecule-1 (VCAM-1) in immunological disorders and cancer. *Int. J. Mol. Sci.* **19**, 1–16 (2018).
209. Renner, F. & Schmitz, M. L. Autoregulatory feedback loops terminating the NF-kappaB response. *Trends Biochem. Sci.* **34**, 128–35 (2009).
210. Shih, V. F.-S. *et al.* Kinetic control of negative feedback regulators of NF-kappaB/RelA determines their pathogen- and cytokine-receptor signaling specificity. *PNAS* **106**, 9619–24 (2009).
211. Jono, H. *et al.* NF-kB Is Essential for Induction of CYLD, the Negative Regulator of NF-kB: Evidence for a novel inducible autoregulatory feedback pathway. *J. Biol. Chem.* **279**, 36171–36174 (2004).
212. Omagari, D. *et al.* Nuclear factor kappa B plays a pivotal role in polyinosinic-polycytidylic acid-induced expression of human β -defensin 2 in intestinal epithelial cells. *Clin. Exp. Immunol.* **165**, 85–93 (2011).
213. Bafadhel, M. *et al.* Profiling of Sputum Inflammatory Mediators in Asthma and Chronic Obstructive Pulmonary Disease. *Respiration* **83**, 36–44 (2012).
214. Pizzichini, E., Pizzichini, M. M., Efthimiadis, A., Hargreave, F. E. & Dolovich, J. Measurement of inflammatory indices in induced sputum: effects of selection of sputum to minimize salivary contamination. *Eur. Respir. J.* **9**, 1174–80 (1996).
215. Rousseaux-Prévost, R., Rousseaux, J., Bazin, H. & Biserte, G. Differential reduction of the inter-chain disulfide bonds of rat immunoglobulin E: Relation to biological activity. *Mol. Immunol.* **21**, 233–241 (1984).
216. Okuno, T. & Kondelis, N. Evaluation of dithiothreitol (DTT) for inactivation of IgM antibodies. *J. Clin. Pathol.* **31**, 1152–1155 (1978).
217. Underdown, B. J. & Dorrington, K. J. Studies on the structural and conformational basis for the relative resistance of serum and secretory immunoglobulin A to proteolysis. *J. Immunol.* **112**, 949–959 (1974).
218. Abdollahpour-Alitappeh, M. *et al.* Evaluation of factors influencing antibody reduction for development of antibody drug conjugates. *Iran. Biomed. J.* **21**, 270–274 (2017).
219. Biesbrock, A. R., Reddy, M. S. & Levine, M. J. Interaction of a salivary mucin-secretory immunoglobulin A complex with mucosal pathogens. *Infect. Immun.* **59**, 3492–3497 (1991).

220. Louis, R. *et al.* The effect of processing on inflammatory markers in induced sputum. *Eur. Respir. J.* **13**, 660–667 (1999).
221. Mukherjee, M. *et al.* Sputum autoantibodies in patients with severe eosinophilic asthma. *J. Allergy Clin. Immunol.* **141**, 1269–1279 (2018).
222. Herwig, M. C., Müller, K. M. & Müller, A. M. Endothelial VE-cadherin expression in human lungs. *Pathol. Res. Pract.* **204**, 725–730 (2008).
223. Ware, L. B. *et al.* Donor smoking is associated with pulmonary edema, inflammation and epithelial dysfunction in ex vivo human donor lungs. *Am. J. Transplant.* **14**, 2295–2302 (2014).
224. Wu, W. *et al.* Long-term cigarette smoke exposure dysregulates pulmonary T cell response and IFN- γ protection to influenza virus in mouse. *Respir. Res.* **22**, 1–14 (2021).
225. de Azevedo, A. M. & Goldberg Tabak, D. Life-threatening capillary leak syndrome after G-CSF mobilization and collection of peripheral blood progenitor cells for allogeneic transplantation. *Bone Marrow Transplant.* **28**, 311–312 (2001).
226. Yamamoto, K. *et al.* Case Report Severe Hypoxemia in a Healthy Donor for Allogeneic Hematopoietic Stem Cell Transplantation after Only the First Administration of Granulocyte-Colony Stimulating Factor. *Transfus Med Hemother* **43**, 433–435 (2016).
227. Dagdemir, A., Albayrak, D., Dilber, C. & Totan, M. G-CSF Related Capillary Leak Syndrome in a Child with Leukemia. *Leuk. Lymphoma* **42**, 1445–1447 (2001).
228. Taha, M., Sharma, A. & Soubani, A. Clinical deterioration during neutropenia recovery after G-CSF therapy in patient with COVID-19. *Respir. Med. Case Reports* **31**, 1–4 (2020).
229. Nawar, T. *et al.* Granulocyte-colony stimulating factor in COVID-19: Is it stimulating more than just the bone marrow? *Am. J. Hematol.* **95**, E208–E210 (2020).
230. Dwivedi, P. & Greis, K. D. Granulocyte colony-stimulating factor receptor signaling in severe congenital neutropenia, chronic neutrophilic leukemia, and related malignancies. *Exp. Hematol.* **46**, 9–20 (2017).
231. Gibbings, S. L. *et al.* Three unique interstitial macrophages in the murine lung at steady state. *Am. J. Respir. Cell Mol. Biol.* **57**, 66–76 (2017).
232. Steuerman, Y. *et al.* Dissection of Influenza Infection In Vivo by Single-Cell RNA Sequencing. *Cell Syst.* **6**, 679-691.e4 (2018).

233. Zhang, J. *et al.* Two waves of pro-inflammatory factors are released during the influenza A virus (IAV)-driven pulmonary immunopathogenesis. *PLOS Pathog.* **16**, 1–24 (2020).
234. García-López, M. Á. *et al.* CXCR3 chemokine receptor distribution in normal and inflamed tissues: Expression on activated lymphocytes, endothelial cells, and dendritic cells. *Lab. Investig.* **81**, 409–418 (2001).
235. Croxford, A. L. *et al.* The Cytokine GM-CSF Drives the Inflammatory Signature of CCR2+ Monocytes and Licenses Autoimmunity. *Immunity* **43**, 502–514 (2015).
236. Ariga, M. *et al.* Nonredundant Function of Phosphodiesterases 4D and 4B in Neutrophil Recruitment to the Site of Inflammation. *J. Immunol.* **173**, 7531–7538 (2004).
237. El Kasmi, K. C. *et al.* A Transcriptional Repressor and Corepressor Induced by the STAT3-Regulated Anti-Inflammatory Signaling Pathway. *J. Immunol.* **179**, 7215–7219 (2007).
238. Tanaka, Y. *et al.* Six-transmembrane epithelial antigen of prostate 4 (STEAP4) is expressed on monocytes/neutrophils, and is regulated by TNF antagonist in patients with rheumatoid arthritis. *Clin Exp Rheumatol* **30**, 99–102 (2012).
239. Croker, B. A. *et al.* SOCS3 Is a Critical Physiological Negative Regulator of G-CSF Signaling and Emergency Granulopoiesis. *Immunity* **20**, 153–165 (2004).
240. Chen, W., FitzGerald, J. M., Sin, D. D. & Sadatsafavi, M. Excess economic burden of comorbidities in COPD: a 15-year population-based study. *Eur. Respir. J.* **50**, 1700393 (2017).
241. Gould, V. M. W. *et al.* Nasal IgA provides protection against human influenza challenge in volunteers with low serum influenza antibody titre. *Front. Microbiol.* **8**, 1–9 (2017).
242. PHAC. Canadian Immunization Guide: Part 4 - Active Vaccines. <https://www.canada.ca/en/public-health/services/publications/healthy-living/canadian-immunization-guide-part-4-active-vaccines.html> (2021).
243. Wern, J. E., Sorensen, M. R., Olsen, A. W., Andersen, P. & Follmann, F. Simultaneous subcutaneous and intranasal administration of a CAF01- adjuvanted Chlamydia vaccine elicits elevated IgA and protective Th1/Th17 responses in the genital tract. *Front. Immunol.* **8**, 1–11 (2017).
244. Gallichan, W. S. *et al.* Intranasal Immunization with CpG Oligodeoxynucleotides as an Adjuvant Dramatically Increases IgA and Protection Against Herpes Simplex Virus-2 in the Genital Tract. *J.*

- Immunol.* **166**, 3451–3457 (2001).
245. Stämpfli, M. R. & Anderson, G. P. How cigarette smoke skews immune responses to promote infection, lung disease and cancer. *Nat. Rev. Immunol.* **9**, 377–384 (2009).
246. Gouglas, D. *et al.* Estimating the cost of vaccine development against epidemic infectious diseases: a cost minimisation study. *Lancet Glob. Heal.* **6**, e1386–e1396 (2018).
247. Behzadi, M. A. & Leyva-Grado, V. H. Overview of current therapeutics and novel candidates against influenza, respiratory syncytial virus, and Middle East respiratory syndrome coronavirus infections. *Front. Microbiol.* **10**, 1–16 (2019).
248. Toots, M. & Plemper, R. K. Next-generation direct-acting influenza therapeutics. *Transl. Res.* **220**, 33–42 (2020).
249. Yip, T. F., Selim, A. S. M., Lian, I. & Lee, S. M. Y. Advancements in host-based interventions for influenza treatment. *Front. Immunol.* **9**, 1–21 (2018).
250. Siddiqi, H. K. & Mehra, M. R. COVID-19 illness in native and immunosuppressed states: A clinical–therapeutic staging proposal. *J. Hear. Lung Transplant.* **39**, 405–407 (2020).
251. Ni, Y. N., Chen, G., Sun, J., Liang, B. M. & Liang, Z. A. The effect of corticosteroids on mortality of patients with influenza pneumonia: A systematic review and meta-analysis. *Crit. Care* **23**, (2019).
252. Zhou, Y. *et al.* Use of corticosteroids in influenza-associated acute respiratory distress syndrome and severe pneumonia: a systemic review and meta-analysis. *Sci. Rep.* **10**, 1–10 (2020).
253. Sterne, J. A. C. *et al.* Association between Administration of Systemic Corticosteroids and Mortality among Critically Ill Patients with COVID-19: A Meta-analysis. *JAMA* **324**, 1330–1341 (2020).
254. Li, H. *et al.* Impact of corticosteroid therapy on outcomes of persons with SARS-CoV-2, SARS-CoV, or MERS-CoV infection: a systematic review and meta-analysis. *Leukemia* **34**, 1503–1511 (2020).
255. van Paassen, J. *et al.* Corticosteroid use in COVID-19 patients: a systematic review and meta-analysis on clinical outcomes. *Crit. Care* **24**, 1–22 (2020).
256. Horby, P. *et al.* Dexamethasone in Hospitalized Patients with Covid-19. *N. Engl. J. Med.* **384**, 693–704 (2021).

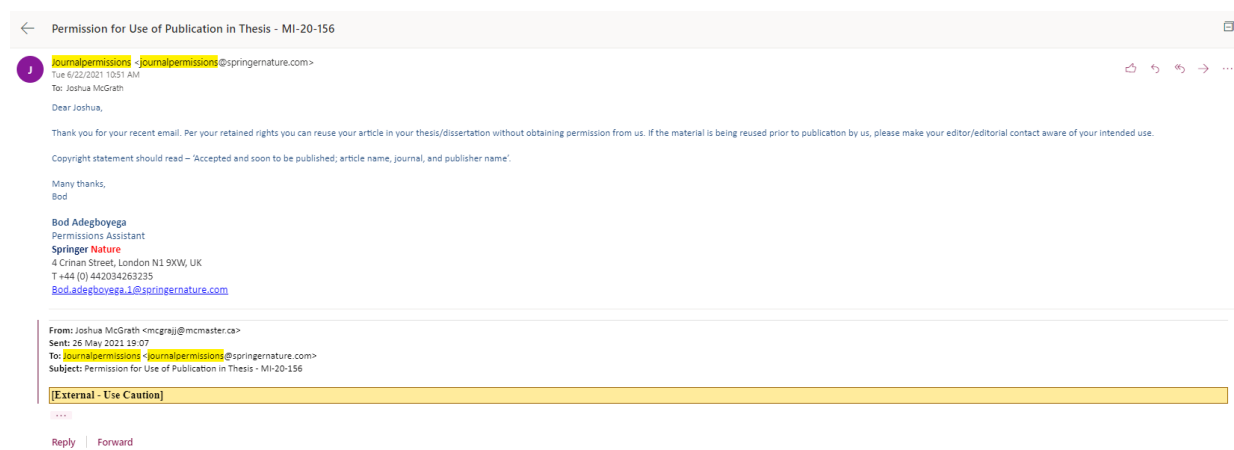
257. Ramakrishnan, S. *et al.* Inhaled budesonide in the treatment of early COVID-19 (STOIC): a phase 2, open-label, randomised controlled trial. *Lancet Respir. Med.* **9**, 763–772 (2021).
258. Torres, A., Loeches, I. M., Sligl, W. & Lee, N. Severe flu management: a point of view. *Intensive Care Med.* **46**, 153–162 (2020).
259. Jaspers, I. *et al.* Reduced Expression of IRF7 in Nasal Epithelial Cells from Smokers after Infection with Influenza. *Am. J. Respir. Cell Mol. Biol.* **43**, 368–375 (2010).
260. Yang, E. & Li, M. M. H. All About the RNA: Interferon-Stimulated Genes That Interfere With Viral RNA Processes. *Front. Immunol.* **11**, 1–18 (2020).
261. Xing, Z. *et al.* IL-6 is an antiinflammatory cytokine required for controlling local or systemic acute inflammatory responses. *J. Clin. Invest.* **101**, 311–320 (1998).
262. Wang, H., Aloe, C., Wilson, N. & Bozinovski, S. G-CSFR antagonism reduces neutrophilic inflammation during pneumococcal and influenza respiratory infections without compromising clearance. *Sci. Rep.* **9**, 1–12 (2019).
263. Rutigliano, J. A. *et al.* Highly Pathological Influenza A Virus Infection Is Associated with Augmented Expression of PD-1 by Functionally Compromised Virus-Specific CD8⁺ T Cells. *J. Virol.* **88**, 1636–1651 (2014).
264. Liu, Q., Zhou, Y. H. & Yang, Z. Q. The cytokine storm of severe influenza and development of immunomodulatory therapy. *Cell. Mol. Immunol.* **13**, 3–10 (2016).
265. Hermesh, T., Moran, T. M., Jain, D. & López, C. B. Granulocyte colony-stimulating factor protects mice during respiratory virus infections. *PLoS One* **7**, 1–8 (2012).
266. Dienz, O. *et al.* Essential role of IL-6 in protection against H1N1 influenza virus by promoting neutrophil survival in the lung. *Mucosal Immunol.* **5**, 258–266 (2012).
267. Yang, M. L. *et al.* IL-6 ameliorates acute lung injury in influenza virus infection. *Sci. Rep.* **7**, 1–11 (2017).
268. Sussan, T. E. *et al.* Targeting Nrf2 with the triterpenoid CDDO-imidazolidine attenuates cigarette smoke-induced emphysema and cardiac dysfunction in mice. *Proc. Natl. Acad. Sci. U. S. A.* **106**, 250–255 (2009).
269. Southam, D. S., Dolovich, M., O’Byrne, P. M. & Inman, M. D.

- Distribution of intranasal instillations in mice: effects of volume, time, body position, and anesthesia. *Am. J. Physiol. - Lung Cell. Mol. Physiol.* **282**, L833–L839 (2002).
270. Oster, W., Lindemann, A., Mertelsmann, R. & Herrmann, F. Production of macrophage-, granulocyte-, granulocyte-macrophage- and multi-colony-stimulating factor by peripheral blood cells. *Eur. J. Immunol.* **19**, 543–548 (1989).
271. Yang, T. C., Chang, P. Y., Kuo, T. L. & Lu, S. C. Electronegative L5-LDL induces the production of G-CSF and GM-CSF in human macrophages through LOX-1 involving NF- κ B and ERK2 activation. *Atherosclerosis* **267**, 1–9 (2017).
272. Zsebo, K. M. *et al.* Vascular endothelial cells and granulopoiesis: Interleukin-1 stimulates release of G-CSF and GM-CSF. *Blood* **71**, 99–103 (1988).
273. Koeffler, H. P. *et al.* Recombinant human TNF(α) stimulates production of granulocyte colony-stimulating factor. *Blood* **70**, 55–59 (1987).
274. Ordelheide, A. M. *et al.* Granulocyte colony-stimulating factor (G-CSF): A saturated fatty acid-induced myokine with insulin-desensitizing properties in humans. *Mol. Metab.* **5**, 305–316 (2016).
275. Wong, J., Saravolac, E., Clement, J. & Nagata, L. Development of a murine hypothermia model for study of respiratory tract influenza virus infection. *Lab Anim Sci.* **47**, 143–147 (1997).
276. Paquette, S. G., Banner, D., Zhao, Z., Fang, Y. & Huang, S. S. H. Interleukin-6 Is a Potential Biomarker for Severe Pandemic H1N1 Influenza A Infection. *PLoS One* **7**, 1–10 (2012).
277. Aggarwal, A., Baker, C. S., Evans, T. W. & Haslam, P. L. G-CSF and IL-8 but not GM-CSF correlate with severity of pulmonary neutrophilia in acute respiratory distress syndrome. *Eur. Respir. J.* **15**, 895–901 (2000).
278. McBride, J. M. *et al.* Phase 2 randomized trial of the safety and efficacy of MHAA4549A, a broadly neutralizing monoclonal antibody, in a human influenza a virus challenge model. *Antimicrob. Agents Chemother.* **61**, 1–12 (2017).
279. Ramos, E. L. *et al.* Efficacy and safety of treatment with an anti-M2e monoclonal antibody in experimental human influenza. *J. Infect. Dis.* **211**, 1038–1044 (2015).
280. Zhu, J. *et al.* Bronchial mucosal inflammation and illness severity in response to experimental rhinovirus infection in COPD. *J. Allergy Clin. Immunol.* **146**, 840-850.e7 (2020).

APPENDIX 1

Permission to Reprint (Chapter 2):

Accepted and soon to be published; Cigarette smoke exposure attenuates the induction of antigen-specific IgA in the murine upper respiratory tract. *Mucosal Immunology*, Springer Nature. Copyright © 2021 The Authors.



Permission to Reprint (Chapter 3):

Allergy

Article: Detecting immunoglobulins in processed sputa

GENERAL INFORMATION

Request ID	600054247	Request Date	10 Sep 2021
Request Status	Accepted	Price	0.00 CAD ?

▼ ALL DETAILS

ISSN:	0105-4538	Publisher:	BLACKWELL MUNKSGAARD
Type of Use:	Republish in a thesis/dissertation	Portion:	Chapter/article

LICENSED CONTENT

Publication Title	Allergy	Country	Denmark
Article Title	Detecting immunoglobulins in process...	Rightsholder	John Wiley & Sons - Books
Author/Editor	European Academy of Allergology and ...	Publication Type	Journal
Date	01/01/1978		

REQUEST DETAILS

Page range(s)	1-3	Distribution	Worldwide
Total number of pages	3	Translation	Original language of publication
Format (select all that apply)	Electronic	Copies for the disabled?	No
Who will republish the content?	Author of requested content	Minor editing privileges?	No
Duration of Use	Life of current edition	Incidental promotional use?	No
Lifetime Unit Quantity	Up to 499	Currency	CAD
Rights Requested	Main product		

NEW WORK DETAILS

Title	Delineating the impact of cigarette sm...	Institution name	McMaster University
Instructor name	Martin R. Stampfli	Expected presentation date	2021-09-11

ADDITIONAL DETAILS

The requesting person / organization to appear on the license

Joshua McGrath

REUSE CONTENT DETAILS

Title, description or numeric reference of the portion(s)	Chapter 3	Title of the article/chapter the portion is from	Detecting immunoglobulins in process...
Editor of portion(s)	Cass, Steven P; McGrath, Joshua JC; So...	Author of portion(s)	Cass, Steven P; McGrath, Joshua JC; So...
Volume of serial or monograph	N/A	Publication date of portion	2021-08-21
Page or page range of portion	83-91		